E. WOLF, PROGRESS IN OPTICS XXVI


# I

# PHOTON BUNCHING AND ANTIBUNCHING*

BY

MALVIN C. TEICH

*Columbia Radiation Laboratory and Center for Telecommunications Research*
*Department of Electrical Engineering, Columbia University*
*New York, NY 10027, USA*

BAHAA E. A. SALEH

*Department of Electrical and Computer Engineering*
*University of Wisconsin*
*Madison, WI 53706, USA*

* This work was supported by the Joint Services Electronics Program at Columbia University and by the National Science Foundation.

M. C. Teich and B. E. A. Saleh, "Photon Bunching and Ant bunching," in Progress in Optics, vol. 26, edited by E. Wolf (North-Holland, Amsterdam, 1988), ch. 1, pp. 1-104.

CONTENTS




M. C. Teich and B. E. A. Saleh, "Photon Bunching and Ant bunching," in Progress in Optics, vol. 26, edited by E. Wolf (North-Holland, Amsterdam, 1988), ch. 1, pp. 1-104.

## § 1. Introduction

The photon correlation experiments carried out by HANBURY-BROWN and TWISS [1956a,b] and the invention of the laser by SCHAWLOW and TOWNES [1958] fostered a strong interest in photon statistics in the 1960s. As it turned out, the semiclassical theory of light provided an adequate theoretical framework for understanding the observed photon correlations from conventional sources of light as well as from lasers (MANDEL [1959a, 1963]). In 1963 GLAUBER [1963a,b] developed a fully quantum-mechanical theory of light that encompassed the semiclassical theory. One intriguing aspect of the new quantum optics was that it admitted the possibility of photon anticorrelations as well as photon correlations. Within this expanded framework it became possible to conceive of new forms of light that had never before been realized: antibunched light, sub-Poisson light, and quadrature-squeezed light.

These three characteristics of nonclassical light have recently received a great deal of attention because they have now been observed in the laboratory (KIMBLE, DAGENAIS and MANDEL [1977], SHORT and MANDEL [1983], TEICH and SALEH [1985], SLUSHER, HOLLBERG, YURKE, MERTZ and VALLEY [1985]). In any given light source these characteristics may, but need not, accompany each other (TEICH, SALEH and STOLER [1983], PEŘINA, PEŘINOVÁ and KOĎOUSEK [1984], SHORT and MANDEL [1984], SCHLEICH and WHEELER [1987], YAMAMOTO, MACHIDA, IMOTO, KITAGAWA and BJÖRK [1987]). There are other manifestations of nonclassical light as well; examples include a photon interevent-time probability density function that is underdispersed relative to the exponential and a violation of Bell's inequalities in a photon correlation experiment (REID and WALLS [1984]). Nonclassical light should be useful in providing new insights into various physical and biological processes, such as spectroscopy and the behavior of the human visual system at low levels of light (TEICH, PRUCNAL, VANNUCCI, BRETON and MCGILL [1982]). It is also expected to find use in applications such as optical signal processing, interferometry, gravitational-wave detection, and lightwave communications.

This review pertains to the generation and characterization of antibunched and sub-Poisson light (sub-Poisson light is alternatively called photon-number-

M. C. Teich and B. E. A. Saleh, "Photon Bunching and Ant bunching," in Progress in Optics, vol. 26, edited by E. Wolf (North-Holland, Amsterdam, 1988), ch. 1, pp. 1-104.

squeezed light). These characteristics are manifested in direct-detection experiments, in which the phase of the light wave is ignored. This is in contrast to the observation of quadrature-squeezed light, which requires the use of an auxiliary light source (a local oscillator) and a heterodyne (coherent) detection process. (Useful sources of recent literature pertinent to the generation and detection of quadrature-squeezed light include articles by WALLS [1983], SHAPIRO [1985], CAVES [1986], LOUDON and KNIGHT [1987], and TEICH and SALEH [1988]). In the course of this presentation, we also review the generation of bunched and super-Poisson (classical) light from collections of independent radiators.

The discussion is readily initiated by the analogy with a gun illustrated in fig. 1.1. Photon guns naturally generate random (Poisson) streams of photons, as shown in fig. 1.1a. The production of antibunched or sub-Poisson light can be achieved in three ways: by regulating the times at which the trigger is pulled, by introducing constraints into the firing mechanism, and/or by selectively deleting some of the Poisson bullets after they are fired. Each of these techniques involves the introduction of anticorrelations, which results in a more predictable number of events. These anticorrelations are introduced by means of a feedback (or feedforward) process of one kind or another.

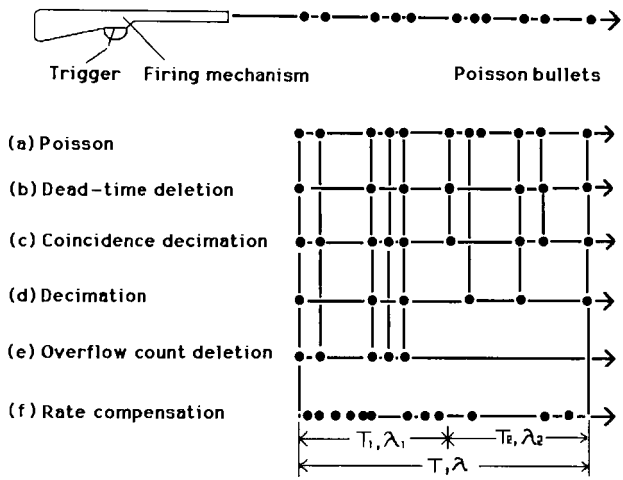


Fig. 1.1. Schematic representation of three components of a simple photon-generation system. A trigger process excites a photon emitter (firing mechanism), which in turn emits photons (Poisson bullets). Anticorrelations can be induced in any of the three elements. Mechanisms for generating antibunched and sub-Poisson light from (a) Poisson light can make use of (b) dead-time deletion, (c) coincidence decimation, (d) decimation, (e) overflow count deletion, or (f) rate compensation.

M. C. Teich and B. E. A. Saleh, "Photon Bunching and Ant bunching," in Progress in Optics, vol. 26, edited by E. Wolf (North-Holland, Amsterdam, 1988), ch. 1, pp. 1-104.

Several specific schemes for introducing such photon anticorrelations are presented in fig. 1.1. Dead-time deletion, illustrated in fig. 1.1b, prohibits photons from being arbitrarily close to each other. This effect can result from a requirement that the trigger or firing mechanism reset between consecutive shots. We will show in § 5.1 that this is, in fact, the way in which isolated atoms behave in the course of emitting resonance fluorescence photons. Under appropriate conditions, dead time can instead be imposed on the bullets after they are fired, as discussed in § 6.2. The dead-time deletion process regularizes the events, as is apparent from fig. 1.1, thereby reducing the randomness of the number of events registered in the fixed counting time $T$.

Photon anticorrelations can also be introduced by coincidence decimation, which is a process in which closely spaced pairs of photons are removed from the stream, as shown in fig. 1.1c. Optical second-harmonic generation (SHG), for example, is a nonlinear process in which two photons are exchanged for a third photon at twice the frequency (see § 6.1). Both photons must be present within the intermediate-state lifetime of the SHG process for the nonlinear photon interaction to occur. Again, the removal of closely spaced pairs of events regularizes the photon stream.

The process of decimation is defined as every $\mathcal{N}$th photon ($\mathcal{N} = 2, 3, \ldots$) of an initially Poisson photon stream being passed while deleting all intermediate photons. The passage of every other photon ($\mathcal{N} = 2$) is explicitly illustrated in fig. 1.1d. The regularization effect on the photon stream is similar to that imposed by dead-time deletion. This mechanism can be used when sequences of correlated photon pairs are emitted; one member of the pair can be detected and used to operate a gate that selectively passes every $\mathcal{N}$th companion photon (see § 6.2.1).

Overflow count deletion is another feedback mechanism that can introduce photon anticorrelations. As shown in fig. 1.1e, the number of photons is counted in a set of preselected time intervals $[0, T]$, $[T, 2T]$, ...; the first $n_0$ photons in each interval are retained and the remainder deleted. If the average number of photons in $[0, T]$ of the initial process is $\gg n_0$, then the transformed process will almost always contain $n_0$ counts per time interval (MANDEL [1976a]).

Finally, rate compensation is illustrated in fig. 1.1f. In this case the (random) number of photons is counted in a short time $T_1$; this information is fed back to control the future rate at which the trigger is pulled. If the random number measured in $T_1$ happens to be below average, the trigger is subsequently pulled at a greater rate and vice versa. More generally, each photon registration at time $t_i$ of a hypothetical Poisson photon process causes the rate $\lambda$ of the transformed

M. C. Teich and B. E. A. Saleh, "Photon Bunching and Ant bunching," in Progress in Optics, vol. 26, edited by E. Wolf (North-Holland, Amsterdam, 1988), ch. 1, pp. 1-104.

point process to be modulated by the factor $h(t - t_i)$ (which vanishes for $t < t_i$). In linear negative feedback the rate of the transformed process becomes $\mu_t = \lambda_0 - \sum_i h(t - t_i)$, where $\lambda_0$ is the rate of the Poisson process. A variety of techniques can be used to implement rate compensation, such as quantum nondemolition measurements (see § 6.2.4) or correlated photon pairs (see § 6.2.2). Dead-time deletion can be viewed as a special case of rate compensation in which the occurrence of each event sets the rate of the process equal to zero for a specified period of time after the registration (SHAPIRO, SAPLAKOGLU, HO, KUMAR, SALEH and TEICH [1987]).

In the course of this review we will find that an attractive way of producing antibunched and sub-Poisson photons is to regulate the times at which the trigger is pulled, using a control mechanism located right at the trigger (see § 7). This is most readily achieved by using an electron stream as the trigger and a collection of atoms in a solid as the firing mechanism. An electron stream exhibits natural anticorrelations in the presence of space charge. Because of their mutual Coulomb repulsion, the electrons repel each other so that the trigger can be pulled with a great deal of regularity. Indeed, the behavior of such a stream of electrons can be understood from a mathematical point of view (SRINIVASAN [1965]) in terms of rate compensation with linear negative feedback.

In § 2 we review the theory pertaining to the generation of bunched and super-Poisson light within the semiclassical theory. We elucidate the distinctions among Poisson, super-Poisson, and sub-Poisson photocounts; unbunched, bunched, and antibunched light; and chaotic, superchaotic light. The roles of wavelike and particle-like fluctuations are discussed. Particular attention is devoted to the statistical characteristics of light arising from the superposition of independent emissions where there is randomness either in the number of emissions or in the times at which the emissions are initiated. Light of this nature often arises in luminescence, scattering, and speckle experiments.

The quantum theory of light generation from superpositions of independent emissions is developed in § 3. A stationary stream of antibunched and/or sub-Poisson light can be generated if sub-Poisson statistics are obeyed by both the random times at which the emissions are initiated and the individual photon emissions themselves. For sufficiently large counting times and large detection areas, interference effects do not appear, and the photons can be shown to behave purely as classical particles. If the emissions are (deterministic) single photons, the overall photon statistics then directly mimic the statistics of the excitations. Uniquely quantum effects can therefore be observed within the domain of linear (single-photon) optics. The implementation of physical mechanisms that lead

M. C. Teich and B. E. A. Saleh, "Photon Bunching and Ant bunching," in Progress in Optics, vol. 26, edited by E. Wolf (North-Holland, Amsterdam, 1988), ch. 1, pp. 1-104.

to this kind of light is discussed in § 7. Although the theory presented in § 3 is geared principally to independent emissions, it can also be applied to certain physical processes that operate on the basis of nonindependent emissions. Several important examples considered in § 6 and § 7 fall in this category.

In § 4 we demonstrate that the loss of photons generally randomizes the statistical properties of an anticorrelated stream of photons, ultimately converting it into random (Poisson) form. Effects such as attenuation, scattering, and the presence of background photons are deleterious to sub-Poisson light.

In § 5 we discuss two nonlinear optics mechanisms (atomic resonance fluorescence and parametric downconversion) that generate small clusters of *conditionally* sub-Poisson photons. A cluster may comprise 2 or 3 photons for resonance fluorescence from an isolated atom in a typical experiment, or a single photon for parametric downconversion. This effect can only be observed by gating the detector for a prespecified time window to ensure that only a single cluster is detected. Sub-Poisson behavior is destroyed by the presence of a Poisson stream of clusters, as discussed in § 3.3.2. Thus unconditionally (cw or stationary) sub-Poisson light cannot be generated without controlling the excitations.

Photon feedback is discussed as a means of producing cw *unconditionally* sub-Poisson light in § 6. Photons generated by a particular process are fed back to control it, which may be accomplished by the use of a variety of nonlinear optics techniques. Methods using feedback intrinsic to a physical process, simply stated, remove selected clusters of photons from the incident pump beam, leaving behind an antibunched residue. External feedback can also be used. A simple example is a process in which photon pairs are produced (e.g., parametric downconversion), with one member of the pair being used to control its twin. Control mechanisms such as decimation, dead-time deletion and rate compensation, illustrated in fig. 1.1, can be used to achieve these ends.

The use of excitation feedback for generating useful antibunched and cw *unconditionally* sub-Poisson light is discussed in § 7. In this case the radiators are controlled before photon emission. Many of the limitations associated with photon-feedback methods are avoided. The technique operates by initiating single-photon emissions at antibunched and sub-Poisson times. For sufficiently long detection times and areas the emitted photons behave like classical particles; their statistics mimic those of the excitations. Perhaps the simplest example of an excitation feedback scheme is provided by the space-charge-limited Franck–Hertz experiment. The anticlustering properties of an electron stream, resulting from Coulomb repulsion, are transferred to the photons. The direction of transfer is the inverse of that encountered in the usual photo-

M. C. Teich and B. E. A. Saleh, "Photon Bunching and Ant bunching," in Progress in Optics, vol. 26, edited by E. Wolf (North-Holland, Amsterdam, 1988), ch. 1, pp. 1-104.

detection process, in which the statistical character of the photons is imparted to the photoelectrons. Any number of solid-state implementations of this concept can be envisaged. Even a simple emitter such as a LED, driven by a constant current source from a battery, will emit sub-Poisson photons. Configurations in which the feedback signal is externally carried have also been suggested. Excitation feedback appears to be the most useful scheme for producing useful antibunched and sub-Poisson light.

In § 8 we consider the use of sub-Poisson light for carrying information, such as in a direct-detection lightwave communication system. As a matter of principle, the channel capacity of such a system, when based on the observation of the photoevent *point process*, cannot be increased by the use of sub-Poisson light. On the other hand, the channel capacity of a *photon-counting* system can be increased by the use of such light. In this latter case, error performance will either be degraded or enhanced by using sub-Poisson light, depending on where the power constraint is placed. Sources of light considered for use in direct-detection lightwave communications should be strongly sub-Poisson, exhibit a large photon flux, be small in size, be fast, and produce a collimated output.

## § 2. Bunched Light from Independent Radiators

The fluctuation properties of light have traditionally been derived from a thermodynamic study of the interacting radiators, atoms and molecules, and the radiated field, treating the source as a continuum. It has been argued that when large numbers of individual radiators are treated discretely, the central limit theorem leads to chaotic behavior. When the number of radiators is small and random, however, it becomes possible to observe deviations from the results predicted by the central limit theorem, and to discern the dependence on the source-number fluctuations.

The problem of studying the interaction of light with matter is often complicated by the fact that the radiated light itself affects the radiating matter. This is the case, for example, with black-body radiation, which results from thermodynamic equilibrium between the radiation and matter in a cavity. It is also the case with laser light in which the emitted photons are fed back to interact with the atoms by the continuing processes of absorption and stimulated emission.

There are a number of problems in which the source and the ensuing radiation may be separated, however. In these cases it is possible to find an explicit relationship for the radiated field in terms of the characteristics of the source. Consider the following examples: (1) a stream of electrons or photons

M. C. Teich and B. E. A. Saleh, "Photon Bunching and Ant bunching," in Progress in Optics, vol. 26, edited by E. Wolf (North-Holland, Amsterdam, 1988), ch. 1, pp. 1-104.

impinges on a phosphorescent screen in which each electron (or photon) produces a packet of radiation in the form of a cluster of photons. The emitted radiation escapes and does not interact with the stream of incoming electrons. (2) A laser beam illuminates a dilute solution of moving particles, resulting in the emission of scattered light. In the first Born approximation an explicit linear relation between the scattered field and the fluctuating density of the medium can be established. The radiated light does not influence the density itself.

In this section we discuss the bunching properties of light generated by a collection of statistically independent radiators excited by an external source. It is assumed that the emitted photons affect neither the excitation process nor the emission process (i.e., there is no feedback from the emitted photons to the source). Our approach makes use of the semiclassical theory of light; we begin with a brief review of semiclassical coherence theory. The quantum treatment is presented in § 3.

### 2.1. SEMICLASSICAL THEORY OF OPTICAL COHERENCE

The semiclassical theory of light treats the radiation field classically while using the quantum theory to describe the interaction of the light with the atoms of the detector. This method has proved to be adequate for a great many purposes (see, for example, SARGENT, SCULLY and LAMB [1974] and MANDEL [1976b]). In the confines of this theory, light is represented by means of a random complex analytic signal $V(\boldsymbol{x})$ [where $\boldsymbol{x}$ is the space–time point $(\boldsymbol{r}, t)$], whose squared absolute value $I(\boldsymbol{x}) = |V(\boldsymbol{x})|^2$ is the optical intensity (GABOR [1946], BORN and WOLF [1980]). Light fluctuations are completely characterized by the statistics of the stochastic process $V(\boldsymbol{x})$. A hierarchy of statistical moments and probability distribution functions of $V(\boldsymbol{x})$ and $I(\boldsymbol{x})$ for different $\boldsymbol{x}$ are defined (see, for example, MANDEL and WOLF [1965], SALEH [1978] and PEŘINA [1985]). At a space–time point $\boldsymbol{x}$ the most important descriptor is the probability density $P(I)$ of the intensity $I = I(\boldsymbol{x})$, its mean $\langle I \rangle$, and its variance $\mathrm{Var}(I)$. The bracket $\langle \cdot \rangle$ denotes ensemble averaging.

Fluctuations at two space–time points $\boldsymbol{x}_1$ and $\boldsymbol{x}_2$ are characterized by the amplitude correlation function

$$G^{(1)}(\boldsymbol{x}_1, \boldsymbol{x}_2) = \langle V^*(\boldsymbol{x}_1) V(\boldsymbol{x}_2) \rangle \tag{2.1}$$

M. C. Teich and B. E. A. Saleh, "Photon Bunching and Ant bunching," in Progress in Optics, vol. 26, edited by E. Wolf (North-Holland, Amsterdam, 1988), ch. 1, pp. 1-104.

and the intensity correlation function (also called the second-order correlation function)

$$G^{(2)}(x_1, x_2) = \langle I(x_1)I(x_2)\rangle , \tag{2.2}$$

as well as their normalized versions

$$g^{(1)}(x_1, x_2) = G^{(1)}(x_1, x_2)/[\langle I(x_1)\rangle \langle I(x_2)\rangle ]^{1/2} , \tag{2.3}$$

$$g^{(2)}(x_1, x_2) = G^{(2)}(x_1, x_2)/[\langle I(x_1)\rangle \langle I(x_2)\rangle ] . \tag{2.4}$$

These quantities are also known as the degrees of first- and second-order coherence, respectively. The degrees of coherence satisfy the following inequalities

$$0 \leqslant |g^{(1)}(x_1, x_2)| \leqslant 1 , \tag{2.5}$$

$$g^{(2)}(x, x) \geqslant 1 , \tag{2.6}$$

$$g^{(2)}(x_1, x_2) \leqslant [g^{(2)}(x_1, x_1)g^{(2)}(x_2, x_2)]^{1/2} . \tag{2.7}$$

When light is detected by a photodetector such as a photomultiplier tube, the photoelectron arrivals at different locations and times are describable by a doubly stochastic Poisson point process (DSPP) (Cox [1955]), whose rate is the stochastic function $\eta I(x)$, where $\eta$ is the quantum efficiency of the detector. The probability of detecting a photoelectron within an incremental area $\Delta A$ and incremental time $\Delta T$, surrounding the point $x$, is given by

$$\eta G^{(1)}(x, x)\Delta A\Delta T = \eta\langle I(x)\rangle \Delta A\Delta T ,$$

whereas the probability of coincidence of two photoevents within incremental areas $\Delta A$ and time intervals $\Delta T$, surrounding the space–time points $x_1$ and $x_2$, is given by $\eta^2 G^{(2)}(x_1, x_2)\,(\Delta A\Delta T)^2$ (Mandel [1959a, 1963], Gagliardi and Karp [1976], Saleh [1978], Shapiro [1985]). The normalized intensity correlation function $g^{(2)}(x_1, x_2)$ therefore represents the joint probability of occurrence of one photoevent detected at $x_1$ and another at $x_2$, normalized by the product of the marginal probabilities that a photoevent occurs at $x_1$ and that a photoevent occurs at $x_2$. The quantity $g^{(2)}(x_1, x_2)$ can be thought of as a normalized photoevent coincidence rate. This approach is valid only in the absence of feedback paths from the detector to the source. In the presence of such paths, the photoelectron arrivals are described by a self-exciting point process (SEPP) (Snyder [1975]) rather than a DSPP (Shapiro, Teich, Saleh, Kumar and Saplakoglu [1986]).

The function $g^{(2)}(r, t, r, t + \tau)$ can be measured by means of a single detector placed at position $r$, where the delayed coincidence rate of photoelectron arrival

M. C. Teich and B. E. A. Saleh, "Photon Bunching and Ant bunching," in Progress in Optics, vol. 26, edited by E. Wolf (North-Holland, Amsterdam, 1988), ch. 1, pp. 1-104.

times is determined. The delay $\tau$ may also be introduced optically by splitting the light beam into two parts (using a beamsplitter) and monitoring the coincidence of photoelectrons registered by two photodetectors. The function $g^{(2)}(\boldsymbol{r}_1, t, \boldsymbol{r}_2, t+\tau)$ is determined by using two detectors, placed at $\boldsymbol{r}_1$ and $\boldsymbol{r}_2$, and measuring the delayed coincidence of photoelectrons registered by the two detectors.

The number of photoelectrons $n$ collected in a time interval $T$, by a detector placed in an area $A$, is a random number whose probability distribution is given by (MANDEL [1959a, 1963])

$$p(n) = \int_0^\infty P(W)\left[\frac{W^n e^{-W}}{n!}\right] \mathrm{d}W \,. \tag{2.8}$$

The counting distribution $p(n)$ is readily seen to be the Poisson transform of the probability density $P(W)$, where

$$W = \eta \int_{\boldsymbol{D}} I(\boldsymbol{x})\, \mathrm{d}\boldsymbol{x} \,.$$

The quantity $W$ represents the total energy collected by the detector, multiplied by the quantum efficiency $\eta$. $\boldsymbol{D}$ is the domain of integration, represented by

$$t \in [0, T] \,, \quad \boldsymbol{r} \in A \,.$$

The moments of $n$ can be easily computed from the moments of $W$ by the use of well-known relations (MANDEL [1958], SALEH [1978]); in particular,

$$\langle n \rangle = \langle W \rangle = \eta \int_{\boldsymbol{D}} G^{(1)}(\boldsymbol{x}, \boldsymbol{x})\, \mathrm{d}\boldsymbol{x} \tag{2.9}$$

and

$$\mathrm{Var}(n) = \langle n \rangle + \mathrm{Var}(W) \tag{2.10}$$

from which

$$\mathrm{Var}(n) = \langle n \rangle + \eta^2 \int_{\boldsymbol{D}} \int_{\boldsymbol{D}} \langle I(\boldsymbol{x}_1) \rangle \langle I(\boldsymbol{x}_2) \rangle \left[g^{(2)}(\boldsymbol{x}_1, \boldsymbol{x}_2) - 1\right] \mathrm{d}\boldsymbol{x}_1\, \mathrm{d}\boldsymbol{x}_2 \,. \tag{2.11}$$

If $A$ and $T$ are sufficiently small, $\langle n \rangle = \eta A T \langle I(\boldsymbol{x}) \rangle$ and

$$\mathrm{Var}(n) = \langle n \rangle + \langle n \rangle^2 [g^{(2)}(\boldsymbol{x}, \boldsymbol{x}) - 1] \,. \tag{2.12}$$

M. C. Teich and B. E. A. Saleh, "Photon Bunching and Ant bunching," in Progress in Optics, vol. 26, edited by E. Wolf (North-Holland, Amsterdam, 1988), ch. 1, pp. 1-104.

For the purpose of this presentation, the most important descriptors of the photoelectron statistics are the normalized photocoincidence rate (i.e., the degree of second-order coherence, or the normalized intensity correlation function) $g^{(2)}(x_1, x_2)$, and the photocount variance $\mathrm{Var}(n)$.

We first examine the case of coherent light, which may be regarded as a standard for comparison with other sources of light.

### 2.1.1. *Coherent light*

Coherent light is characterized by a deterministic intensity $I(x)$, and by degrees of coherence whose absolute value is unity, that is, $|g^{(1)}(x_1, x_2)| = g^{(2)}(x_1, x_2) = 1$. Photoevents occur independently, and their coincidence is totally random. Photocounts have a Poisson distribution regardless of the counting time or the detector area. The Poisson distribution is represented by

$$p(n) = \frac{\langle n \rangle^n \exp(-\langle n \rangle)}{n!}, \tag{2.13}$$

which has a variance equal to the mean, that is,

$$\mathrm{Var}(n) = \langle n \rangle . \tag{2.14}$$

The most important source of coherent light is an ideal single-mode, amplitude-stabilized laser operated well above the threshold of oscillation (see, for example, SARGENT, SCULLY and LAMB [1974]).

### 2.1.2. *Poisson, super-Poisson, and sub-Poisson photocounts*

The ratio between the variance and the mean of the photocounts $n$ is an important descriptor of the photocount statistics, and is known as the *Fano factor* (FANO [1947])

$$\mathrm{F}_n(\boldsymbol{D}) = \frac{\mathrm{Var}(n)}{\langle n \rangle} . \tag{2.15}$$

In view of eq. (2.11) the Fano factor depends on the counting area and time (represented by $\boldsymbol{D}$). The quantity $[\mathrm{F}_n(\boldsymbol{D}) - 1]$ is sometimes referred to in the literature as $Q$ (MANDEL [1979]). For coherent light $n$ is Poisson distributed and $\mathrm{F}_n(\boldsymbol{D}) = 1$, independent of $\boldsymbol{D}$. Light for which $\mathrm{F}_n(\boldsymbol{D}) > 1$ is said to exhibit super-Poisson behavior in the domain $\boldsymbol{D}$ in which this inequality is obeyed.

M. C. Teich and B. E. A. Saleh, "Photon Bunching and Ant bunching," in Progress in Optics, vol. 26, edited by E. Wolf (North-Holland, Amsterdam, 1988), ch. 1, pp. 1-104.

Such light suffers from fluctuations larger than those of the Poisson. When $F_n(D) < 1$, the photocounts are said to exhibit sub-Poisson behavior. In view of eq. (2.10) it is readily apparent that $F_n(D)$ cannot fall below unity so that sub-Poisson photocount statistics are not permitted within the framework of the semiclassical theory of light. A DSSP always exhibits Poisson or super-Poisson counts. However, sub-Poisson photocount statistics are admitted in the quantum theory of light, as will become apparent in § 3.1.

### 2.1.3. *Unbunched, bunched, and antibunched light*

As indicated earlier, the coincidence rate $g^{(2)}(x_1, x_2) = 1$ for coherent light, signifying that the joint probability of coincidence of a photoevent at $x_1$ and another at $x_2$ equals the product of the marginal probabilities of an event at each point – that is, photoevents occur independently, or in total randomness. Photoevents are then said to be *unbunched*. When $g^{(2)}(x_1, x_2) > 1$, occurrences of events at the two points are positively correlated, that is, when one occurs, the other is more likely to occur. Alternatively, when $g^{(2)}(x_1, x_2) < 1$, photoevents are anticorrelated, that is, when one occurs, the other is less likely to occur. In the limit when the two space–time points are very close to each other, that is, when $x_1 \approx x_2 = x$, the normalized coincidence rate is measured by the function $g^{(2)}(x, x)$. If $g^{(2)}(x, x) > 1$, photoevents (at this point $x$) are said to be *bunched*, that is, they have a tendency to be clustered together. Bunching of light was experimentally illustrated in a number of early experiments (TWISS and LITTLE [1959], ARECCHI, GATTI and SONA [1966], MORGAN and MANDEL [1966]).

On the other hand, if $g^{(2)}(x, x) < 1$, photoevents at this point are said to be *antibunched*, that is, they tend to be separated. Within the framework of the semiclassical theory, light cannot be antibunched. This is because $g^{(2)}(x, x)$ can never be smaller than 1, as indicated by the inequality (2.6). However, as will become apparent in § 3.1, the generation of antibunched light is possible within the quantum theory (GLAUBER [1963a,b], MOLLOW and GLAUBER [1967a,b], STOLER [1974], KIMBLE and MANDEL [1976], CARMICHAEL and WALLS [1976a,b], WALLS [1979], LOUDON [1980, 1983], PAUL [1982], PEŘINA [1985]), and this phenomenon has indeed been observed in the laboratory (KIMBLE, DAGENAIS and MANDEL [1977, 1978], DAGENAIS and MANDEL [1978], RATEIKE, LEUCHS and WALTHER as cited in CRESSER, HÄGER, LEUCHS, RATEIKE and WALTHER [1982]). As with sub-Poisson light, the observation of antibunched light provides an example of nonclassical light because it is, in fact, a manifestation of a quantum effect.

M. C. Teich and B. E. A. Saleh, "Photon Bunching and Ant bunching," in Progress in Optics, vol. 26, edited by E. Wolf (North-Holland, Amsterdam, 1988), ch. 1, pp. 1-104.

An alternative definition of bunching and antibunching is related to the behavior of the normalized coincidence rate $g^{(2)}(x, x + \Delta x)$, as a function of the separation $\Delta x$, in the vicinity of a space–time point $x$. If the normalized coincidence rate has its peak value when the two points coincide ($\Delta x = 0$) and decreases when they are separated ($\Delta x > 0$), photoevents are more likely to arrive together and the light is said to be bunched by this definition. If the coincidence rate increases as $\Delta x$ increases (positive derivative), then photoevents are more likely to be separated than to arrive together; the light is then said to be antibunched by this definition. In view of the inequality (2.7) the coincidence rate must drop as the points are separated. Therefore, by this definition as well, the semiclassical theory mandates that light cannot be antibunched.

Several simple hypothetical normalized intensity correlation functions, $g^{(2)}(\tau) = g^{(2)}(r, t; r, t + \tau)$ vs $\tau$, are illustrated in fig. 2.1. The function in fig. 2.1a corresponds to bunched light. The other three functions represent nonclassical light; figs. 2.1c and 2.1d represent antibunching according to the definition based on the property $g^{(2)}(0) < 1$, whereas figs. 2.1b and 2.1d represent antibunching according to the positive-derivative definition. In this chapter we use the property $g^{(2)}(x, x) < 1$ to define antibunching.

The super- or sub-Poisson nature of a source of light is strongly related to its bunched or antibunched characteristics (TEICH, SALEH and STOLER

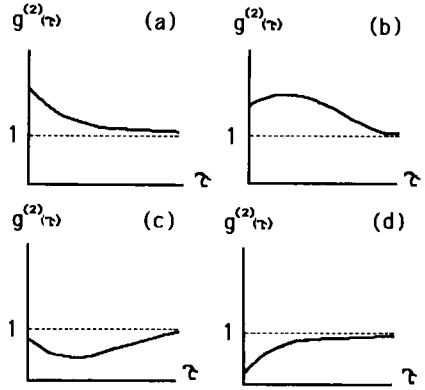


Fig. 2.1. Several hypothetical normalized intensity correlation functions $g^{(2)}(\tau)$ versus the time difference $\tau$. This quantity is also referred to as the normalized second-order degree of coherence or the normalized photoevent coincidence rate. The function in (a) corresponds to bunched light. The other three functions represent nonclassical light; (c) and (d) represent antibunched light according to the definition based on the property $g^{(2)}(0) < 1$, whereas (b) and (d) represent antibunched light according to the definition based on the positive derivative at $\tau = 0$. In this chapter we use the property $g^{(2)}(0) < 1$ to define antibunching. (After JAKEMAN [1986]).

M. C. Teich and B. E. A. Saleh, "Photon Bunching and Ant bunching," in Progress in Optics, vol. 26, edited by E. Wolf (North-Holland, Amsterdam, 1988), ch. 1, pp. 1-104.

[1983]). This is because the Fano factor $F_n(\boldsymbol{D})$ is directly related to the normalized coincidence rate $g^{(2)}(\boldsymbol{x}_1, \boldsymbol{x}_2)$ (see eqs. 2.15 and 2.11),

$$F_n(\boldsymbol{D}) - 1 = \frac{\langle n \rangle}{D^2} \int_{\boldsymbol{D}} \int_{\boldsymbol{D}} [g^{(2)}(\boldsymbol{x}_1, \boldsymbol{x}_2) - 1] \, d\boldsymbol{x}_1 \, d\boldsymbol{x}_2 , \tag{2.16}$$

where, for simplicity, we have assumed that the average intensity $\langle I(\boldsymbol{x}) \rangle$ is constant within the detection domain $\boldsymbol{D}$, and $D = AT$. Super- or sub-Poisson behavior of counts within $\boldsymbol{D}$ depends on whether the normalized coincidence rate at pairs of points within $\boldsymbol{D}$ is greater or smaller than unity. In the special case when $A$ and $T$ are sufficiently small so that the domain $\boldsymbol{D}$ can be regarded as a point, that is, $\boldsymbol{D} \to 0$, eq. (2.16) reduces to

$$[F_n(0) - 1] = \langle n \rangle \, [g^{(2)}(\boldsymbol{x}, \boldsymbol{x}) - 1] , \tag{2.17}$$

indicating that the bunching/antibunching and super/sub-Poisson attributes of the light are in one-to-one correspondence (TEICH, SALEH and STOLER [1983]).

### 2.1.4. *Chaotic light*

Another important model of light is chaotic (or thermal) light (MANDEL [1959a, 1963]). It is characterized by an analytic signal $V(\boldsymbol{x})$ that is a complex Gaussian stochastic process of circular symmetry in the complex plane. At every point $\boldsymbol{x}$, its amplitude $|V|$ has a Rayleigh distribution, whereas its intensity $I$ has an exponential distribution

$$P(I) = \langle I \rangle^{-1} \exp\left(\frac{-I}{\langle I \rangle}\right), \tag{2.18}$$

for which

$$\mathrm{Var}(I) = \langle I \rangle^2 . \tag{2.19}$$

At pairs of points $\boldsymbol{x}_1$ and $\boldsymbol{x}_2$, the normalized intensity and amplitude correlation functions are related by the Siegert relation (SIEGERT [1954])

$$g^{(2)}(\boldsymbol{x}_1, \boldsymbol{x}_2) = 1 + |g^{(1)}(\boldsymbol{x}_1, \boldsymbol{x}_2)|^2 . \tag{2.20}$$

The second term on the right-hand side of eq. (2.20) represents bunching. It is responsible for the effect first observed by HANBURY-BROWN and TWISS [1956a,b]; see HANBURY-BROWN [1974] for a review.

M. C. Teich and B. E. A. Saleh, "Photon Bunching and Ant bunching," in Progress in Optics, vol. 26, edited by E. Wolf (North-Holland, Amsterdam, 1988), ch. 1, pp. 1-104.

Photoelectrons counted in an area $A$ and time interval $T$ have a distribution that can be determined from eq. (2.8). If the time $T$ and area $A$ are sufficiently small, the integrated intensity $W$ also has an exponential distribution and its Poisson transform yields the Bose–Einstein distribution,

$$p(n) = \frac{\langle n \rangle^n}{(\langle n \rangle + 1)^{n+1}}, \tag{2.21}$$

which is characterized by the variance

$$\mathrm{Var}(n) = \langle n \rangle + \langle n \rangle^2 . \tag{2.22}$$

The first term on the right-hand side of this equation was associated by EINSTEIN [1909] with the photon (particle) nature of light, since it has a Poisson particle-like variance (see eq. 2.14). At the same time he associated the second term with the wavelike nature of light because of its exponential wavelike variance (see eq. 2.19). Equation (2.22) is known as Einstein's fluctuation formula for black-body radiation; it provided the first clear indication of wave–particle duality (WOLF [1979]).

In general, for arbitrary $A$ and $T$, the photocount variance is given by a generalized version of eq. (2.22) that is associated with the negative-binomial rather than the Bose–Einstein distribution (MANDEL [1959a]). Using eq. (2.11), and assuming that the average intensity $\langle I(\boldsymbol{x}) \rangle$ is constant within $D$, we obtain

$$\mathrm{Var}(n) = \langle n \rangle + \frac{\langle n \rangle^2}{M} . \tag{2.23}$$

The parameter $M$, which is known as the degrees-of-freedom parameter (MANDEL [1963], PEŘINA [1985], SALEH [1978], GOODMAN [1985]), is given by

$$M^{-1} = \frac{1}{D^2} \int_D \int_D |g^{(1)}(\boldsymbol{x}_1, \boldsymbol{x}_2)|^2 \, \mathrm{d}\boldsymbol{x}_1 \, \mathrm{d}\boldsymbol{x}_2 , \tag{2.24}$$

with $D = AT$. The corresponding Fano factor is

$$\mathrm{F}_n(D) = 1 + \frac{\langle n \rangle}{M} . \tag{2.25}$$

For small $A$ and $T$ it is apparent that $M = 1$ and that the photocounting distribution reverts to the Bose–Einstein distribution. Chaotic light is rendered

M. C. Teich and B. E. A. Saleh, "Photon Bunching and Ant bunching," in Progress in Optics, vol. 26, edited by E. Wolf (North-Holland, Amsterdam, 1988), ch. 1, pp. 1-104.

super-Poisson by the second term comprising the wavelike noise. For large $A$ (relative to the characteristic coherence area $A_c$) and/or large $T$ (relative to the characteristic coherence time $\tau_c$), $M$ is large so that eq. (2.23) reduces to $\mathrm{Var}(n) = \langle n \rangle$, as for the Poisson distribution. In this limit the wavelike fluctuations are averaged out, leaving only the Poisson particle-like fluctuations behind.

Light from a black-body radiator is well described by the thermal model (see, for example, MANDEL and WOLF [1965]). Black-body radiation is a result of the mutual thermal equilibrium between atoms and photons, in which emitted photons interact with atoms by absorption and stimulated emission processes. Feedback from the radiation to the atoms is an important element of the equilibrium process. It will become apparent in § 2.2, however, that independent emissions without feedback from radiation to source can also result in radiation with the same properties as thermal light.

### 2.1.5. *Chaotic, superchaotic, and subchaotic light*

In view of the importance of chaotic light, we regard it as another benchmark with which light sources can be compared. We coin the term *superchaotic* to describe light for which $g^{(2)}(x, x)$ is greater than 2. Light for which $g^{(2)}(x, x)$

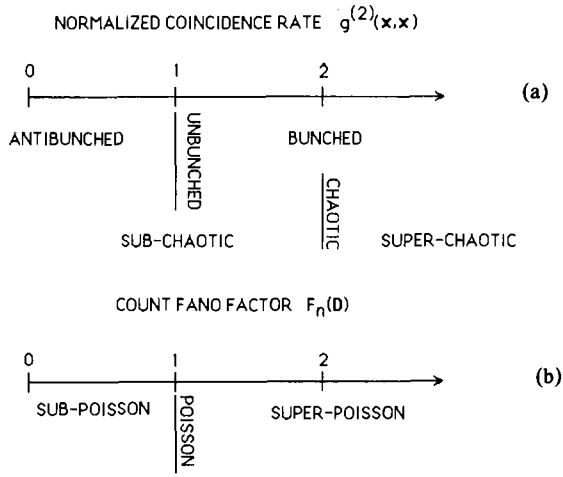


Fig. 2.2. (a) Regions and boundaries of the normalized coincidence rate $g^{(2)}(x, x)$ that define bunched/antibunched and superchaotic/subchaotic behavior for photoevents at the space–time point $x$. (b) Regions and boundaries of the Fano factor $F_n(D)$ that define Poisson, super-Poisson, and sub-Poisson behavior for photoevents counted by a detector of space–time volume $D$ (area $A$ and time interval $T$).

M. C. Teich and B. E. A. Saleh, "Photon Bunching and Ant bunching," in Progress in Optics, vol. 26, edited by E. Wolf (North-Holland, Amsterdam, 1988), ch. 1, pp. 1-104.

is smaller than 2 is referred to as *subchaotic*. For photoevents counted by a small detector ($D \to 0$), these regions correspond to $F_n(0)$ being greater or smaller than $1 + \langle n \rangle$, respectively. Superchaotic light will then obviously be super-Poisson, but subchaotic light may be either sub- or super-Poisson.

Figure 2.2 portrays a schematic illustration of the aforedefined regions and boundaries of the normalized coincidence rate $g^{(2)}(x, x)$ and the count Fano factor $F_n(D)$.

Representative examples for three different measures of the statistical properties of a light source are illustrated in fig. 2.3: the normalized intensity correlation function (normalized photoevent coincidence rate) $g^{(2)}(\tau)$ versus the time difference $\tau$, the inter-event-time probability density $P(\tau)$ versus the inter-event time $\tau$, and the photoevent counting probability distribution $p(n)$

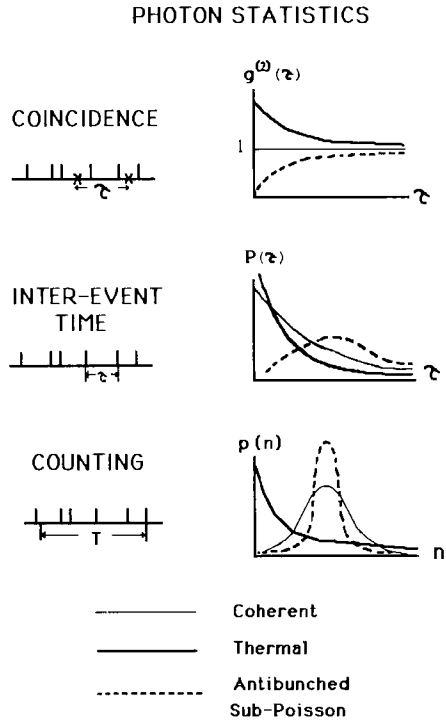


Fig. 2.3. Representative examples for three measures of the statistical properties of a light source: the normalized intensity correlation function (normalized photoevent coincidence rate) $g^{(2)}(\tau)$ versus the time difference $\tau$, the inter-event time probability density function $P(\tau)$ versus the inter-event time $\tau$, and the photon-counting probability distribution $p(n)$ versus the count number $n$. The thin solid curve, the thick solid curve, and the dotted curve correspond to coherent, thermal (chaotic), and nonclassical light, respectively.

M. C. Teich and B. E. A. Saleh, "Photon Bunching and Ant bunching," in Progress in Optics, vol. 26, edited by E. Wolf (North-Holland, Amsterdam, 1988), ch. 1, pp. 1-104.

versus the count number $n$. The thin solid curve, thick solid curve, and dotted curve correspond to coherent, thermal, and nonclassical light, respectively.

### 2.1.6. *Inter-event time statistics*

As indicated in the Introduction, there are many measures that can be used to characterize nonclassical light. One measure that has received relatively little attention in the literature is the inter-event time probability density $P(\tau)$ versus $\tau$ (SALEH [1978]), illustrated in fig. 2.3.

A measure of this distribution that is analogous to the Fano factor is the coefficient of variation $c$, which is defined as

$$c = \frac{[\mathrm{Var}(\tau)]^{1/2}}{\langle \tau \rangle}, \tag{2.26}$$

where $\mathrm{Var}(\tau)$ and $\langle \tau \rangle$ are the variance and mean of the inter-event time probability density, respectively. Coherent light, associated with the Poisson distribution, displays an exponential inter-event time probability density function, as is well known (COX [1962], PARZEN [1962]), so that $c = 1$. For chaotic light $c > 1$ (SALEH [1978]), as is $g^{(2)}(\boldsymbol{x}, \boldsymbol{x})$ and $\mathrm{F}_n(\boldsymbol{D})$. The distribution $P(\tau)$ in this case is said to be overdispersed relative to the exponential (for which $c = 1$). Within the framework of the semiclassical theory, light cannot be underdispersed relative to the exponential (i.e., it cannot exhibit $c < 1$). It will become apparent in § 3, however, that underdispersed light is possible within the quantum theory.

## 2.2. SUPERPOSITION OF INDEPENDENT EMISSIONS

Many common sources of radiation comprise a number of radiators that radiate independently. Consider $N$ such radiators (as illustrated schematically

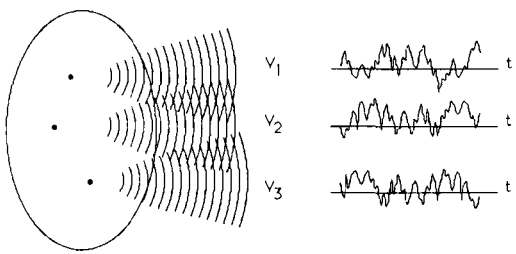


Fig. 2.4. Schematic representation of the amplitudes of a number of statistically independent stationary emissions.

in fig. 2.4). This model of light is suitable for a great variety of situations, including radiation from independent luminescent or incandescent points of a large source, as well as light from independent scatterers such as encountered in speckle (JAKEMAN [1980a]).

The complex analytic signal of the total radiation can then be expressed as the sum of $N$ statistically independent contributions, viz.,

$$V(x) = \sum_{k=1}^{N} V_k(x) . \tag{2.27}$$

It will be useful to relate the statistics of the total radiation $V(x)$ to the statistics of the individual emissions $\{V_k(x)\}$. We first consider the case in which $N$ is deterministic, we then extend the results to permit $N$ to be random in the following section.

Confining our attention to one space–time point $x = (r, t)$, we write eq. (2.27) in the form

$$V = \sum_{k=1}^{N} V_k , \tag{2.28}$$

where $V = V(x)$ and $V_k = V_k(x)$. For simplicity we assume that the complex random variables $V_k$ have circular symmetry in the complex plane. (This applies when the real and imaginary parts of each of the random variables $V_k$ are independent and identically distributed, or when the phase is uniformly distributed.) It follows that the mean values, as well as all odd-order moments, of $V_k$ are zero. It also follows that the sum $V(x)$ is circularly symmetrical.

The determination of the statistics of the sum $V$ of a set of statistically independent phasors $V_k$, whose phases are uniformly distributed, is the same as the well-known random walk problem. Its solution dates back to Lord Rayleigh. More recent work (in the context of light scattering) includes contributions by TROUP [1965], MITCHELL [1968], CHEN and TARTAGLIA [1972], SCHAEFER and PUSEY [1972], PUSEY, SCHAEFER and KOPPEL [1974], BARAKAT [1974, 1976], BARAKAT and BLAKE [1976], SCHAEFER [1975], JAKEMAN and PUSEY [1976], and O'DONNELL [1982].

The moments of $V$ may be related to those of $V_k$ by the straightforward (but rather lengthy) use of eq. (2.28) in the definition of the moments, exploiting the property of statistical independence and the fact that the odd moments vanish. The simplest moments of $I = |V|^2$ are

$$\langle I \rangle = \sum_{k=1}^{N} \langle I_k \rangle , \tag{2.29}$$

M. C. Teich and B. E. A. Saleh, "Photon Bunching and Ant bunching," in Progress in Optics, vol. 26, edited by E. Wolf (North-Holland, Amsterdam, 1988), ch. 1, pp. 1-104.

$$\mathrm{Var}(I) = \langle I \rangle^2 [1 + \gamma], \tag{2.30}$$

where

$$I_k = |V_k|^2,$$

$$\gamma = \sum_k r_k^2 \gamma_k, \tag{2.31}$$

$$r_k = \frac{\langle I_k \rangle}{\langle I \rangle}, \tag{2.32}$$

$$\gamma_k = \frac{[\mathrm{Var}(I_k) - \langle I_k \rangle^2]}{\langle I_k \rangle^2}. \tag{2.33}$$

The parameters $\gamma_k$ and $\gamma$ represent deviations from chaotic behavior for the $k$th emission and for the total field, respectively (see eq. 2.19). The symbol $\gamma$ (with different modifiers) will be used to denote deviations from chaotic properties throughout this chapter.

We now move on to two space–time points $x_1, x_2$. The correlation functions of the total field may be related to the correlation functions of the individual emissions by the following relations, which can be obtained by systematic algebraic manipulations using the assumptions of circular symmetry and statistical independence of the different emissions:

$$g^{(1)}(x_1, x_2) = \sum_k [r_k(x_1)\, r_k(x_2)]^{1/2} g_k^{(1)}(x_1, x_2), \tag{2.34}$$

$$g^{(2)}(x_1, x_2) = 1 + |g^{(1)}(x_1, x_2)|^2 + \gamma(x_1, x_2), \tag{2.35}$$

where

$$\gamma(x_1, x_2) = \sum_k r_k(x_1)\, r_k(x_2)\, \gamma_k(x_1, x_2), \tag{2.36}$$

$$\gamma_k(x_1, x_2) = g_k^{(2)}(x_1, x_2) - 1 - |g_k^{(1)}(x_1, x_2)|^2, \tag{2.37}$$

and

$$r_k(x) = \frac{\langle I_k(x) \rangle}{\langle I(x) \rangle}. \tag{2.38}$$

Here $g_k^{(1)}(x_1, x_2)$ and $g_k^{(2)}(x_1, x_2)$ are the degrees of first-order coherence and degrees of second-order coherence for the $k$th emission, respectively. The functions $\gamma(x_1, x_2)$ and $\gamma_k(x_1, x_2)$ represent deviations from chaotic behavior of the superposed light and of the $k$th emission, respectively (see eq. 2.20). These functions may attain positive or negative values.

M. C. Teich and B. E. A. Saleh, "Photon Bunching and Ant bunching," in Progress in Optics, vol. 26, edited by E. Wolf (North-Holland, Amsterdam, 1988), ch. 1, pp. 1-104.

Although it is difficult to obtain expressions for the photocount probability distribution for a detector of arbitrary area and arbitrary counting time, an expression for the photocount variance can be easily obtained by use of eq. (2.11). The corresponding Fano factor turns out to be

$$\mathrm{F}_n(\boldsymbol{D}) = 1 + \frac{\langle n \rangle}{M} + \langle n \rangle \bar{\gamma}\,, \tag{2.39}$$

where $1/M$ is given by eq. (2.24), and $\bar{\gamma}$ is determined from a similar expression:

$$\bar{\gamma} = \frac{1}{D^2} \int_{\boldsymbol{D}} \int_{\boldsymbol{D}} \gamma(\boldsymbol{x}_1, \boldsymbol{x}_2)\, \mathrm{d}\boldsymbol{x}_1\, \mathrm{d}\boldsymbol{x}_2\,. \tag{2.40}$$

The term $\langle n \rangle \bar{\gamma}$ represents the excess nonchaotic contribution to the Fano factor. For small $T$ and $A$ (i.e., $D \to 0$), $\bar{\gamma} = \gamma = \gamma(\boldsymbol{x}, \boldsymbol{x})$. Since $M = 1$ we then have

$$\mathrm{F}_n(0) = 1 + \langle n \rangle + \langle n \rangle \gamma\,. \tag{2.41}$$

### 2.2.1. *Chaotic emissions*

If the individual emissions are chaotic, it is evident from eqs. (2.31), (2.33), (2.36) and (2.37) that $\gamma_k(\boldsymbol{x}_1, \boldsymbol{x}_2)$, $\gamma(\boldsymbol{x}_1, \boldsymbol{x}_2)$, and $\gamma$ vanish; furthermore

$$\mathrm{Var}(I) = \langle I \rangle^2\,, \qquad g^{(2)}(\boldsymbol{x}_1, \boldsymbol{x}_2) = 1 + |g^{(1)}(\boldsymbol{x}_1, \boldsymbol{x}_2)|^2\,,$$

$$\mathrm{F}_n(\boldsymbol{D}) = 1 + \frac{\langle n \rangle}{M}\,,$$

indicating that the resultant total field itself becomes chaotic. This is not surprising. When the individual emissions are Gaussian (i.e., $V_k$ are Gaussian), the sum $V$ is also Gaussian (because the sum of Gaussian random variables is Gaussian).

### 2.2.2. *Statistically identical emissions*

Assume now that the emissions are statistically identical and stationary. An individual emission is described by the mean and variance of its intensity, $\langle I_0 \rangle$ and $\mathrm{Var}(I_0)$, and its correlation functions $g_0^{(1)}(\boldsymbol{x}_1, \boldsymbol{x}_2)$ and $g_0^{(2)}(\boldsymbol{x}_1, \boldsymbol{x}_2)$, where the subscript 0 denotes an individual emission. The deviation from chaotic

M. C. Teich and B. E. A. Saleh, "Photon Bunching and Ant bunching," in Progress in Optics, vol. 26, edited by E. Wolf (North-Holland, Amsterdam, 1988), ch. 1, pp. 1-104.

behavior is then described by the parameters

$$\gamma_0 = \frac{[\mathrm{Var}(I_0) - \langle I_0 \rangle^2]}{\langle I_0 \rangle^2}, \tag{2.42}$$

$$\gamma_0(\boldsymbol{x}_1, \boldsymbol{x}_2) = g_0^{(2)}(\boldsymbol{x}_1, \boldsymbol{x}_2) - 1 - |g_0^{(1)}(\boldsymbol{x}_1, \boldsymbol{x}_2)|^2, \tag{2.43}$$

$$\bar{\gamma}_0 = \frac{1}{D^2} \int_{\boldsymbol{D}} \int_{\boldsymbol{D}} \gamma_0(\boldsymbol{x}_1, \boldsymbol{x}_2)\, \mathrm{d}\boldsymbol{x}_1\, \mathrm{d}\boldsymbol{x}_2 . \tag{2.44}$$

If $\alpha$ denotes the number of photocounts associated with an individual emission in a region $\boldsymbol{D}$, its mean is

$$\langle \alpha \rangle = \eta T A \langle I_0 \rangle , \tag{2.45}$$

whereas its Fano factor is

$$\mathrm{F}_\alpha(\boldsymbol{D}) = 1 + \frac{\langle \alpha \rangle}{M} + \langle \alpha \rangle \bar{\gamma}_0 , \tag{2.46}$$

where

$$M^{-1} = \frac{1}{D^2} \int_{\boldsymbol{D}} \int_{\boldsymbol{D}} |g_0^{(1)}(\boldsymbol{x}_1, \boldsymbol{x}_2)|^2\, \mathrm{d}\boldsymbol{x}_1\, \mathrm{d}\boldsymbol{x}_2 . \tag{2.47}$$

The corresponding parameters for the superposed radiation are obtained from eqs. (2.29)–(2.33):

$$\langle I \rangle = N \langle I_0 \rangle ,$$

$$\mathrm{Var}(I) = \langle I \rangle^2 \left[ 1 + \frac{\gamma_0}{N} \right], \tag{2.48}$$

$$g^{(1)}(\boldsymbol{x}_1, \boldsymbol{x}_2) = g_0^{(1)}(\boldsymbol{x}_1, \boldsymbol{x}_2), \tag{2.49}$$

$$g^{(2)}(\boldsymbol{x}_1, \boldsymbol{x}_2) = 1 + |g^{(1)}(\boldsymbol{x}_1, \boldsymbol{x}_2)|^2 + \frac{1}{N} \gamma_0(\boldsymbol{x}_1, \boldsymbol{x}_2), \tag{2.50}$$

$$\mathrm{F}_n(\boldsymbol{D}) = 1 + \frac{\langle n \rangle}{M} + \frac{\langle n \rangle \bar{\gamma}_0}{N} . \tag{2.51}$$

M. C. Teich and B. E. A. Saleh, "Photon Bunching and Ant bunching," in Progress in Optics, vol. 26, edited by E. Wolf (North-Holland, Amsterdam, 1988), ch. 1, pp. 1-104.

A comparison of these properties with those of chaotic light leads us to observe that the deviation from chaotic behavior is inversely proportional to the number $N$ of superposed emissions. As $N \to \infty$, the superposed light tends toward chaotic behavior whatever the statistics of the original emissions. This too, in fact, is expected as a result of the central limit theorem (MIDDLETON [1967a,b]). A theory of chaotic radiation has been constructed in terms of superpositions of discrete independent radiators (BERAN and PARRENT [1964], KARP, GAGLIARDI and REED [1968], LOUDON [1983]). Light emitted by a collision-broadened source has been modeled as a wave broken into discrete sections, each with fixed phase. The phase is assumed to change randomly when a collision occurs, and the intercollision times are taken to be random (exponentially distributed). In the limit of a large number of collisions, the result has been shown to approach chaotic behavior (LOUDON [1983]).

The terms $(1/N)\gamma_0(x_1, x_2)$ and $(1/N)\bar{\gamma}_0\langle n\rangle$ represent an excess bunching and an excess Fano factor above and beyond the chaotic values. These terms may also be negative, resulting in a reduction of bunching below the chaotic level, as will become apparent in the examples below. Deviations from chaotic behavior can be observed when $N$ is not large (FORRESTER [1972], KARP [1975], TEICH and SALEH [1981a], SALEH and TEICH [1982], SALEH, STOLER and TEICH [1983]).

Equation (2.51) can also be written in terms of the Fano factor of the photoevents for an independent emission,

$$\mathrm{F}_n(D) - 1 - \frac{\langle n\rangle}{M} = \mathrm{F}_\alpha(D) - 1 - \frac{\langle \alpha\rangle}{M}, \tag{2.52}$$

indicating that *the excess Fano factor* (above chaotic behavior) *for the total radiation is equal to that for a single emission.* When the degrees-of-freedom parameter $M$ is sufficiently large, as is the case for a large detector area $A$ and/or a large counting time $T$, so that the wave interference terms $\langle n\rangle/M$ and $\langle \alpha\rangle/M$ are negligible, we obtain

$$\mathrm{F}_n(D) \approx \mathrm{F}_\alpha(D), \tag{2.53}$$

that is, *the Fano factor for the total photocount is approximately equal to the Fano factor for the single emission count.* This result is obtained by simply treating photoevents as particles, arguing that the total number of photoevents is simply the sum of $N$ independent numbers $\alpha_1, \alpha_2, \ldots, \alpha_N$ of photons associated with the $N$ emissions, each of mean $\langle \alpha\rangle$ and Fano factor $\mathrm{F}_\alpha(D)$.

M. C. Teich and B. E. A. Saleh, "Photon Bunching and Ant bunching," in Progress in Optics, vol. 26, edited by E. Wolf (North-Holland, Amsterdam, 1988), ch. 1, pp. 1-104.

The way in which the probability distributions $P(I)$ and $p(n)$ approach the distributions associated with chaotic light, as $N$ increases, has been studied by a number of authors (for a review see BARAKAT and BLAKE [1980]).

*Example: Identical emissions of deterministic intensity.* When the individual emissions have deterministic intensities, we have

$$|g_0^{(1)}(x_1, x_2)| = g_0^{(2)}(x_1, x_2) = 1\,,$$

$$\gamma_0(x_1, x_2) = -1\,, \qquad \gamma_0 = \bar{\gamma}_0 = -1\,,$$

$$M = 1\,, \qquad \mathrm{F}_\alpha(D) = 1\,.$$

The total radiation exhibits the following properties:

$$\mathrm{Var}(I) = \langle I \rangle^2 \left(1 - \frac{1}{N}\right), \tag{2.54}$$

$$g^{(2)}(x_1, x_2) = 2 - \frac{1}{N}, \tag{2.55}$$

$$\mathrm{F}_n(D) = 1 + \langle n \rangle \left(1 - \frac{1}{N}\right). \tag{2.56}$$

It is evident that the superposed light is subchaotic. For $N > 1$, $g^{(2)}(x_1, x_2) > 1$ and $\mathrm{F}_n(D) > 1$, indicating that the superposed light remains bunched and super-Poisson (as expected for semiclassically described light). Again, eqs. (2.19) and (2.20) are reproduced in the limit of large $N$, and chaotic behavior results.

## 2.3. NUMBER FLUCTUATIONS

When the number of emissions is itself random, the statistical averages considered in § 2.2 should be regarded as conditioned on a fixed value of $N$. A subsequent average over the fluctuations of $N$ is then required to yield the overall averages. This problem has been studied by a number of authors using different distributions of $N$. The model is applicable to radiation emitted from an ensemble of atoms that are excited at random (FORRESTER [1972], KARP, GAGLIARDI and REED [1968], KARP [1975]) and to light scattering from a random number of scatterers (JAKEMAN [1980a]).

M. C. Teich and B. E. A. Saleh, "Photon Bunching and Ant bunching," in Progress in Optics, vol. 26, edited by E. Wolf (North-Holland, Amsterdam, 1988), ch. 1, pp. 1-104.

2.3.1. *Poisson number fluctuations*

We assume that the number of statistically identical emissions is Poisson distributed with mean $\langle N \rangle$,

$$P(N) = \frac{\langle N \rangle^N \exp(-\langle N \rangle)}{N!}. \tag{2.57}$$

This problem has been studied by BARAKAT and BLAKE [1976], PUSEY, SCHAEFER and KOPPEL [1974], SCHAEFER and PUSEY [1972], and SCHAEFER [1975]. Averaging the statistical moments derived in § 2.2.2 over the fluctuations of $N$ gives rise to

$$g^{(2)}(x_1, x_2) = 1 + |g^{(1)}(x_1, x_2)|^2 + \frac{1}{\langle N \rangle} g_0^{(2)}(x_1, x_2), \tag{2.58}$$

$$\mathrm{F}_n(D) = 1 + \frac{\langle n \rangle}{M} + \frac{\langle n \rangle \Gamma_0}{\langle N \rangle}, \tag{2.59}$$

where

$$\Gamma_0 = \frac{1}{D^2} \int_D \int_D g_0^{(2)}(x_1, x_2)\, \mathrm{d}x_1\, \mathrm{d}x_2. \tag{2.60}$$

Equation (2.59) can also be written in the form

$$\mathrm{F}_n(D) = 1 + \frac{\langle n \rangle}{M} + [\mathrm{F}_\alpha(D) - 1 + \langle \alpha \rangle]. \tag{2.61}$$

The excess coincidence rate above that for chaotic light [the third term of eq. (2.58)] is proportional to the normalized coincidence rate for a single emission, which is always nonnegative. The light is therefore superchaotic. This is to be compared with the deterministic-$N$ case, for which the excess coincidence rate is proportional to the excess coincidence rate of an individual emission (eq. 2.50), a term that may be positive or negative. *When the number of emitters N is Poisson distributed, the light is superchaotic; when N is deterministic, the light is merely bunched.*

We now compare the Poisson-$N$ photocount Fano factor, given in eqs. (2.59)–(2.61), with the deterministic-$N$ Fano factor, given in eqs. (2.51) and (2.52). The positive sign in the right-most term in eq. (2.61) reflects an increased

M. C. Teich and B. E. A. Saleh, "Photon Bunching and Ant bunching," in Progress in Optics, vol. 26, edited by E. Wolf (North-Holland, Amsterdam, 1988), ch. 1, pp. 1-104.

Fano factor resulting from randomness in the number of emissions. This distinction is important inasmuch as $N$ is random for most natural sources of light.

*Example*: *Identical emissions of deterministic intensity.* When the individual emissions have deterministic intensities, as in the example considered in § 2.2.2., we have

$$g^{(2)}(\boldsymbol{x}_1, \boldsymbol{x}_2) = 2 + \frac{1}{\langle N \rangle}, \tag{2.62}$$

$$\Gamma_n(\boldsymbol{D}) = 1 + \langle n \rangle \left(1 + \frac{1}{\langle N \rangle}\right). \tag{2.63}$$

These results should be compared with those presented in eqs. (2.55) and (2.56). The light is obviously superchaotic and the photocounts are super-Poisson.

As the mean number of emissions $\langle N \rangle \to \infty$, eqs. (2.62) and (2.63) approach their chaotic limits. It is of interest to note that this asymptotic limit, which applies when $N$ is Poisson, does not necessarily apply for numbers of emissions governed by other distributions. The case where $N$ is distributed in accordance with the negative-binomial (rather than the Poisson) distribution, for example, has been considered in some detail (JAKEMAN and PUSEY [1978]). If the intensity of the individual emissions is assumed to fall off in proportion to $1/\langle N \rangle$, then in the limit $\langle N \rangle \to \infty$ the amplitude of the total field is governed by a distribution proportional to a modified Bessel function of the second kind (the so-called $K$-distribution), rather than by the Rayleigh distribution as for chaotic light, regardless of the distribution of the individual emissions (JAKEMAN and PUSEY [1976, 1978], JAKEMAN [1980a,b]). This model has been applied to the study of non-Rayleigh scattering from diffusers by many authors (e.g., HOENDERS, JAKEMAN, BALTES and STEINLE [1979], EBELING [1980], JAKEMAN [1982, 1983], JAKEMAN and HOENDERS [1982], O'DONNELL [1982], OLIVER [1984]). The $K$-distribution has also been applied to the study of laser light propagating through the atmosphere (PARRY and PUSEY [1979], ANDREWS and PHILLIPS [1986]).

### 2.4. EMISSIONS INITIATED AT POISSON TIMES

The independent-radiator model considered in § 2.2 and § 2.3 was formulated under the assumption that the number of radiators is a random variable

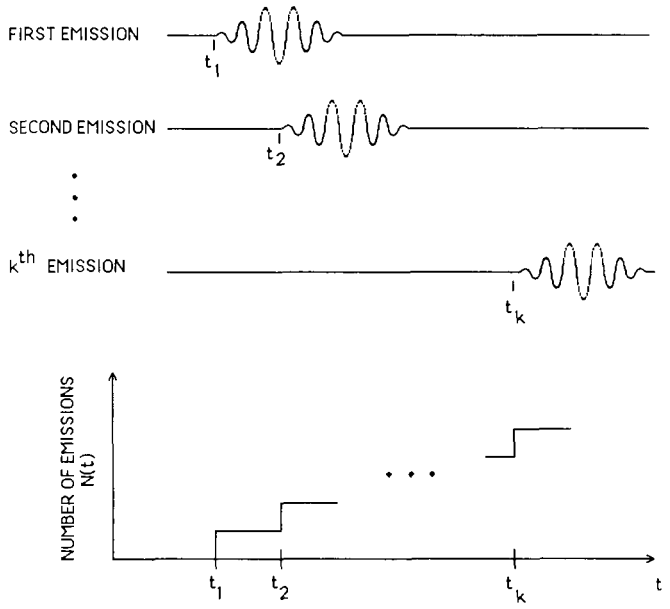


Fig. 2.5. Schematic representation of the amplitudes $\{V_k(t)\}$ of a sequence of short-duration emissions initiated at times $\{t_1, t_2, \ldots, t_k, \ldots\}$ described by a Poisson point process. The function $N(t)$ is a stochastic counting process representing the number of radiators that have begun to radiate prior to time $t$.

$N$ ($N$ deterministic is a special case). This model is not applicable when the number of active radiators is a random process, that is, a stochastic function of time $N(t)$. We now proceed to this situation.

Consider radiation formed by a sequence of short-duration emissions initiated at the times $\{t_1, t_2, \ldots, t_k, \ldots\}$. Let $N(t)$ represent the number of radiators that begin to radiate prior to time $t$, as illustrated in fig. 2.5. The function $N(t)$ represents a stochastic counting process with jumps at the times $\{t_1, t_2, \ldots, t_k, \ldots\}$, where $t_k$ is the time at which the $k$th emission is initiated. We limit ourselves to the case for which $N(t)$ is a homogeneous Poisson counting process of rate $\mu$ (events per second). We further assume that the emissions are random, statistically independent, and identically distributed (except for the fact that they begin at different times).

The complex analytic signal of the total field can be written as the sum

$$V(\boldsymbol{r}, t) = \sum_{k=-\infty}^{N(t)} V_k(\boldsymbol{r}, t - t_k), \tag{2.64}$$

where $V_k(\boldsymbol{r}, t - t_k)$ represents the $k$th emission. Each individual emission is assumed to have known mean intensity $\langle I_0(\boldsymbol{r}, t)\rangle$, amplitude correlation function $G_0^{(1)}(\boldsymbol{r}_1, t_1, \boldsymbol{r}_2, t_2)$, and intensity correlation function $G_0^{(2)}(\boldsymbol{r}_1, t_1, \boldsymbol{r}_2, t_2)$. We wish to determine the statistics of the overall radiation, particularly the correlation functions $G^{(1)}(\boldsymbol{r}_1, \boldsymbol{r}_2, \tau)$ and $G^{(2)}(\boldsymbol{r}_1, \boldsymbol{r}_2, \tau)$. It is important to note that although the individual emissions are nonstationary, the overall field is stationary because of the stationarity of the underlying emission-time point process. This is why the correlation functions of the total field are written as functions of $\tau = t_2 - t_1$, rather than functions of $t_1$ and $t_2$ separately.

The function $V(\boldsymbol{r}, t)$ can be regarded as a filtered marked stationary Poisson process (SNYDER [1975]). Using the properties of shot-noise processes (RICE [1944], GILBERT and POLLAK [1960], PAPOULIS [1984]), the total radiation can be shown to have the following statistical properties (SALEH, STOLER and TEICH [1983]):

$$\langle I(\boldsymbol{r}, t)\rangle = \mu \int_0^\infty \langle I_0(\boldsymbol{r}, t)\rangle \, \mathrm{d}t, \tag{2.65}$$

$$G^{(1)}(\boldsymbol{r}_1, \boldsymbol{r}_2, \tau) = \mu \int_0^\infty G_0^{(1)}(\boldsymbol{r}_1, t, \boldsymbol{r}_2, t + \tau) \, \mathrm{d}t, \tag{2.66}$$

$$g^{(2)}(\boldsymbol{r}_1, \boldsymbol{r}_2, \tau) = 1 + |g^{(1)}(\boldsymbol{r}_1, \boldsymbol{r}_2, \tau)|^2 + \gamma(\boldsymbol{r}_1, \boldsymbol{r}_2, \tau), \tag{2.67}$$

where the excess normalized coincidence rate

$$\gamma(\boldsymbol{r}_1, \boldsymbol{r}_2, \tau) = \frac{\mu \int_0^\infty G_0^{(2)}(\boldsymbol{r}_1, t, \boldsymbol{r}_2, t + \tau) \, \mathrm{d}t}{\langle I(\boldsymbol{r}_1, t)\rangle \, \langle I(\boldsymbol{r}_2, t)\rangle} \tag{2.68}$$

is now given by an average over the normalized coincidence rate of an individual emission. The photoevents have a normalized coincidence rate given by eq. (2.67) and a photocount Fano factor, determined by the use of eqs. (2.11) and (2.15), which is

$$\mathrm{F}_n(D) = 1 + \frac{\langle n\rangle}{M} + \langle n\rangle \bar{\gamma}, \tag{2.69}$$

where $\bar{\gamma}$ is the average of $\gamma(\boldsymbol{r}_1, \boldsymbol{r}_2, \tau)$ as given by eq. (2.40). The result is similar to that obtained for the addition of a Poisson number of identical emissions (see § 2.3.1).

M. C. Teich and B. E. A. Saleh, "Photon Bunching and Ant bunching," in Progress in Optics, vol. 26, edited by E. Wolf (North-Holland, Amsterdam, 1988), ch. 1, pp. 1-104.

### 2.4.1. *Quasi-coherent emissions*

As a particular example, we assume that each emission is represented as a pulse of deterministic field with random phase. For simplicity the spatial dependence is ignored by limiting our interest to a single point $r$. The individual emissions may then be expressed in the form

$$V_k(t - t_k) = V_0(t) \exp(i\theta_k) . \tag{2.70}$$

The phases $\theta_k$ are drawn from a uniform distribution. This is the model used by SALEH, STOLER and TEICH [1983, Sec. IIA]. The results are

$$\langle I(t) \rangle = \mu \int_0^\infty I_0(t) \mathrm{d}t , \tag{2.71}$$

$$G^{(1)}(\tau) = \mu \int_0^\infty V_0^*(t)\, V_0(t + \tau)\, \mathrm{d}t , \tag{2.72}$$

$$g^{(2)}(\tau) = 1 + |g^{(1)}(\tau)|^2 + \frac{1}{\mu \tau_p} \bar{g}_0^{(2)}(\tau) , \tag{2.73}$$

where

$$\tau_p = \frac{\left[\int_{-\infty}^{\infty} I_0(t)\, \mathrm{d}t\right]^2}{\int_{-\infty}^{\infty} I_0^2(t)\, \mathrm{d}t} . \tag{2.74}$$

The quantity $\tau_p$ is the characteristic decay time of the intensity of an individual emission, $I_0(t) = |V_0(t)|^2$. The quantity

$$\bar{g}_0^{(2)}(\tau) = \frac{\bar{I}_0(\tau)}{\bar{I}_0(0)} \tag{2.75}$$

depends on the normalized time-averaged autocorrelation function of the intensity of an individual emission

$$\bar{I}_0(\tau) = \int_0^\infty I_0(t)\, I_0(t + \tau)\, \mathrm{d}t . \tag{2.76}$$

M. C. Teich and B. E. A. Saleh, "Photon Bunching and Ant bunching," in Progress in Optics, vol. 26, edited by E. Wolf (North-Holland, Amsterdam, 1988), ch. 1, pp. 1-104.

Comparing eqs. (2.73) and (2.58) leads us to see that the parameter $\mu\tau_p$ can be associated with the average number of independent emissions overlapping at a given time, that is, $\langle N \rangle = \mu\tau_p$. This interpretation is sensible in view of the strong underlying similarity between the two models, although in the case considered here the contributions are not strictly identical because the emissions are initiated at different times.

The radiation emanating from such a process is superchaotic (as is the radiation modeled in § 2.3). In addition to the usual chaotic fluctuations manifested by the first two terms on the right-hand side of eq. (2.73), the third term represents excess bunching. It is directly proportional to $\bar{g}_0^{(2)}(\tau)$ and inversely proportional to $\mu\tau_p$, the average number of emissions per emission lifetime. The third term therefore becomes significant when $\mu\tau_p \ll 1$, that is, when the emissions are sparse and seldom overlap. This result is similar to that obtained by LOUDON [1980]. On the other hand, when $\mu\tau_p \gg 1$, that is, when the emissions overlap strongly, $V(t)$ approaches the complex Gaussian process that is characteristic of a chaotic field (PICINBONO, BENDJABALLAH and POUGET [1970]); in this case the third term becomes negligible and the results for chaotic light apply (CARMICHAEL and WALLS [1976a,b]).

We now examine the photocounting properties of such light, assuming a point detector with counting time $T$, quantum efficiency $\eta$, and incremental area $\Delta A$ (which is here taken to be unity for convenience). The mean photon count is

$$\langle n \rangle = \mu \langle \alpha \rangle T, \tag{2.77}$$

where

$$\langle \alpha \rangle = \eta \int_0^\infty I_0(t)\, dt \tag{2.78}$$

can be interpreted as the average number of photocounts per emission, and $\mu T$ is the average number of emissions initiated within $T$. The Fano factor, which depends on the counting time $T$, can be written in the form

$$F_n(T) = 1 + \frac{\langle n \rangle}{M} + \frac{\langle n \rangle \Gamma_0}{\mu\tau_p}, \tag{2.79}$$

where

$$\Gamma_0 = \frac{2}{T} \int_0^T \left(1 - \frac{\tau}{T}\right) \bar{g}_0^{(2)}(\tau)\, d\tau. \tag{2.80}$$

M. C. Teich and B. E. A. Saleh, "Photon Bunching and Ant bunching," in Progress in Optics, vol. 26, edited by E. Wolf (North-Holland, Amsterdam, 1988), ch. 1, pp. 1-104.

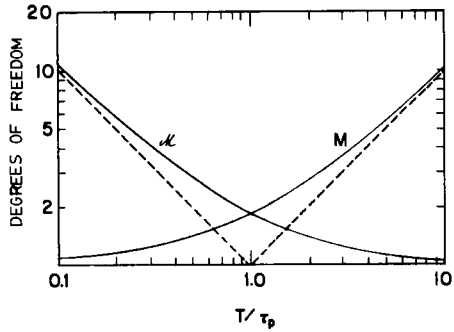


Fig. 2.6. Dependence of the degrees-of-freedom parameters $M$ and $\mathscr{M}$ on the ratio $T/\tau_p$ for exponentially decaying coherent emissions. $M$ is the usual degrees-of-freedom parameter for chaotic light, whereas $\mathscr{M}$ is the special degrees-of-freedom parameter for shot-noise light. The dependences of $M$ and $\mathscr{M}$ on the ratio $T/\tau_p$ are almost symmetrically opposite. The dashed lines represent unity slope. (After SALEH, STOLER and TEICH [1983].)

It is also convenient to write it in the form

$$\mathrm{F}_n(T) = 1 + \frac{\langle n \rangle}{M} + \frac{\langle \alpha \rangle}{\mathscr{M}}, \tag{2.81}$$

where $\mathscr{M}^{-1} = \Gamma_0 T/\tau_p$, from which

$$\mathscr{M}^{-1} = \frac{2}{\tau_p} \int_0^T \left(1 - \frac{\tau}{T}\right) \frac{\bar{I}_0(\tau)}{\bar{I}_0(0)} \, \mathrm{d}\tau. \tag{2.82}$$

It is now apparent that the third term on the right-hand side of the expression for the Fano factor in eq. (2.81) is independent of the mean count $\langle n \rangle$. It is therefore of the same nature as the first term; both represent particle-like noise as opposed to the wavelike noise represent by the second term. Further evidence of this is centered on the degrees-of-freedom parameters.

The parameter $M$ in eq. (2.81) is the usual degrees-of-freedom parameter for chaotic light with amplitude correlation function $g^{(1)}(\tau)$, whereas the parameter $\mathscr{M}$ in this equation is a special degrees-of-freedom parameter that has been recently introduced to describe light whose intensity fluctuates in accordance with a shot-noise random process (TEICH and SALEH [1981a], SALEH and TEICH [1982], SALEH, STOLER and TEICH [1983]). These parameters are displayed in fig. 2.6 for exponentially decaying coherent emissions. The dependences of $M$ and $\mathscr{M}$ on the ratio $T/\tau_p$ are almost symmetrically opposite. When $T \ll \tau_p$, $M \approx 1$ while $\mathscr{M} \approx \tau_p/T \gg 1$. As $T/\tau_p$ increases, $M$ increases while $\mathscr{M}$ decreases. In the limit $T \gg \tau_p$, $M \approx T/\tau_p \gg 1$ and $\mathscr{M} \approx 1$.

M. C. Teich and B. E. A. Saleh, "Photon Bunching and Ant bunching," in Progress in Optics, vol. 26, edited by E. Wolf (North-Holland, Amsterdam, 1988), ch. 1, pp. 1-104.

The value of the ratio $T/\tau_p$ affects the Fano factor dramatically. For $T \ll \tau_p$,

$$F_n(T) = 1 + \langle n \rangle + \frac{\langle n \rangle}{\mu \tau_p} = 1 + \langle n \rangle + \langle \alpha \rangle \frac{T}{\tau_p}. \tag{2.83}$$

As $T/\tau_p \to 0$, $F_n(T)$ approaches $1 + \langle n \rangle$, which characterizes the Bose–Einstein distribution. On the other hand, for $T \gg \tau_p$,

$$F_n(T) = 1 + \langle \alpha \rangle, \tag{2.84}$$

which characterizes the Neyman Type-A (NTA) distribution. This distribution is obtained when each of a Poisson-distributed number of primary events contributes a Poisson-distributed number of secondary events and the total number of events are counted (TEICH [1981], SALEH and TEICH [1982, 1983], SALEH, STOLER and TEICH [1983]). In our case the primary events correspond to the emissions and the secondary events correspond to the photoevents associated with each emission. The processes associated with light of this nature (shot-noise light), as well as the ensuing photocounting distributions and pulse-interval distributions, have been studied in great detail in a number of papers (TEICH and SALEH [1981a,b], SALEH, TAVOLACCI and TEICH [1981], SALEH and TEICH [1982, 1983], MATSUO, TEICH and SALEH [1983], SALEH, STOLER and TEICH [1983], TEICH and SALEH [1987]).

Spatial effects have not been considered in this presentation. A more general treatment has been provided by TEICH, SALEH and PEŘINA [1984], in which each individual emission is assumed to originate at a random position within a source of finite volume. This model leads to generalized versions of eqs. (2.65)–(2.69). Expressions have been derived for the photoevent coincidence rates at arbitrary points located in a detection plane that is at a specified distance from the source, as well as the photocount Fano factor for a detector of arbitrary area. The calculations lead naturally to the introduction of a spatial degrees-of-freedom parameter $M_s$, which plays a role analogous to the temporal degrees-of-freedom parameter $M$ in determining both the coincidence rate and the Fano factor.

## § 3. Antibunched Light from Independent Radiators

In § 2 we demonstrated that light composed of many independent emissions tends toward chaotic behavior; the photoevents are bunched and the photocounts are super-Poisson. The individual emissions themselves were constrained to be either unbunched or bunched, since the semiclassical theory of light does not admit antibunched emissions.

M. C. Teich and B. E. A. Saleh, "Photon Bunching and Ant bunching," in Progress in Optics, vol. 26, edited by E. Wolf (North-Holland, Amsterdam, 1988), ch. 1, pp. 1-104.

In this section we address the same situations – a superposition of identical independent emissions, and a superposition of identical independent emissions initiated at random times. But we now use a quantum formulation of the problem, which allows the individual emissions to be antibunched and sub-Poisson. When the emission times are Poisson, we will see that the superposed radiation is again bunched and super-Poisson, approaching chaotic behavior when the emissions overlap strongly. We will conclude that *sub-Poisson light cannot be generated by a collection of independent emissions initiated at Poisson times, even if the emissions are deterministic.* The statistics of the times at which the emissions are initiated must be rendered sub-Poisson in order to generate antibunched and/or sub-Poisson light.

### 3.1. QUANTUM THEORY OF OPTICAL COHERENCE: A BRIEF REVIEW

In the quantum theory of coherence (GLAUBER [1963a,b], LOUDON [1983], PEŘINA [1985]), amplitude and intensity correlation functions are defined in terms of the positive- and negative-frequency parts of the optical electric field operator, $\hat{E}^+(\boldsymbol{x})$ and $\hat{E}^-(\boldsymbol{x})$, respectively. The first- and second-order correlation functions (or coherence functions) correspond to the quantum-mechanical expectation values

$$G^{(1)}(\boldsymbol{x}_1, \boldsymbol{x}_2) = \mathrm{Tr}\{\hat{\varrho}\,\hat{E}^-(\boldsymbol{x}_1)\,\hat{E}^+(\boldsymbol{x}_2)\}\,, \tag{3.1}$$

$$G^{(2)}(\boldsymbol{x}_1, \boldsymbol{x}_2) = \mathrm{Tr}\{\hat{\varrho}\,\hat{E}^-(\boldsymbol{x}_1)\,\hat{E}^-(\boldsymbol{x}_2)\,\hat{E}^+(\boldsymbol{x}_2)\,\hat{E}^+(\boldsymbol{x}_1)\}\,, \tag{3.2}$$

respectively. Here $\hat{\varrho}$ is the density operator of the field. Normalized versions of these functions, $g^{(1)}(\boldsymbol{x}_1, \boldsymbol{x}_2)$ and $g^{(2)}(\boldsymbol{x}_1, \boldsymbol{x}_2)$, are defined in analogy with the classical theory (see eqs. 2.3 and 2.4) and these go by the same names.

The probability distribution of the number of photon counts collected by a detector of area $A$, in the time interval $T$, is (KELLEY and KLEINER [1964], LAX and ZWANZIGER [1973], SHAPIRO, YUEN and MACHADO MATA [1979], YUEN and SHAPIRO [1980], SHAPIRO [1985])

$$p(n) = \left\langle : \frac{\hat{W}^n \exp(-\hat{W})}{n!} : \right\rangle, \tag{3.3}$$

where

$$\hat{W} = \eta \int_D \hat{E}^-(\boldsymbol{x})\,\hat{E}^+(\boldsymbol{x})\,\mathrm{d}\boldsymbol{x}\,.$$

M. C. Teich and B. E. A. Saleh, "Photon Bunching and Ant bunching," in Progress in Optics, vol. 26, edited by E. Wolf (North-Holland, Amsterdam, 1988), ch. 1, pp. 1-104.

Here : : denotes normal ordering and time-ordering (LOUDON [1983]). $\boldsymbol{D}$ again denotes the region $r \in A$ and $t \in [0, T]$, and $\eta$ denotes the detector quantum efficiency. The photon-count mean and Fano factor (ratio of count variance to count mean) can be obtained from the coherence functions by use of relations that are identical to those of the semiclassical theory, eqs. (2.9) and (2.16), which we repeat here for convenience:

$$\langle n \rangle = \eta \int_{\boldsymbol{D}} G^{(1)}(\boldsymbol{x}, \boldsymbol{x}) \, \mathrm{d}\boldsymbol{x} , \tag{3.4}$$

$$\mathrm{F}_n(\boldsymbol{D}) - 1 = \frac{\langle n \rangle}{D^2} \int_{\boldsymbol{D}} \int_{\boldsymbol{D}} [g^{(2)}(\boldsymbol{x}_1, \boldsymbol{x}_2) - 1] \, \mathrm{d}\boldsymbol{x}_1 \, \mathrm{d}\boldsymbol{x}_2 , \tag{3.5}$$

where $D = AT$. We have assumed that $\langle I(\boldsymbol{x}) \rangle$ is constant within $\boldsymbol{D}$. When the detector area and counting time are sufficiently small ($\boldsymbol{D} \to 0$), this reduces to

$$[\mathrm{F}_n(0) - 1] = \langle n \rangle [g^{(2)}(\boldsymbol{x}, \boldsymbol{x}) - 1] , \tag{3.6}$$

which is identical with eq. (2.17). Again, we assume that there are no feedback paths from detector to source. A quantum theory of detection that is valid in the presence of such paths has recently been developed (SHAPIRO, SAPLAKOGLU, HO, KUMAR, SALEH and TEICH [1987]).

The difference between the semiclassical and quantum results lies in the procedures used to calculate $G^{(1)}(\boldsymbol{x}_1, \boldsymbol{x}_2)$ and $G^{(2)}(\boldsymbol{x}_1, \boldsymbol{x}_2)$ and in their physical interpretation. As in the semiclassical theory, $\eta G^{(1)}(\boldsymbol{x}, \boldsymbol{x}) \Delta T \Delta A$ represents the probability that a photoevent is detected within an incremental area $\Delta A$ and incremental time $\Delta T$ surrounding a point $\boldsymbol{x}$. Likewise, as discussed in § 2.1, $g^{(2)}(\boldsymbol{x}_1, \boldsymbol{x}_2)$ represents the normalized coincidence rate for two photoevents at $\boldsymbol{x}_1$ and $\boldsymbol{x}_2$. However, in the quantum theory, $g^{(2)}(\boldsymbol{x}_1, \boldsymbol{x}_2)$ is no longer defined or interpreted as a normalized statistical correlation function of the optical intensity. It is therefore no longer bounded by the inequalities satisfied by classical correlation functions, viz. eqs. (2.6) and (2.7). The function $g^{(2)}(\boldsymbol{x}, \boldsymbol{x})$ can dip below unity, thus violating eq. (2.6). Antibunched photon registrations are consequently possible (see the reviews of LOUDON [1980] and PAUL [1982]). The correlation function is required to be nonnegative, however (GLAUBER [1963a]). If $g^{(2)}(\boldsymbol{x}_1, \boldsymbol{x}_2)$ falls below unity over some subregion of $\boldsymbol{D}$, the integral in eq. (3.5) can become negative and result in a photon-count Fano factor below unity, that is, sub-Poisson photocounts. Photon antibunching and sub-Poisson photon counting statistics are among a handful of optical phenomena that require the full quantum theory of light for an explanation.

M. C. Teich and B. E. A. Saleh, "Photon Bunching and Ant bunching," in Progress in Optics, vol. 26, edited by E. Wolf (North-Holland, Amsterdam, 1988), ch. 1, pp. 1-104.

In the semiclassical theory, when there is no feedback from the detector to the source, photoevents occur in accordance with a doubly stochastic Poisson point process. In the quantum theory this is no longer the case. Photoevents follow a more general self-exciting point process (SHAPIRO [1985]), which may be characterized by its multicoincidence rates (see, for example, PEŘINA [1985]).

### 3.2. SUPERPOSITION OF INDEPENDENT EMISSIONS

An optical field generated by $N$ independent emissions may be described by the superposition

$$\hat{E}^+(x) = \sum_k \hat{E}_k^+(x), \tag{3.7}$$

where $\hat{E}_k^+(x)$ is the positive-frequency part of the field operator for the $k$th emission. This, in turn, may be written in terms of the annihilation operators $\hat{a}_l$ of the different radiation modes as

$$\hat{E}_k^+(x) = \sum_l V_{kl}(x)\hat{a}_l. \tag{3.8}$$

The functions $\{V_{kl}(x)\}$ are assumed to be random classical functions with $V_{kl}(x)$ and $V_{k'l}(x)$ (corresponding to the $k$th and $k'$th emissions) taken to be statistically independent. This defines what we mean by independent emissions. Therefore, in addition to the usual quantum-mechanical randomness embedded in the properties of the operators $\{\hat{a}_k\}$, there is a distinct classical randomness that is associated with the stochastic functions $\{V_{kl}(x)\}$.

When determining the optical coherence functions, we must average over both kinds of randomness; therefore,

$$G^{(1)}(x_1, x_2) = \langle \mathrm{Tr}\{\hat{\varrho}\hat{E}^-(x_1)\hat{E}^+(x_2)\}\rangle, \tag{3.9}$$

$$G^{(2)}(x_1, x_2) = \langle \mathrm{Tr}\{\hat{\varrho}\hat{E}^-(x_1)\hat{E}^-(x_2)\hat{E}^+(x_2)\hat{E}^+(x_1)\}\rangle, \tag{3.10}$$

where $\langle\cdot\rangle$ designates an average over the fluctuations of the classical functions $V_{kl}(x)$. In the following we assume that the $\{V_{kl}(x)\}$ have zero mean, that is, we restrict ourselves to states for which $\langle \mathrm{Tr}\{\hat{\varrho}\hat{E}_k^+(x)\}\rangle = 0$, so that the mean values of optical fields vanish. This restriction is convenient in simplifying the algebraic form of the results.

We are now in a position to determine the coincidence rate and Fano factor for photoevents associated with the total field. It can be shown that the

M. C. Teich and B. E. A. Saleh, "Photon Bunching and Ant bunching," in Progress in Optics, vol. 26, edited by E. Wolf (North-Holland, Amsterdam, 1988), ch. 1, pp. 1-104.

coherence functions of the total field $G^{(1)}(x_1, x_2)$ and $G^{(2)}(x_1, x_2)$ are related to those of the individual emissions $G_k^{(1)}(x_1, x_2)$ and $G_k^{(2)}(x_1, x_2)$ by the *same* formulas that we reported in § 2.2 using the classical formulation. This is not surprising because those relations were derived with the benefit of only classical arguments. For identical emissions these relations are as follows (see eqs. 2.43, 2.44, 2.49–2.52):

$$g^{(1)}(x_1, x_2) = g_0^{(1)}(x_1, x_2)$$

$$g^{(2)}(x_1, x_2) = 1 + |g^{(1)}(x_1, x_2)|^2 + \frac{1}{N}\gamma_0(x_1, x_2), \tag{3.11}$$

$$F_n(D) = 1 + \frac{\langle n\rangle}{M} + \frac{\langle n\rangle \bar{\gamma}_0}{N}, \tag{3.12}$$

$$= 1 + \frac{\langle n\rangle}{M} + \left[F_\alpha(D) - 1 - \frac{\langle \alpha\rangle}{M}\right], \tag{3.13}$$

where

$$\gamma_0(x_1, x_2) = g_0^{(2)}(x_1, x_2) - 1 - |g_0^{(1)}(x_1, x_2)|^2, \tag{3.14}$$

$$\bar{\gamma}_0 = \frac{1}{D^2}\int_D \int_D \gamma_0(x_1, x_2)\, dx_1\, dx_2. \tag{3.15}$$

The quantity $M$ is the degrees-of-freedom parameter in eq. (2.47) and $\langle \alpha\rangle$ is the mean number of photoevents associated with an individual emission. Equation (3.11) gives

$$g^{(2)}(x, x) = 2 + \frac{1}{N}[g_0^{(2)}(x, x) - 2],$$

which was also obtained by LOUDON [1980] and applied to radiation from a few atoms in resonance fluorescence.

When using the preceding relations, the coherence functions of the individual emissions, $g_0^{(1)}(x_1, x_2)$ and $g_0^{(2)}(x_1, x_2)$, must be calculated by using quantum rules.

### 3.2.1. *Quasi-coherent single-mode emissions*

Consider a simple example in which the individual identical emissions are single-mode emissions (TITULAER and GLAUBER [1965]) characterized by

$$\hat{E}_k^+(\boldsymbol{x}) = V_0(\boldsymbol{x}) \exp(\mathrm{i}\theta_k)\hat{a} \tag{3.16}$$

where $V_0(\boldsymbol{x})$ is an arbitrary deterministic function, the $\theta_k$ are statistically independent and uniformly distributed random phases, and $\hat{a}$ is the annihilation operator for that mode.

The individual emissions then have the following statistical averages:

$$|g_0^{(1)}(\boldsymbol{x}_1, \boldsymbol{x}_2)| = 1\,,$$

$$g_0^{(2)}(\boldsymbol{x}_1, \boldsymbol{x}_2) = 2 + \gamma_0\,, \tag{3.17}$$

$$\gamma_0(\boldsymbol{x}_1, \boldsymbol{x}_2) = \gamma_0\,, \qquad \bar{\gamma}_0 = \gamma_0\,, \qquad M = 1\,,$$

$$\mathrm{F}_\alpha(\boldsymbol{D}) = 1 + \langle\alpha\rangle + \gamma_0\langle\alpha\rangle\,, \tag{3.18}$$

where $\langle\alpha\rangle = \langle n\rangle/N$ is the mean number of photoevents per emission and

$$\gamma_0 = \frac{\langle \hat{a}^\dagger\hat{a}^\dagger\hat{a}\hat{a}\rangle}{\langle \hat{a}^\dagger\hat{a}\rangle^2} - 2 \tag{3.19}$$

is a parameter that depends on the quantum state of the individual emissions ($\hat{a}$ is the annihilation operator). Note that all averages are independent of $\boldsymbol{x}_1$ and $\boldsymbol{x}_2$ because of the single-mode assumption.

It follows that the total radiation has the following properties

$$g^{(2)}(\boldsymbol{x}_1, \boldsymbol{x}_2) = 2 + \frac{1}{N}\gamma_0\,, \tag{3.20}$$

$$\mathrm{F}_n(\boldsymbol{D}) = 1 + \langle n\rangle + \frac{1}{N}\gamma_0\langle n\rangle$$

$$= 1 + \langle n\rangle + [\mathrm{F}_\alpha(\boldsymbol{D}) - 1 - \langle\alpha\rangle] = \mathrm{F}_\alpha(\boldsymbol{D}) + (N-1)\langle\alpha\rangle\,. \tag{3.21}$$

Again, the deviation from chaotic behavior is inversely proportional to the number of emissions $N$ and is directly proportional to the deviation of the Fano factor for the individual emissions from the chaotic value. If the individual emissions are themselves chaotic [$\gamma_0 = 0$ or $\mathrm{F}_\alpha(\boldsymbol{D}) = 1 + \langle\alpha\rangle$], the overall light is chaotic. If the individual emissions are subchaotic but super-Poisson [$-1 < \gamma_0 < 0$ or $1 < \mathrm{F}_\alpha(\boldsymbol{D})$], the overall light is also subchaotic and super-

M. C. Teich and B. E. A. Saleh, "Photon Bunching and Ant bunching," in Progress in Optics, vol. 26, edited by E. Wolf (North-Holland, Amsterdam, 1988), ch. 1, pp. 1-104.

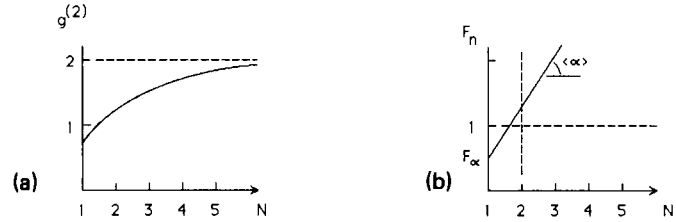


Fig. 3.1. $N$-dependence of the statistical properties of light that is composed of a superposition of $N$ statistically independent and identical emissions: (a) normalized coincidence rate $g^{(2)}(x, x)$; (b) Fano factor $F_n(D)$. $\langle \alpha \rangle$ (the slope) and $F_\alpha$ represent the mean number of photons and the Fano factor for an individual emission, respectively. The statistics change from antibunched and sub-Poisson to bunched and super-Poisson as $N$ increases above 1.

Poisson. If the individual emissions are Poisson [$\gamma_0 = -1$ or $F_\alpha(D) = 1$], then

$$g^{(2)}(x_1, x_2) = 2 - \frac{1}{N}, \tag{3.22}$$

$$F_n(D) = 1 + \langle n \rangle \left(1 - \frac{1}{N}\right), \tag{3.23}$$

reproducing the classical results in eqs. (2.55) and (2.56).

Finally, if the individual emissions are sub-Poisson [$F_\alpha(D) < 1$], the overall light is subchaotic but super-Poisson if $N > 1 + [1 - F_\alpha(D)]/\langle \alpha \rangle$. The dependence of $g^{(2)}(x, x)$ and $F_n(D)$ on $N$ for this case is illustrated in fig. 3.1. As an example, consider individual emissions described by the one-photon number state ($\alpha = 1$), for which $F_\alpha(D) = 0$ and $\gamma_0 = -2$. Then,

$$g^{(2)}(x_1, x_2) = 2 - \frac{2}{N}, \tag{3.24}$$

$$F_n(D) = N - 1. \tag{3.25}$$

For $N = 1$ (a single one-photon emission) the light is antibunched and sub-Poisson (by assumption). For $N = 2$ the light is unbunched, since $g^{(2)}(x_1, x_2) = F_n(D) = 1$. For $N > 2$ the light is bunched and super-Poisson.

To conclude, when $N$ statistically independent identical antibunched emissions are superposed, the resultant light has a normalized coincidence rate $g^{(2)}(x, x)$ that increases with increasing $N$, making the superposed radiation bunched even for modest $N$. It also has a photocount Fano factor that increases linearly with $N$, so that for sufficiently large $N$ ($N > 2$ in the single-photon emission case) the overall light becomes super-Poisson.

M. C. Teich and B. E. A. Saleh, "Photon Bunching and Ant bunching," in Progress in Optics, vol. 26, edited by E. Wolf (North-Holland, Amsterdam, 1988), ch. 1, pp. 1-104.

### 3.3. EMISSIONS INITIATED AT POISSON TIMES

We now examine the case of statistically independent identical emissions initiated at Poisson random times. We have already developed the main equations that relate the statistical properties of the superposed radiation to those of the individual emissions (see eqs. 2.65–2.68). Those equations are also applicable here, provided that the correlation functions of the individual emissions are determined using the quantum theory of light.

#### 3.3.1. *Quasi-coherent single-mode emissions*

Assume again that the individual emissions are in a single mode described by

$$\hat{E}_k^+ = V_0(t) \exp(\mathrm{i}\theta_k)\hat{a}\,, \tag{3.26}$$

where $V_0(t)$ is a deterministic pulse of intensity $I_0(t) = |V_0(t)|^2$, the $\theta_k$ are random independent phases, and $\hat{a}$ is the annihilation operator of the radiation mode. Spatial effects are ignored for simplicity.

An individual emission initiated at $t = 0$ has the following properties:

$$g_0^{(2)}(t, t+\tau) = \beta\,, \tag{3.27}$$

$$\langle \alpha \rangle = \langle \hat{a}^\dagger \hat{a} \rangle\, \eta \int_0^\infty I_0(t)\,\mathrm{d}t\,, \tag{3.28}$$

$$\mathrm{F}_\alpha(\infty) = 1 + \langle \alpha \rangle\, (\beta - 1)\,, \tag{3.29}$$

where $\alpha$ is the total number of photoevents associated with an individual emission (over $t \in [0, \infty]$) and the coincidence rate of its photoevents $\beta$ is given by

$$\beta = \frac{\langle \hat{a}^\dagger \hat{a}^\dagger \hat{a}\, \hat{a} \rangle}{\langle \hat{a}^\dagger \hat{a} \rangle^2}\,. \tag{3.30}$$

To determine the properties of the superposed radiation, we substitute in eqs. (2.72), (2.73) and (2.79) to obtain

$$g^{(1)}(\tau) = \frac{\displaystyle\int_0^\infty V_0^*(t)\, V_0(t+\tau)\,\mathrm{d}t}{\displaystyle\int_0^\infty I_0(t)\,\mathrm{d}t}\,, \tag{3.31}$$

M. C. Teich and B. E. A. Saleh, "Photon Bunching and Ant bunching," in Progress in Optics, vol. 26, edited by E. Wolf (North-Holland, Amsterdam, 1988), ch. 1, pp. 1-104.

$$g^{(2)}(\tau) = 1 + |g^{(1)}(\tau)|^2 + \frac{1}{\mu\tau_p}\bar{g}_0^{(2)}(\tau), \tag{3.32}$$

$$F_n(T) = 1 + \frac{\langle n\rangle}{M} + \langle n\rangle\frac{\Gamma_0}{\mu\tau_p}, \tag{3.33}$$

where $\bar{g}_0^{(2)}(\tau) = \beta\bar{I}_0(\tau)/\bar{I}_0(0)$, $\bar{I}_0(\tau)$ being the time-averaged correlation function of the intensity of an emission pulse (see eq. 2.76), and

$$\Gamma_0 = \frac{2}{T}\int_0^T\left(1 - \frac{\tau}{T}\right)\bar{g}_0^{(2)}(\tau)\,d\tau, \tag{3.34}$$

as in eq. (2.80). Equation (3.33) can be written in the alternate forms

$$F_n(T) = 1 + \frac{\langle n\rangle}{M} + \beta\frac{\langle\alpha\rangle}{\mathcal{M}}, \tag{3.35}$$

$$F_n(T) = 1 + \frac{\langle n\rangle}{M} + \frac{[F_\alpha(\infty) - 1 + \langle\alpha\rangle]}{\mathcal{M}}, \tag{3.36}$$

where $\mathcal{M}$ is the degrees-of-freedom parameter given by eq. (2.82). Equation (3.36) is the relation between the Fano factor of the total radiation and that of an individual emission.

Note that eqs. (3.31)–(3.36) are the same as the results obtained from the semiclassical theory, except for the factor $\beta$, which depends on the quantum state of the individual emissions. For a quasi-coherent state, $F_\alpha(\infty) = 1$ and $\beta = 1$, so that the classical results are reproduced exactly. For a chaotic state, $F_\alpha(\infty) = 1 + \langle\alpha\rangle$ and $\beta = 2$, corresponding to superchaotic light. The state that is likely to generate the least bunching is the one-photon number state (i.e., a single-photon emission), for which $\langle\alpha\rangle = 1$, $F_\alpha(\infty) = 0$, and $\beta = 0$. As evidenced by eqs. (3.32)–(3.34), even in this case the stream of emitted photons remains as bunched as chaotic light.

If the observation time is long ($T \gg \tau_p$), then $M = T/\tau_p \gg 1$ and $\mathcal{M} \approx 1$. In that case

$$F_n(T) \approx \langle\alpha\rangle + F_\alpha(\infty). \tag{3.37}$$

This is the result that would be obtained by ignoring photon interference, treating photons purely as particles, and arguing that $n$ is the sum of a Poisson-distributed random number $m$ of emissions, each containing a random

number $\alpha$ of photons. For example, if each emission contains a single photon, then $\langle \alpha \rangle = 1$, $F_\alpha(\infty) = 0$, and $F_n(T) = 1$, indicating that the resulting photon counts are Poisson. This is not surprising. We have a stream of single photons emitted about Poisson times; a Poisson number of photons is observed.

### 3.3.2. *Radiation from an atomic beam*

Consider radiation emanating from a beam of atoms moving with a constant velocity $v$, monitored through a window of length $d$. The total radiation may be described by

$$\hat{E}^+(t) = \sum_k \hat{E}_k^+(t - t_k) R_T(t - t_k),$$

where $E_k(t)$ represents the $k$th emission, $t_k$ is the time at which the $k$th atom enters the window region, $R_T(t)$ is a rectangular function of value 1 for $t \in [0, T]$ and zero elsewhere, and $T = d/v$ is the atomic transit time across the window. The length $d$ may represent a scattering region (radiation is then produced by scattering from the incoming atoms) or a region within which atoms are excited by an energy source to undergo luminescence or fluorescence. If it is assumed that the times of atomic entries into the window region are describable as a homogeneous Poisson point process (of rate $\mu$), then the theory presented in § 3.2 (eqs. 3.11–3.15) can be used to provide

$$g^{(2)}(\tau) = 1 + |g^{(1)}(\tau)|^2 + \frac{1}{\mu T} \bar{g}^{(2)}(\tau),$$

$$\bar{g}^{(2)}(\tau) = \left(1 - \frac{\tau}{T}\right) g_0^{(2)}(\tau), \quad |\tau| < T,$$

$$= 0, \qquad \text{elsewhere,}$$

where $g_0^{(2)}(\tau)$ is the normalized coincidence rate for radiation from a single atom (assumed to be stationary). In particular,

$$g^{(2)}(0) = 2 + \frac{1}{\mu T} g_0^{(2)}(0).$$

This result is consistent with the results of § 2.3, if $\mu T = \langle N \rangle$ is taken to be the average number of radiators. It is immediately obvious that the total radiation is not only bunched but it is superchaotic, regardless of the nature of the individual atomic emissions.

M. C. Teich and B. E. A. Saleh, "Photon Bunching and Ant bunching," in Progress in Optics, vol. 26, edited by E. Wolf (North-Holland, Amsterdam, 1988), ch. 1, pp. 1-104.

This reveals the root of the difficulty in obtaining sub-Poisson light from sub-Poisson atomic emissions, for example, atoms undergoing resonance fluorescence (KIMBLE and MANDEL [1976], CARMICHAEL and WALLS [1976a,b]). The antibunching and sub-Poisson properties of the resonance-fluorescence photon clusters cannot be expressed unless the randomness in the number of radiators is removed (JAKEMAN, PIKE, PUSEY and VAUGHAN [1977]). This problem may be alleviated to some extent by gating the detector, as implemented by SHORT and MANDEL [1983], but the best that can then be achieved is the generation of conditionally sub-Poisson photon clusters. This issue will be addressed in § 5.

In summary, it is apparent that independent emissions initiated at Poisson times stand no chance of producing unconditionally antibunched or sub-Poisson photons. The best they can achieve is unbunched, Poisson behavior. One effective way to alter the situation is to initiate the sub-Poisson emissions at sub-Poisson times (TEICH, SALEH and STOLER [1983], TEICH, SALEH and PEŘINA [1984]). This is discussed from a mathematical point of view in the next subsection and from a physical point of view (in terms of excitation feedback) in § 7. More delicate implementations may be provided by the methods outlined in § 6.

### 3.4. EMISSIONS INITIATED AT SUB-POISSON TIMES

Consider the superposition of a sequence of statistically independent and identical emissions initiated at times $\{t_1, t_2, \ldots, t_k, \ldots\}$ described by an arbitrary stationary point process (no longer restricted to Poisson). This is referred to as the excitation process because these times will be determined by an excitation mechanism, as will become apparent in § 7. Even though the individual emissions are nonstationary (typically taking the form of pulses lasting a short time), the overall radiation is stationary because of the assumed stationarity of the excitation process.

#### 3.4.1. *Characterization of the excitation point process*

Two of the most important descriptors of a stationary point process are the rate $\mu$ (events per second) and the rate of coincidence $\mu^2 g_e^{(2)}(\tau)$ of pairs of events at times separated by $\tau$. These descriptors are not sufficient to characterize an arbitrary point process completely (COX [1962], SNYDER [1975], SALEH [1978]); in general, knowledge of the probability of multicoincidences

M. C. Teich and B. E. A. Saleh, "Photon Bunching and Ant bunching," in Progress in Optics, vol. 26, edited by E. Wolf (North-Holland, Amsterdam, 1988), ch. 1, pp. 1-104.

of events at $k$ points, for $k = 1, 2, \ldots, \infty$, is required. If $m$ is the number of events that occur in a time interval $[0, T]$, then its mean is

$$\langle m \rangle = \mu T \tag{3.38}$$

and its Fano factor (ratio of variance to mean) is

$$\mathrm{F}_m(T) = 1 + \frac{\langle m \rangle}{M_e}, \tag{3.39}$$

where

$$M_e^{-1} = \frac{2}{T}\int_0^\infty \left(1 - \frac{\tau}{T}\right)[g_e^{(2)}(\tau) - 1]\,\mathrm{d}\tau. \tag{3.40}$$

The simplest example is the Poisson point process, for which $g_e^{(2)}(\tau) = 1$ and $\mathrm{F}_m(T) = 1$. If $g_e^{(2)}(0) < 1$, the excitation process is said to be antibunched or anticorrelated, whereas if $g_e^{(2)}(0) > 1$, it is said to be bunched or correlated. The characteristic time associated with the function $[g_e^{(2)}(\tau) - 1]$ is denoted $\tau_e$. Similarly, if $\mathrm{F}_m(T) < 1$, the excitation counts are said to be sub-Poisson (for this counting time $T$), whereas if $\mathrm{F}_m(T) > 1$, the counts are said to be super-Poisson. These are, of course, the same terms used earlier to characterize the photoevent point process. The Poisson point process has neither memory nor aftereffects.

For the self-exciting point process (SEPP), on the other hand, the probability of occurrence of an event at a particular time depends on the times and numbers of previous occurrences (SNYDER [1975]). Renewal point processes (RPPs) form an important subclass of SEPPs for which the rate $\mu$ and the normalized coincidence rate $g_e^{(2)}(\tau)$ do characterize the process completely (COX [1962]). These are processes for which the interevent time intervals are statistically independent and identically distributed. The following are important examples of renewal point processes that exhibit antibunched events and sub-Poisson counts:

(1). The gamma-$\mathcal{N}$ process. This process is obtained from a Poisson process by decimation, that is, by selecting every $\mathcal{N}$th event and discarding all others as illustrated in fig. 1.1d (COX [1962], PARZEN [1962]). The process is so named because the inter-event-time interval distribution $P(\tau)$ (see fig. 2.3) is a gamma distribution of order $\mathcal{N}$. For the particular case when $\mathcal{N} = 2$ (shown in fig. 1.1d), it turns out that (TEICH, SALEH and PEŘINA [1984])

$$g_e^{(2)}(\tau) = 1 - \exp(-4\mu|\tau|), \tag{3.41}$$

$$\mathrm{F}_m(T) \approx \tfrac{1}{2}. \tag{3.42}$$

M. C. Teich and B. E. A. Saleh, "Photon Bunching and Ant bunching," in Progress in Optics, vol. 26, edited by E. Wolf (North-Holland, Amsterdam, 1988), ch. 1, pp. 1-104.

(2). The nonparalyzable dead-time-modified Poisson process. This process is obtained from a Poisson process by deleting events that fall within a specified dead time $\tau_d$ following the registration of an event, as illustrated in fig. 1.1b (COX [1962], PARZEN [1962], RICCIARDI and ESPOSITO [1966], MÜLLER [1974], CANTOR and TEICH [1975], TEICH and VANNUCCI [1978]). It is characterized by (TEICH, SALEH and PEŘINA [1984])

$$g_e^{(2)}(\tau) = 1 - \frac{1}{\mu} \sum_{l=1}^{\infty} \frac{[\lambda(\tau - l\tau_d)]^{l-1}}{(l-1)!} \exp[-\lambda(\tau - l\tau_d)]\, U(\tau - l\tau_d) \quad (3.43)$$

$$F_m(T) \approx (1 - \mu\tau_d)^2 , \quad (3.44)$$

with

$$\lambda = \frac{\mu}{(1 - \mu\tau_d)} , \quad (3.45)$$

where $U(t)$ is the unit step function, $\lambda$ is the initial rate of the process, and $\mu$ is the rate after dead-time modification. Its inter-event-time density function is a decaying exponential function displaced from $\tau = 0$ to the minimum permissible inter-event time, $\tau_d$.

Another example is a pulse train with random time of initiation (LOUDON [1980], TEICH, SALEH and PEŘINA [1984]).

### 3.4.2. *Photon statistics for emissions at antibunched times*

When the underlying excitation process has known rate $\mu$ and normalized coincidence rate $g_e^{(2)}(\tau)$, but is otherwise arbitrary, what can be said about the statistics of the radiation? Because of their finite lifetime, emissions overlap and interfere (as we have seen in earlier sections). To determine their bunching properties, it is necessary to know not only the rate of coincidence of the excitation process at pairs of time instants, but it is also necessary to know coincidence rates at triple points, and so on. If such information is not available, the bunching properties of the superposed radiation cannot be determined.

However, in the limit in which the counting time $T$ is much longer than the lifetime $\tau_p$ of the individual emissions, interference has a negligible effect on the total number of collected photocounts. The total number of photons $n$ is then

simply the sum of the number of photons emitted *independently* by the individual emissions. If $m$ is the number of emissions and $\alpha_k$ is the number of photoevents associated with the $k$th emission, then $n = \sum_{k=1}^{m} \alpha_k$. Using the fact that the $\{\alpha_k\}$ are statistically independent and identical, it is not difficult to show that the mean and variance of $n$ are

$$\langle n \rangle = \langle \alpha \rangle \langle m \rangle , \tag{3.46}$$

$$\mathrm{Var}(n) = \langle \alpha \rangle^2 \mathrm{Var}(m) + \langle m \rangle \mathrm{Var}(\alpha) , \tag{3.47}$$

from which it follows that the corresponding Fano factors are related by

$$\mathrm{F}_n = \langle \alpha \rangle \mathrm{F}_m + \mathrm{F}_\alpha \tag{3.48}$$

or

$$\mathrm{F}_n = 1 + [\mathrm{F}_\alpha - 1 + \langle \alpha \rangle] + \langle \alpha \rangle (\mathrm{F}_m - 1) . \tag{3.49}$$

Equation (3.47) is known as the cascade variance formula (SHOCKLEY and PIERCE [1938], MANDEL [1959b], BURGESS [1961]). Equation (3.49) shows that the Fano factor comprises three contributions. The first term is that of a Poisson process. The second term represents excess noise due to randomness in the number of photons per emission (if $\alpha = 1$, then $\mathrm{F}_\alpha = 0$ and it vanishes). The third term admits the possibility of noise reduction due to anticorrelations in the excitation process (this term vanishes if the excitation process is Poisson).

As an example, we can apply this formula to the case considered in § 3.3 in which the excitation process was a Poisson point process. When $m$ is Poisson, $\mathrm{F}_m = 1$ and eq. (3.48) becomes

$$\mathrm{F}_n = \langle \alpha \rangle + \mathrm{F}_\alpha , \tag{3.50}$$

which reproduces eq. (3.37).

We now consider another example in which each of the individual emissions is described by a one-photon number state (i.e., single-photon emissions and $\alpha = 1$). This corresponds to $\langle \alpha \rangle = 1$ and $\mathrm{F}_\alpha = 0$, from which eq. (3.48) yields

$$\mathrm{F}_n = \mathrm{F}_m .$$

This is to be expected. For single-photon emissions the number of photons counted over a long time interval is approximately equal to the number of excitations (assuming there are no losses). If the excitation point process is sub-Poisson, the photons will also be sub-Poisson. It is of interest to note that

M. C. Teich and B. E. A. Saleh, "Photon Bunching and Ant bunching," in Progress in Optics, vol. 26, edited by E. Wolf (North-Holland, Amsterdam, 1988), ch. 1, pp. 1-104.

we need not go outside the domain of linear (single-photon) optics to see such uniquely quantum-mechanical effects.

Equations (3.48) and (3.49) reveal the key to obtaining sub-Poisson photons from sub-Poisson excitations. In order to have $F_n < 1$, $F_\alpha$ must be $< 1$, as is apparent from eq. (3.48). Furthermore, a necessary condition for $F_n < 1$ is that $F_m < 1$ (because the second term in eq. (3.49) is nonnegative). It follows that for $F_n$ to be less than one, both $F_\alpha$ and $F_m$ must be less than one. Therefore, *the generation of a stationary stream of sub-Poisson photons from a superposition of independent emissions requires both the excitation process and the photons of the individual emissions to be sub-Poisson.*

The implementation of physical mechanisms that lead to this kind of model are presented in § 7, where various kinds of excitation feedback are used to generate sub-Poisson excitations. Other ways of producing sub-Poisson light are to generate correlated photon pairs or to use a quantum nondemolition measurement, as discussed in § 6. One member of each correlated photon pair is used to provide a photon feedback signal that controls the twin photon beam. It might appear that the theoretical framework presented here is not appropriate for this paradigm because the photon emissions are not independent (correlated pairs are produced). However, because the control photons are annihilated they can be viewed as simply modifying the excitation statistics for the surviving photon beam, which then may be considered to comprise independent emissions. A fully quantum-mechanical analysis of photon-feedback mechanisms (SHAPIRO, SAPLAKOGLU, HO, KUMAR, SALEH and TEICH [1987]), such as those considered in § 6, confirms that the approach presented here is suitable for describing physical processes involving photon feedback as well as excitation feedback.

### 3.4.3. *Bunching/antibunching properties of emissions initiated at antibunched times*

The determination of the short-time behavior of the photoevents requires knowledge of the normalized photocoincidence rate $g^{(2)}(\tau)$. This is not possible unless the excitation point process is completely specified (higher-order multicoincidence rates specified). TEICH, SALEH and PEŘINA [1984] examined this problem under the assumption that the excitation point process was a renewal point process. Under the additional assumption of single-mode individual emissions, as in eq. (3.26), they showed that

$$g^{(2)}(\tau) = 1 + |g^{(1)}(\tau)|^2 + \frac{1}{\mu \tau_p} \bar{g}^{(2)}(\tau) + r(\tau) . \tag{3.51}$$

M. C. Teich and B. E. A. Saleh, "Photon Bunching and Ant bunching," in Progress in Optics, vol. 26, edited by E. Wolf (North-Holland, Amsterdam, 1988), ch. 1, pp. 1-104.

The first three terms on the right-hand side of eq. (3.51) apply when the excitation process is Poisson (see eq. 3.32). The fourth term, which is given by

$$r(\tau) = \int_0^\infty \psi(\tau, t)\,[g_e^{(2)}(t) - 1]\,\mathrm{d}t\,, \tag{3.52}$$

with

$$\psi(\tau, t) = \int_0^\infty [I_0(t')\,I_0(t' + \tau - t) + V_0^*(t')\,V_0(t' + \tau)\,V_0^*(t + t')\,V_0(t + t' + \tau)]\,\mathrm{d}t'\,, \tag{3.53}$$

represents the effects of deviation of the excitation process from Poisson. When the excitation point process is antibunched, this term is negative, thereby introducing anticorrelation into the photon process. If it is sufficiently strong, it can counterbalance the bunching effects due to wave interference (second term) and to the randomness of the individual emissions (third term).

With the availability of eq. (3.51), the Fano factor for the photon counts in a time interval of arbitrary duration can be determined. The result can be put in the form (TEICH, SALEH and PEŘINA [1984])

$$\mathrm{F}_n(T) = 1 + \frac{\langle n\rangle}{M} + \frac{[\mathrm{F}_\alpha(\infty) - 1 + \langle\alpha\rangle]}{\mathscr{M}} + \frac{\langle n\rangle}{\mathscr{M}'}\,, \tag{3.54}$$

where $M$ and $\mathscr{M}$ are the degrees-of-freedom parameters discussed in § 3.3 and $\mathscr{M}'$ is a new degrees-of-freedom parameter associated with the term $r(\tau)$. $\mathscr{M}'$ depends, in a complex way, on the relation between the counting time $T$, the emission lifetime $\tau_p$, and the excitation point-process memory time $\tau_e$ (width of the function $[g_e^{(2)}(\tau) - 1]$). For counting times that are long ($T \gg \tau_p, \tau_e$), however, it turns out that $M = \infty$ and wavelike (interference) noise is washed out; $\mathscr{M} = 1$ so that the role of noise in the individual emissions is enhanced; and $\mathscr{M}'$ is given by the degrees-of-freedom parameter for the excitation process $M_e$ given in eq. (3.40). It then follows that eq. (3.54) reduces to eq. (3.49), which was directly obtained by use of the cascade variance formula.

This problem has been examined in considerable detail by TEICH, SALEH and PEŘINA [1984]. They also addressed the effects of different locations for the different emissions, and the rates of photon coincidence at pairs of positions

M. C. Teich and B. E. A. Saleh, "Photon Bunching and Ant bunching," in Progress in Optics, vol. 26, edited by E. Wolf (North-Holland, Amsterdam, 1988), ch. 1, pp. 1-104.

in the detection plane. MANDEL [1983] examined photon interference and spatial correlation effects of light produced by two independent sources, each containing either a random or a deterministic number of radiators.

### 3.5. SUMMARY: GENERATION OF ANTIBUNCHED AND SUB-POISSON LIGHT

It has been shown that two key effects regulate the antibunching and sub-Poisson possibilities for light generated by a two-step process of excitation and emission: (1) the statistical properties of the excitations themselves and (2) the statistical properties of the individual emissions. The role of these two factors is readily illustrated, from a heuristic point of view, in terms of the schematic presentation in fig. 3.2.

In fig. 3.2a we show an excitation process that is Poisson. Consider each excitation as generating photons independently. Now if each excitation instantaneously produces a single photon, and if we ignore the effects of interference, the outcome is a Poisson stream of photons, which is neither antibunched nor, obviously, sub-Poisson. This is the least random situation that we could hope to produce, given the Poisson excitation statistics. If interference is present, it will redistribute the photon occurrences, leading to the results for chaotic light (SALEH, STOLER and TEICH [1983]). On the other hand, the individual nonstationary emissions may consist of multiple photons or random numbers of photons. In this case, we encounter two sources of randomness, one associated with the excitations and another associated with the emissions, so that the outcome will be both bunched and super-Poisson.

In particular, if the emissions are also described by Poisson statistics, and the counting time is sufficiently long, we recover the Neyman Type-A counting distribution, as has been discussed in detail elsewhere (TEICH [1981], TEICH and SALEH [1981a], SALEH and TEICH [1982, 1983]). Even if the individual emissions comprise deterministic numbers of photons, the end result is the fixed-multiplicative Poisson distribution, which is super-Poisson (TEICH [1981]). Related results have been obtained when interference is permitted (SALEH, STOLER and TEICH [1983]). It is clear, therefore, that if the excitations themselves are Poisson (or super-Poisson), there is little hope of generating antibunched or sub-Poisson light by such a two-step process.

In fig. 3.2b we consider a situation in which the excitations are more regular than those for the Poisson. For illustration and concreteness we choose the excitation process to be produced by deleting every other event of a Poisson process. The outcome is the gamma-2 (or Erlang-2) renewal process, whose

M. C. Teich and B. E. A. Saleh, "Photon Bunching and Ant bunching," in Progress in Optics, vol. 26, edited by E. Wolf (North-Holland, Amsterdam, 1988), ch. 1, pp. 1-104.

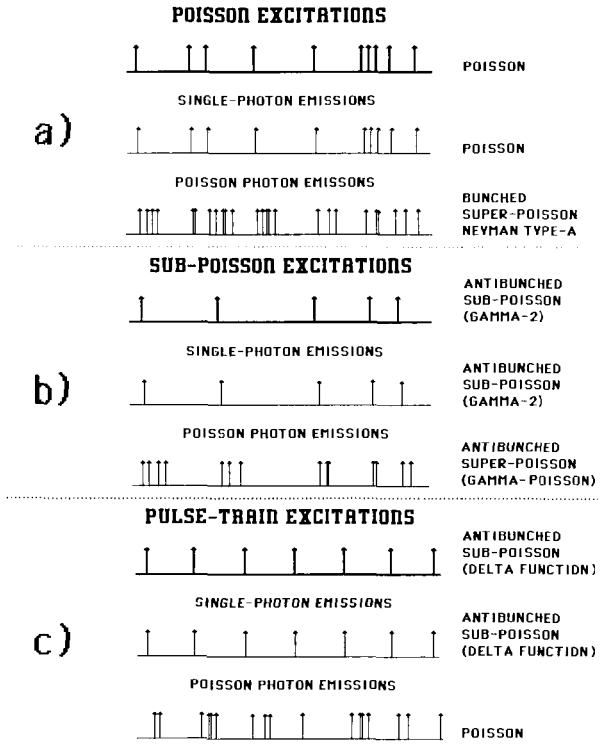


Fig. 3.2. Schematic representation of a two-step process for the generation of light, illustrating stochastic excitations (first line) with either single-photon emissions (second line) or Poisson multiple-photon emissions (third line). Interference effects are ignored in this simple representation. (a) Poisson excitations; (b) antibunched, sub-Poisson excitations (gamma-2); (c) pulse-train excitations (random phase). (After TEICH, SALEH and PEŘINA [1984].)

analytical properties are well understood. Single-photon emissions, in the absence of interference, result in antibunched, sub-Poisson photon statistics. Poisson emissions, on the other hand, result in super-Poisson light statistics. Of course, the presence of interference can introduce additional bunching. Clearly, a broad variety of excitation processes can be invoked for generating many different kinds of light. A process similar to the gamma-2, and for which many analytical results are available, is the nonparalyzable dead-time-modified Poisson process. Resonance fluorescence radiation from a single atom will be described by a process of this type, since after emitting a single photon the atom decays to the ground state where it cannot radiate. The superposition of light from a number of such atoms will wash out the sub-Poisson behavior, however.

M. C. Teich and B. E. A. Saleh, "Photon Bunching and Ant bunching," in Progress in Optics, vol. 26, edited by E. Wolf (North-Holland, Amsterdam, 1988), ch. 1, pp. 1-104.

Finally, in fig. 3.2c we consider the case of pulse-train excitations (with random initial time). This is the limiting result both for the gamma family of processes and for the dead-time-modified Poisson process. In the absence of interference, single-photon emissions in this case yield antibunched, ideally sub-Poisson photon statistics. Interference causes the antibunching to disappear, but the sub-Poisson nature remains in the long-counting-time limit. Poisson emissions give rise to Poisson photon statistics.

The illustration presented in fig. 3.2 is intended to emphasize the importance of the excitation and emission statistics as determinants of the character of the generated light. To produce antibunched and/or sub-Poisson photons, both sub-Poisson excitations and sub-Poisson emissions are required.

The statistical properties of light generated by sub-Poisson excitations, with each excitation leading to a single-photon emission, have been developed earlier in this section. The sub-Poisson excitations are characterized by a time constant $\tau_e$, which represents the time over which excitation events are anticorrelated (antibunched). The single-photon emissions, on the other hand, are characterized by a photon excitation/emission lifetime $\tau_p$. The detected light will be sub-Poisson provided $T \gg \tau_e, \tau_p$; $A \gg A_c$, where $T$ is the detector counting time, $A$ is the detector counting area, and $A_c$ is the coherence area. Different methods of sub-Poisson excitation result in different values of $\tau_e$, whereas different mechanisms of photon generation result in different values of $\tau_p$ and $A_c$.

Invoking these limits assures that all memory of the field from individual emissions lies within the detector counting time and area. The randomization of photon occurrences associated with interference therefore does not extend beyond these limits. Consequently the photon-count statistics are determined by the only remaining source of variability, which is the randomness in the excitation occurrences.

In this limit the photons behave as classical particles, and the photon statistics are governed by the simple rules specified in eqs. (3.48)–(3.50). This kind of picture also provides the basis for understanding the generation of sub-Poisson light by a semiconductor laser (YAMAMOTO, MACHIDA, IMOTO, KITAGAWA and BJÖRK [1987]).

## § 4. Randomization of Sub-Poisson Photon Streams

Photon streams often undergo random deletion (thinning). Obvious examples of importance in quantum optics include optical absorption and the

M. C. Teich and B. E. A. Saleh, "Photon Bunching and Ant bunching," in Progress in Optics, vol. 26, edited by E. Wolf (North-Holland, Amsterdam, 1988), ch. 1, pp. 1-104.

photodetection process itself, for which the quantum efficiency of the detector is invariably less than unity. It has long been known that the Poisson process, which is probably the most ubiquitous of all point processes, remains Poisson under the action of such Bernoulli random selection (PARZEN [1962]).

More recently it has been established (TEICH and SALEH [1982], PEŘINA, SALEH and TEICH [1983]) that the DSPP photon distribution retains its form under the effects of such deletion, but with a reduced integrated rate. A specific example is the negative binomial photon distribution, which, on deletion, remains negative binomial with reduced mean and an unchanged degrees-of-freedom parameter $M$. Another is the shot-noise-driven Poisson (SNDP) photon-counting distribution, which re-emerges on random deletion with the same degrees-of-freedom parameter $\mathscr{M}$, but in this case with reduced mean *and* reduced multiplication parameter.

There is no general result of this nature for sub-Poisson photon counting distributions. On the sub-Poisson side of the Poisson barrier, however, the binomial distribution retains its form under Bernoulli deletion.

Nevertheless, on either side of the barrier, the Fano factor obeys a particularly simple relation under the effect of Bernoulli random deletion, provided that the counting window is sufficiently large. This characteristic is discussed in § 4.1.

Another source of photon-stream randomization is associated with the presence of additive independent Poisson photons, such as those arising from background radiation. The modified Fano factor reduction formula that accounts for this effect is presented in § 4.2.

Finally, we mention parenthetically that the process of photon detection often involves the use of devices that operate by means of electron multiplication. Examples are the photomultiplier tube and the avalanche photodiode. Although the electron multiplication process also adds randomness to the detected signal, it is possible to minimize the deleterious effects of multiplication noise by a judicious choice of detection device and mode of operation (TEICH, MATSUO and SALEH [1986]).

### 4.1. BERNOULLI RANDOM DELETION

A photon stream with Fano factor $\mathrm{F}_m(D)$ emerges, after random deletion, with Fano factor $\mathrm{F}_n(D)$ in accordance with the relation

$$[\mathrm{F}_n(D) - 1] = \eta[\mathrm{F}_m(D) - 1], \qquad T \gg \tau_e, \tau_p; \qquad A \gg A_c, \tag{4.1}$$

M. C. Teich and B. E. A. Saleh, "Photon Bunching and Ant bunching," in Progress in Optics, vol. 26, edited by E. Wolf (North-Holland, Amsterdam, 1988), ch. 1, pp. 1-104.

where $\eta$ is the probability of photon survival (quantum efficiency) and $\langle m \rangle$ is the initial mean photon number. This relation may be obtained directly from eq. (3.48) by using the substitutions $\langle \alpha \rangle = \eta$ and $F_\alpha = 1 - \eta$, which are appropriate for events governed by the Bernoulli (random-deletion) law. If $\eta$ contains the quantum efficiency of the detector, as well as all other losses, $F_n(\boldsymbol{D})$ then represents the expected photoelectron (post-detection) Fano factor. The validity of eq. (4.1) requires that the counting time $T$ be greater than both the characteristic electron correlation time $\tau_e$ and the photon correlation time $\tau_p$, and that the detection area $A$ be greater than the coherence area $A_c$. These conditions ensure that interference has a negligible effect on the total count number (see § 3.4 and § 3.5). Furthermore, eq. (4.1) is only applicable for open-loop photodetection (see SHAPIRO, SAPLAKOGLU, HO, KUMAR, SALEH and TEICH [1987]).

Equation (4.1) has been derived both quantum-mechanically (PAUL [1966, 1982], MILLER and MISHKIN [1967], GHIELMETTI [1976], YUEN and SHAPIRO [1978], PEŘINA, SALEH and TEICH [1983], LOUDON and SHEPHERD [1984]) and semiclassically (TEICH and SALEH [1982]). It is applicable for bilinear interactions of boson quantum systems in the rotating-wave approximation, which lead to Heisenberg–Langevin equations involving only annihilation operators (PEŘINA, SALEH and TEICH [1983]). Such interactions leave the initial statistics of the system unchanged (in particular, a coherent initial state remains coherent). Equation (4.1) is also applicable for interactions in which photons interact with electrons and atoms whose fermion properties play no role. The semiclassical derivation gives the correct result because of the correspondence between semiclassical and normally ordered correlation functions, for which vacuum fluctuations play no role.

It is useful, perhaps, to point out that, in contradistinction to the Fano factor, the magnitude of the second-order correlation function $g^{(2)}(\boldsymbol{x}, \boldsymbol{x})$ is independent of $\eta$. This is because $g^{(2)}(\boldsymbol{x}, \boldsymbol{x})$ reflects the joint detection of pairs of photons (coincidences) at the space–time point $\boldsymbol{x}$. Random deletion has the effect of providing fewer such pairs at each value of $\boldsymbol{x}$, thereby reducing the accuracy of the estimated correlation function.

### 4.2. ADDITIVE INDEPENDENT POISSON PHOTONS

In the presence of additive independent Poisson photons, as well as Bernoulli deletion, the expression analogous to eq. (4.1) is

$$[F_n(\boldsymbol{D}) - 1] = \eta\beta[F_m(\boldsymbol{D}) - 1], \qquad T \gg \tau_e, \tau_p; \qquad A \gg A_c . \tag{4.2}$$

M. C. Teich and B. E. A. Saleh, "Photon Bunching and Ant bunching," in Progress in Optics, vol. 26, edited by E. Wolf (North-Holland, Amsterdam, 1988), ch. 1, pp. 1-104.

Here, $n$ represents the signal-plus-additive-background photon-count (or post-detection photoelectron) random variable and $F_n(\boldsymbol{D})$ is the overall photon-count (or photoelectron) Fano factor. The quantity $\beta$ $(0 \leqslant \beta \leqslant 1)$ is governed by the presence of Poisson additive counts (e.g., background light). In the absence of such counts, $\beta = 1$.

If the additive Poisson noise count mean is $\langle p \rangle$, then $\mathrm{Var}\langle p \rangle = \langle p \rangle$. In the case where the Bernoulli selection occurs before the addition, $\beta$ turns out to be (TEICH and SALEH [1982])

$$\beta = \left(1 + \frac{\langle p \rangle}{\eta \langle m \rangle}\right)^{-1}, \tag{4.3}$$

whereas when the Bernoulli selection occurs after the addition,

$$\beta = \left(1 + \frac{\langle p \rangle}{\langle m \rangle}\right)^{-1}. \tag{4.4}$$

Equation (4.2) clearly shows that all photon distributions move toward the Poisson barrier under the action of Bernoulli deletion and/or additive independent Poisson background events. However, no amount of deletion or additive noise will permit this barrier to be crossed from either direction.

### 4.3. ANALOG RELATIONS

The analog version of eq. (4.2) is useful when the detected photocurrent (or the excitation current discussed in § 7.1.2) is continuous rather than a sequence of discrete events. It can be used to relate the power spectral densities of an excitation current $S_m(\omega)$ and a detected photocurrent $S_n(\omega)$. The ratios $S_j(\omega)/2e\langle i_j \rangle$ may be regarded as Fano factors $F_j(T_j)$, where $j = m, n$, and the $\langle i_j \rangle$ are the mean values of the respective currents. Here the counting times $T_j$ play the role of inverse bandwidths of the filters involved. In the limits $T_j \gg \tau_e, \tau_p$ and for $\omega \ll 1/\tau_e, 1/\tau_p$, we obtain

$$\left(\frac{S_n(\omega)}{2e\langle i_n \rangle} - 1\right) = \eta\beta\left(\frac{S_m(\omega)}{2e\langle i_m \rangle} - 1\right), \qquad \omega \ll \frac{1}{\tau_e}, \frac{1}{\tau_p}; \quad A \gg A_c. \tag{4.5}$$

The quantity $\beta$ accounts for the admixture of independent Poisson background events as discussed earlier.

M. C. Teich and B. E. A. Saleh, "Photon Bunching and Ant bunching," in Progress in Optics, vol. 26, edited by E. Wolf (North-Holland, Amsterdam, 1988), ch. 1, pp. 1-104.

## § 5. Observation of Antibunched and Conditionally Sub-Poisson Photon Emissions

Antibunching was the first characteristic of nonclassical light to be observed in the laboratory. It is an effect that generally becomes less pronounced as the number of radiators increases (this is a result of the increase of accidental coincidences between uncorrelated photons). In 1977 KIMBLE, DAGENAIS and MANDEL [1977] carried out a series of experiments in which they excited sodium vapor with laser light. This led to the production of antibunched resonance fluorescence radiation (KIMBLE, DAGENAIS and MANDEL [1977, 1978], DAGENAIS and MANDEL [1978]). Similar results were achieved by RATEIKE, LEUCHS and WALTHER, as cited in CRESSER, HÄGER, LEUCHS, RATEIKE and WALTHER [1982], using a longer interaction time. Antibunching has also been observed in parametric downconversion by using an event-triggered optical shutter (WALKER and JAKEMAN [1985b]) and in correlated atomic photon emissions (GRANGIER, ROGER and ASPECT [1986]). More recently GRANGIER, ROGER, ASPECT, HEIDMANN and REYNAUD [1986] observed that a multi-atom source in a four-wave-mixing configuration gives rise to antibunched pairs of fluorescence photons traveling in opposite directions.

Antibunching and sub-Poisson behavior need not necessarily accompany each other as discussed in § 3 (TEICH, SALEH and STOLER [1983]); nevertheless, they sometimes do. From an experimental point of view it is generally easier to observe antibunching than sub-Poisson statistics (SHORT and MANDEL [1984], WALKER and JAKEMAN [1985b]). The observation of antibunching and sub-Poisson behavior in resonance fluorescence reflects the fact that the atom makes a quantum jump to its ground state at the time a photon is emitted. The inability of the atom to radiate in the ground state may be viewed as an enforced dead time (TEICH and VANNUCCI [1978]) following a photon emission, during which further emissions are prohibited (KIMBLE and MANDEL [1976]). This regularizes the resonance-fluorescence photon emissions from a single atom, so that it produces an antibunched and sub-Poisson cluster of photons while it traverses the experimental apparatus.

In § 5.1 we discuss the generation of conditionally sub-Poisson resonance-fluorescence photons from single atoms. The use of parametric down-conversion for producing conditionally sub-Poisson single photons is considered in § 5.2. Finally, the destruction of sub-Poisson behavior resulting from the incorporation of excitation statistics (removal of the conditioning) is discussed in § 5.3. Techniques for the generation of unconditionally sub-Poisson light are presented in § 6 and § 7.

M. C. Teich and B. E. A. Saleh, "Photon Bunching and Ant bunching," in Progress in Optics, vol. 26, edited by E. Wolf (North-Holland, Amsterdam, 1988), ch. 1, pp. 1-104.

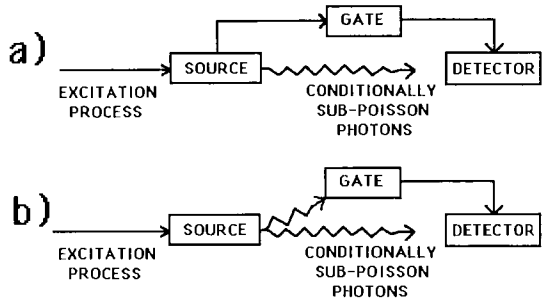


Fig. 5.1. Schematic diagram illustrating the generation of conditionally sub-Poisson photons. (a) Configuration for resonance fluorescence where the entry of a single atom into the field of view of the apparatus gates the detector open for a brief time. (b) Configuration for correlated photon pairs (e.g., spontaneous parametric downconversion or $^{40}Ca$ correlated photon emissions), where one partner of a photon pair gates the detector open for a brief time.

## 5.1. CONDITIONALLY SUB-POISSON PHOTON CLUSTERS FROM RESONANCE FLUORESCENCE

SHORT and MANDEL [1983, 1984] observed individual clusters of sub-Poisson emissions from isolated sodium atoms. The effect is observable only if there is a single atom in the field of view of the apparatus at any given time and if it remains there during the photon counting time. In the Short–Mandel experiment this was achieved by enforcing two conditions: (1) the beam of sodium atoms was made sufficiently weak so that the average interatomic separation was $\sim 10\,\mu s$ in time or $\sim 1$ cm in distance; (2) the detector was gated on for a counting time $T \approx 200$ ns by means of an auxiliary detector that registered the arrival of the atom in the apparatus. A schematic representation is provided in fig. 5.1a; the excitation process was such that the source consisted of only a single atom.

A block diagram of their experimental apparatus is presented in fig. 5.2. A highly collimated sodium atomic beam is intersected perpendicularly by two circularly polarized dye-laser beams, tuned to the $3^2S_{1/2}$, $F = 2$ to $3^2P_{3/2}$, $F = 3$ Na transition, and stabilized in frequency to 1–2 MHz. The two intersection regions are in a weak magnetic field parallel to the dye laser beams. Optical pumping in the first region prepares the sodium atoms to be in the $3^2S_{1/2}$, $F = 2$, $m_F = 2$ magnetic sublevel. The only allowed dipole transition is between this and the higher $3^2P_{3/2}$, $F = 3$, $m_F = 3$ magnetic sublevel, so that the atoms behave essentially as a two-level quantum system. The exciting laser beam causes the atom to shuttle back and forth between the two levels, emitting resonance fluorescence photons.

M. C. Teich and B. E. A. Saleh, "Photon Bunching and Ant bunching," in Progress in Optics, vol. 26, edited by E. Wolf (North-Holland, Amsterdam, 1988), ch. 1, pp. 1-104.

Part of the fluorescence radiation in a region in the center of the second intersection is collected by a microscope objective and imaged onto a rectangular aperture where the field is split into two parts (see fig. 5.2). The light from a 50 μm-long region of the atomic beam, which the atom enters first, is directed to photomultiplier tube A (PMT A), whereas the light from an adjacent 425 μm-long region is sent to photomultiplier tube B, where the principal photon counting process takes place. When PMT A detects the arrival of an atom in the apparatus by registering a photon count, a 90 ns delay is invoked (to allow the atom to move from region A into region B), after which PMT B is gated on to allow the resonance fluorescence photons to be counted during the counting time $T \approx 200$ ns. The atom remains in region B during the measurement about 98% of the time. A histogram is constructed of the number of photon counts registered by PMT B during this time. This is normalized to

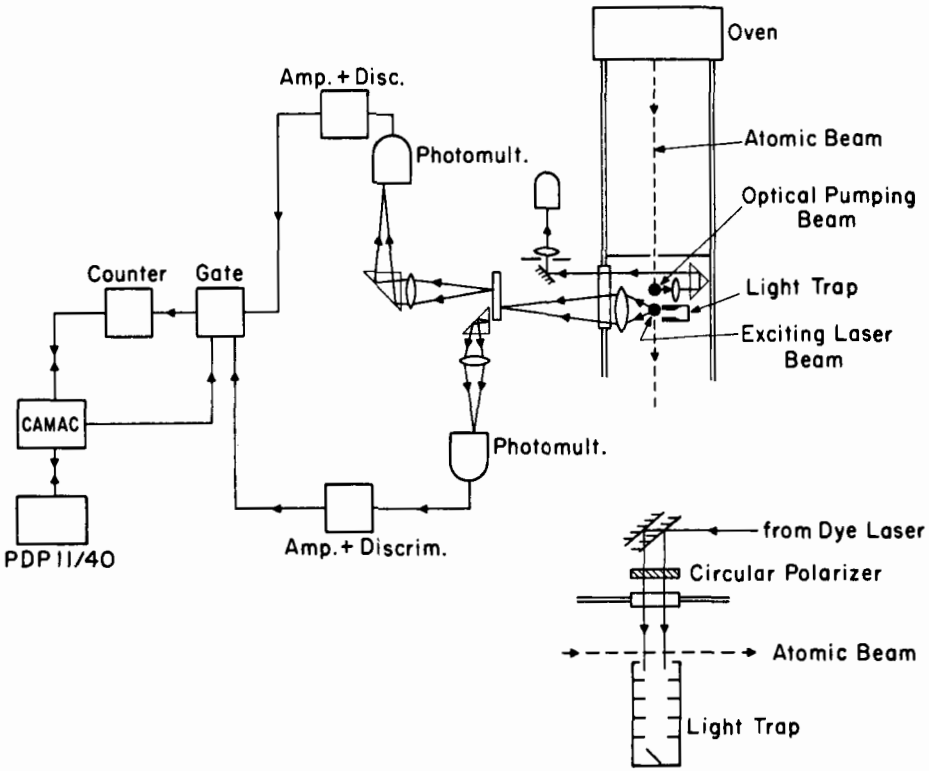


Fig. 5.2. Experimental apparatus for the observation of conditionally sub-Poisson photon clusters from resonance fluorescence. (After SHORT and MANDEL [1984].)

provide the experimental photon-counting distribution $p(n, T)$. Special efforts were made to minimize background and dark counts.

In each of the $24 \times 10^6$ measurements the detector was gated on when it was ascertained that an atom was in the field of view of the apparatus. The collection of a single photon-counting distribution took many hours. After collection of the data, corrections were made for additive background light, occasional pairs of atoms in the apparatus, dead time in the counting electronics, and PMT afterpulsing. The experiment provided a corrected count mean $\langle n \rangle \approx 6.5 \times 10^{-3}$ and a Fano factor $F_n(T) \approx 0.9978 \pm 0.0002$, indicating that the resonance-fluorescence photon clusters were slightly sub-Poisson. The results are in good accord with theoretical calculations for resonance fluorescence (SHORT and MANDEL [1984], MANDEL [1979], COOK [1980, 1981], LENSTRA [1982]).

### 5.2. CONDITIONALLY SUB-POISSON SINGLE PHOTONS FROM PARAMETRIC DOWNCONVERSION

It is easier to observe conditionally sub-Poisson photon emissions by means of spontaneous parametric downconversion. In this process photons from a coherent beam of light are split into lower-frequency signal and idler photons in a crystal that lacks inversion symmetry (LOUISELL, YARIV and SIEGMAN [1961], BURNHAM and WEINBERG [1970]). If a signal photon is detected at some position within a short time interval $T$, there is an idler photon in a one-photon state at a corresponding position at the same time (HONG and MANDEL [1986]).

HONG and MANDEL [1986] conducted a parametric downconversion experiment that made use of an argon-ion laser pump beam at 351.1 nm and a potassium dihydrogen phosphate (KDP) crystal. The downconverted signal and idler photons were collected by lenses and sent to two counting photomultiplier tubes. The idler counter was gated on by the signal counter, as represented schematically in fig. 5.1b. The idler photon-counting probability distribution, conditioned on the occurrence of a signal photon, was therefore measured. Under the paradigm of the experiment, if the collection efficiencies were unity and there were no dark current or background photons, the conditional idler counting distribution would be very nearly ideal, that is, $p(n) = \delta_{n,1}$ corresponding to $F \approx 0$. The experimental results lay far from this, however, exhibiting a post-detection Fano factor $F_n(T) \approx 0.998$. The dilution of sub-Poisson behavior resulted largely from the low detector quantum

M. C. Teich and B. E. A. Saleh, "Photon Bunching and Ant bunching," in Progress in Optics, vol. 26, edited by E. Wolf (North-Holland, Amsterdam, 1988), ch. 1, pp. 1-104.

efficiencies. Correction of the experimental result for background light and random deletion resulted in a photon-counting distribution near the theoretical ideal. Hong and Mandel point out that this scheme achieves a close approximation to a localized one-photon state.

In principle, the same configuration could be applied to other correlated photon-emission processes, for example, cascaded two-photon atomic emissions. Consider the experiment performed by ASPECT, GRANGIER and ROGER [1981, 1982], in which two photons emitted from a single $^{40}$Ca atom (the $4p^2\ ^1S_0 \rightarrow 4s4p\ ^1P_1 \rightarrow 4s^2\ ^1S_0$ cascade) were used in a polarization correlation experiment to demonstrate a strong violation of the generalized Bell inequalities. (It is interesting to note that REID and WALLS [1984] demonstrated that the violation of these inequalities is associated with nonclassical light.) Instead of the coincidence experiment they carried out, however, imagine a photon-counting experiment in which the registration of the upper (green) photon triggers a photon counter maximally sensitive to the lower (violet) photon. The violet photon will clearly be detected in Bernoulli fashion, since individual spontaneous atomic emissions represent single photons that may or may not be detected. As such, the emissions are conditionally sub-Poisson. Unlike the parametric downconversion experiment, however, the spatial atomic-emission pattern gives rise to photons that are not well localized. Thus even a perfect detection system triggered by the first photon will not result in a probability $\delta_{n,1}$ for the second photon.

### 5.3. DESTRUCTION OF SUB-POISSON BEHAVIOR BY EXCITATION STATISTICS

In the experiments just discussed the detector was gated on for a brief time in such a manner as to allow only photons from a single excitation event to be detected. Most emissions in nature (e.g., atomic photon emissions) are intrinsically sub-Poisson, and this character could be readily observed if we were able to gate a detector to respond only during the appropriate short time interval.

Constructing a true sub-Poisson light source from a *collection* of such emissions is difficult, however, because we are faced with randomness in the excitations rather than a single deterministic excitation event. In the resonance-fluorescence experiment the excitation statistics are determined by the random number of atoms in the field of view; indeed this number is not usually regulated (FORRESTER [1972], CARMICHAEL and WALLS [1976a,b], CARMICHAEL, DRUMMOND, MEYSTRE and WALLS [1978], JAKEMAN, PIKE, PUSEY and

M. C. Teich and B. E. A. Saleh, "Photon Bunching and Ant bunching," in Progress in Optics, vol. 26, edited by E. Wolf (North-Holland, Amsterdam, 1988), ch. 1, pp. 1-104.

VAUGHAN [1977]). In the correlated photon-emission experiments these statistics are determined by the occurrence times of the signal photons. When these times follow a Poisson process, as is usual, the resulting stationary source of light will, in fact, be super-Poisson, as is understood from § 3.3.2 and illustrated schematically in fig. 5.3. The sample functions in the top row represent conditionally sub-Poisson emissions from resonance fluorescence (top left) and from $^{40}$Ca violet photons (top right). The character of the results changes drastically when Poisson excitation statistics are taken into account and the gating interval is not preferentially chosen. The resulting photon counts then become super-Poisson for resonance fluorescence radiation (bottom left) and Poisson for correlated photon emissions (bottom right).

The equivalent of a single excitation event can be achieved if a single atom (or atomic ion) undergoing resonance fluorescence can be trapped in the field of view. There will then be no fluctuation in the atomic number. This has recently been accomplished by DIEDRICH and WALTHER [1987], who showed

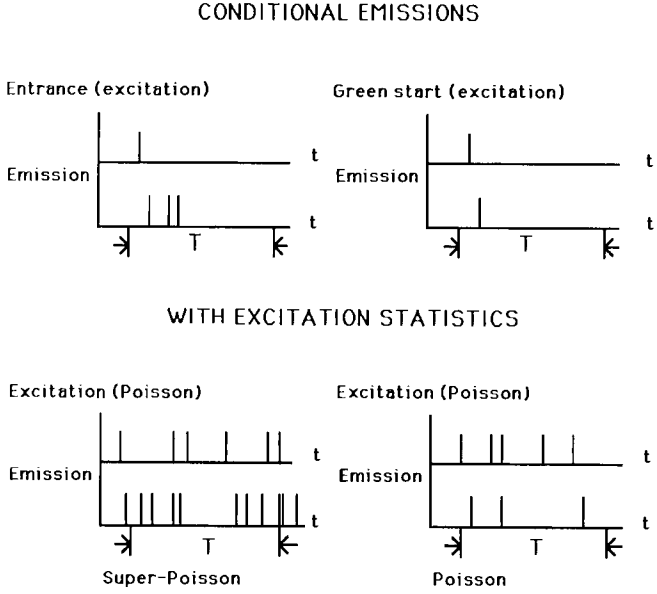


Fig. 5.3. Generation of conditionally sub-Poisson and unconditionally super-Poisson or Poisson light. Top left: sample function for a conditionally sub-Poisson resonance-fluorescence photon cluster. Bottom left: Poisson entries of atoms into the apparatus and unsynchronized gating result in unconditionally super-Poisson resonance-fluorescence radiation. Top right: sample function for a conditionally sub-Poisson $^{40}$Ca violet photon emission. Bottom right: Poisson entries of $^{40}$Ca atoms into the apparatus and unsynchronized gating lead to unconditionally Poisson green and violet photons.

M. C. Teich and B. E. A. Saleh, "Photon Bunching and Ant bunching," in Progress in Optics, vol. 26, edited by E. Wolf (North-Holland, Amsterdam, 1988), ch. 1, pp. 1-104.

that the emitted radiation, though obviously very weak, was both antibunched and unconditionally sub-Poisson.

It is evident that making a source of unconditionally sub-Poisson photons requires that the excitations be rendered sub-Poisson (see § 3.5 and TEICH, SALEH and PEŘINA [1984]). This is shown schematically in fig. 5.4. In the top row, sample functions are presented for conditionally sub-Poisson emissions from $^{40}$Ca pairs (top left) and for a single-photon atomic emission resulting from an electron impact excitation (top right). By the use of a suitable feedback circuit, the green photons can trigger an optical gate to provide selective passage of their violet partners. This can be accomplished in such a way that both the excitations and the violet emissions are unconditionally sub-Poisson (bottom left). A closely related technique was used by RARITY, TAPSTER and JAKEMAN [1987] to produce unconditionally sub-Poisson light in a parametric down-conversion experiment. The generation of unconditionally sub-Poisson light by the use of photon feedback methods such as these is the topic of § 6 (see

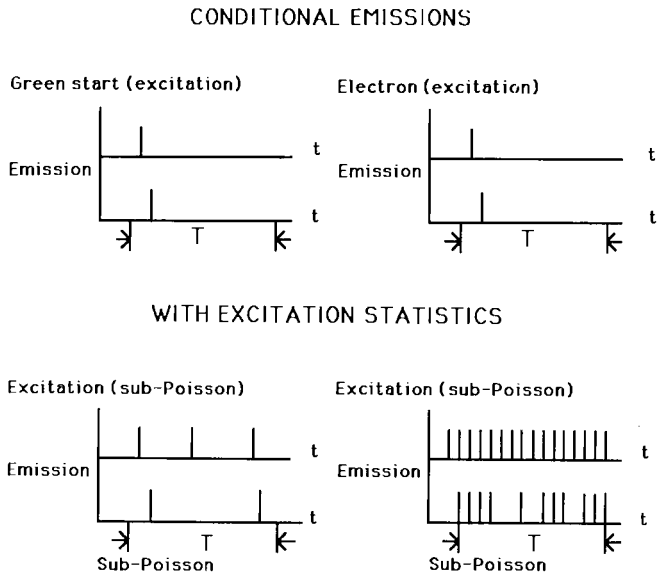


Fig. 5.4. Generation of conditionally and unconditionally sub-Poisson light. Top left: sample function for a conditionally sub-Poisson $^{40}$Ca violet photon emission. Bottom left: selective gating of violet photons by green photons leads to production of unconditionally sub-Poisson violet photons (see § 6). Top right: sample function for a conditionally sub-Poisson single-photon emission resulting from an electron impact excitation. Bottom right: sub-Poisson electron excitations (resulting, for example, from space charge) lead to unconditionally sub-Poisson photon emissions (see § 7).

M. C. Teich and B. E. A. Saleh, "Photon Bunching and Ant bunching," in Progress in Optics, vol. 26, edited by E. Wolf (North-Holland, Amsterdam, 1988), ch. 1, pp. 1-104.

especially § 6.2.1 and § 6.2.2). Electron excitations can also be made sub-Poisson by the use of feedback; one example entails the use of space-charge effects that operate by Coulomb repulsion. The generation of unconditionally sub-Poisson light by the use of excitation feedback methods is the topic of § 7 (see especially § 7.1.1).

## § 6. Generation of Antibunched and Sub-Poisson Light by Photon Feedback

The previous section was concerned with methods useful for observing antibunched and sub-Poisson individual emissions, which was achieved by gating the detector for a specific brief time interval. However, the generation of a *stationary* source of sub-Poisson light cannot be arranged so easily.

The principal mechanisms for generating cw sub-Poisson light rely on photon feedback or excitation feedback. In this section we consider photon feedback, that is, configurations in which the photons generated by the process at hand also provide the feedback signal. The simplest example is a process in which photon pairs are produced with one member of the pair being used to control its twin. This condition of dual purpose means that nonlinear optics must be invoked to achieve the effect.

In addition, the particular feedback process that is used may be intrinsic to the physical light-generation mechanism or it may take the form of an external feedback path. These two possibilities are illustrated schematically in fig. 6.1. In § 6.1 we briefly discuss methods that rely on feedback intrinsic to a physical process; historically, these comprised the first proposals for generating non-

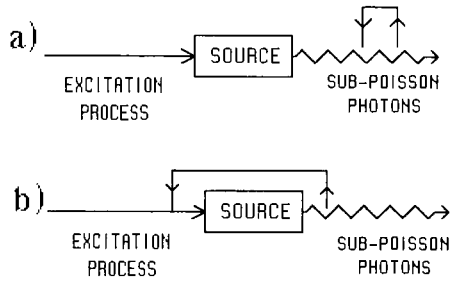


Fig. 6.1. Schematic diagram illustrating the generation of sub-Poisson light by means of photon feedback. (a) Feedback process intrinsic to the physical light-generation mechanism. (b) Feedback process carried by way of an external path. The feedback may take the form of an electrical signal or an optical signal.

M. C. Teich and B. E. A. Saleh, "Photon Bunching and Ant bunching," in Progress in Optics, vol. 26, edited by E. Wolf (North-Holland, Amsterdam, 1988), ch. 1, pp. 1-104.

classical light. This discussion is followed, in § 6.2, by a discussion of several configurations in which the feedback signal from the photons is carried externally. In § 6.3 we discuss the limitations of such methods. A quantum-mechanical theory applicable to these methods shows that it is possible, at least in principle, to synthesize a quantum light beam with arbitrary prescribed photon-counting statistics (SHAPIRO, SAPLAKOGLU, HO, KUMAR, SALEH and TEICH [1987]).

### 6.1. METHODS USING FEEDBACK INTRINSIC TO A PHYSICAL PROCESS

The earliest proposals for generating nonclassical light originated some 20 years ago with TAKAHASI [1965], MOLLOW and GLAUBER [1967a,b], and STOLER [1970, 1971, 1974]; these authors suggested the use of degenerate parametric amplification for generating antibunched and quadrature-squeezed light (see also YUEN [1976]). Since that time there have been numerous suggestions for the use of other nonlinear processes, including two-photon and multiphoton absorption, four-wave mixing, Raman and hyper-Raman scattering, interference in parametric processes, resonance fluorescence, and optical bistability and multistability. All of these interactions, in one way or another, involve higher-order (nonlinear) optical effects.

Viewed in an elementary way, nonlinear optical processes can introduce antibunching by removing selected clusters of photons from the incident (usually Poisson) pump beam, leaving behind an antibunched residue. The example of a two-quantum nonlinear absorber, operating by coincidence decimation, was illustrated in fig. 1.1c. Photon pairs arriving closer in time than the intermediate-state lifetime of the absorber are successful in effecting a two-photon transition and are removed from the beam (CHANDRA and PRAKASH [1970], TORNAU and BACH [1974], SIMAAN and LOUDON [1975], EVERY [1975], LOUDON [1976]). A number of review articles and books have considered the various schemes that rely on intrinsically nonlinear optical effects (LOUDON [1980], PAUL [1982], WALLS [1983], PEŘINA [1984, 1985], SCHUBERT and WILHELMI [1980, 1986]); the reader is referred to these for details.

Although parametric amplification was the first process suggested for generating nonclassical light, it has been so used only recently. WU, KIMBLE, HALL and WU [1986] generated strongly quadrature-squeezed light at 1.06 μm using parametric downconversion in a MgO : $LiNbO_3$ crystal. Indeed, a variety of nonlinear optical interactions have recently been used to generate

M. C. Teich and B. E. A. Saleh, "Photon Bunching and Ant bunching," in Progress in Optics, vol. 26, edited by E. Wolf (North-Holland, Amsterdam, 1988), ch. 1, pp. 1-104.

quadrature-squeezed light (SLUSHER, HOLLBERG, YURKE, MERTZ and VALLEY [1985], SHELBY, LEVENSON, PERLMUTTER, DEVOE and WALLS [1986], MAEDA, KUMAR and SHAPIRO [1987]). However, it appears that none of these nonlinear effects with feedback intrinsic to a physical process has yet been used to directly generate antibunched or sub-Poisson light.

### 6.2. METHODS USING EXTERNAL FEEDBACK

The photon feedback signal may be externally carried to the excitation process or the source, as illustrated schematically in fig. 6.1b. If the feedback is carried on the external path as an electrical signal, the photon timing information must be imparted to it in a special way. This is because the conventional process of detection involves the annihilation of photons as part of the process of creating an electrical signal. In usual circumstances the choice is therefore to have either the photons *or* the electronic residue of their detection. However, several special schemes have recently been suggested for imparting photon timing information onto a electrical signal while leaving the photons intact.

The first such suggestion appears to have been provided by SALEH and TEICH [1985], who proposed a scheme making use of correlated photon pairs from cascaded atomic emissions. In this case the photons from one of the atomic transitions are detected in the conventional manner to provide an external feedback signal. This signal is used to selectively permit certain photons from the second atomic transition to be passed through a gate (by means of the decimation process illustrated in fig. 1.1d). Since the photons are always emitted in correlated pairs, the selected twins survive and contribute to the light at the output. This configuration is illustrated schematically in fig. 6.2a and discussed in § 6.2.1.

There are many variations on this theme. The external feedback signal could be used to control the twin photon beam optically by means of dead-time deletion or rate compensation, instead of by decimation as discussed above (see fig. 1.1). Or the feedback signal could be used to control the source of the photons (the atoms) or the excitation process (the furnace), as illustrated in figs. 6.2b and 6.2c, rather than the twin beam. As an example of source control, the feedback signal from the control photon beam could be used to increase the rate of $^{40}Ca$ atoms entering the system when the detection rate is low and to decrease it when the detection rate is high. (A feedback signal of this kind was used by ASPECT [1986] and his co-workers for atomic beam stabilization;

M. C. Teich and B. E. A. Saleh, "Photon Bunching and Ant bunching," in Progress in Optics, vol. 26, edited by E. Wolf (North-Holland, Amsterdam, 1988), ch. 1, pp. 1-104.

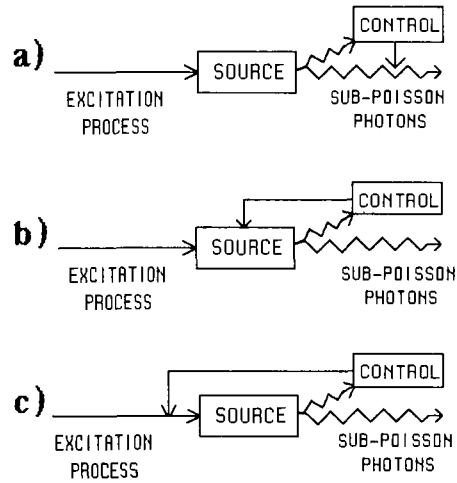


Fig. 6.2. Schematic diagram illustrating the generation of sub-Poisson light by correlated photon pairs and external feedback. One of the twin photon beams is annihilated to generate the control signal. (a) Optical control of one beam by its twin; (b) photon-source control; (c) excitation control.

however, the generation of nonclassical light requires that the characteristic feedback time $\tau_f$ be short in comparison with the counting time $T$.) Nonlinear optics schemes other than two-photon emissions can also be used to generate photon pairs; parametric downconversion is considered in § 6.2.2.

Furthermore, the feedback signal need not be carried electrically; it could be carried optically (e.g., on an optical fiber) with the attendant advantage of higher speed, as discussed in § 6.2.3.

Finally, in § 6.2.4 we discuss the use of a quantum nondemolition (QND) scheme for generating sub-Poisson light. This technique was suggested by YAMAMOTO, IMOTO and MACHIDA [1986a,b]. It allows the measurement of photon number at the output of a semiconductor laser, by means of the optical Kerr effect, without photon destruction, and the subsequent rate compensation of the laser excitation.

### 6.2.1. *Correlated photon pairs from cascaded atomic emissions*

The correlated atomic photon-pair emitters comprise a collection of excited atoms undergoing spontaneous cascaded emissions. For illustrative purposes we focus on the $4p^2\ ^1S_0 \rightarrow 4s4p\ ^1P_1 \rightarrow 4s^2\ ^1S_0$ green/violet cascade in $^{40}Ca$. This system was used by ASPECT, GRANGIER and ROGER [1981, 1982] and

ASPECT, DALIBART and ROGER [1982] as the basis of a polarization correlation experiment that demonstrated a strong violation of the generalized Bell inequalities.

A block diagram illustrating the use of $^{40}Ca$ photon pairs for generating nonclassical light is presented in fig. 6.3. A beam of $^{40}Ca$ atoms is selectively excited to the $4p^2\ ^1S_0$ state by means of optical pumping. This is the source. The atoms decay by the spontaneous emission of a green photon (at a wavelength of 551.3 nm) and a violet photon (at 422.7 nm). The two photons are correlated in emission times and in polarization. The green fluorescence light is collected by a lens and passed through a polarizer and green-transmitting interference filter to a photomultiplier tube (PMT)/discriminator, which produces the control signal. The green photoelectron events, in turn, feed a digital electronic trigger circuit that produces brief pulses of duration $\tau_g$ ($\approx 10$ ns) in accordance with a rule for selection, to be discussed subsequently. The violet fluorescence light is collected from the other side of the source. It is fed through a polarizer and violet-transmitting interference filter, into an optical delay path, and then through an optical gate that is opened for a period of $\tau_g$ s each time a pulse arrives from the selected trigger circuit. The optical delay path is adjusted so that the electrical trigger pulse (arising from the registration of a green photon) and its companion violet photon arrive at the optical gate simultaneously.

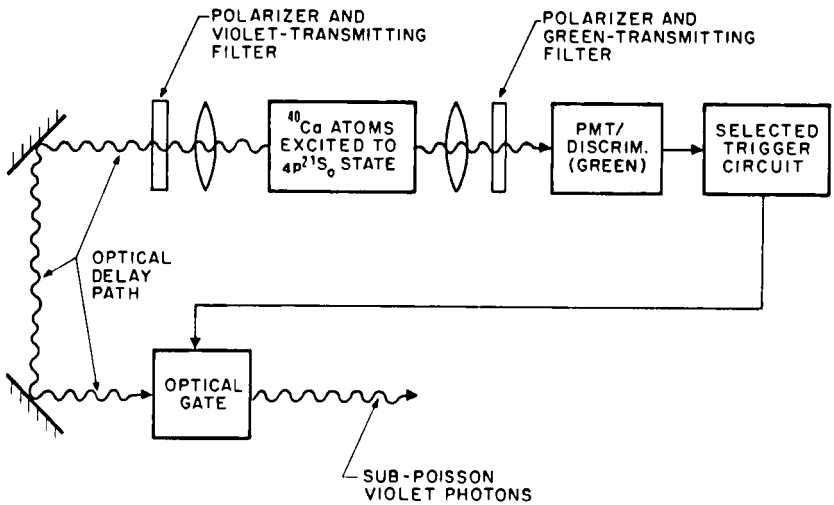


Fig. 6.3. Block diagram for sub-Poisson light generation using correlated photon pairs, in this case cascaded photon emissions from $^{40}Ca$ atoms. (After SALEH and TEICH [1985].)

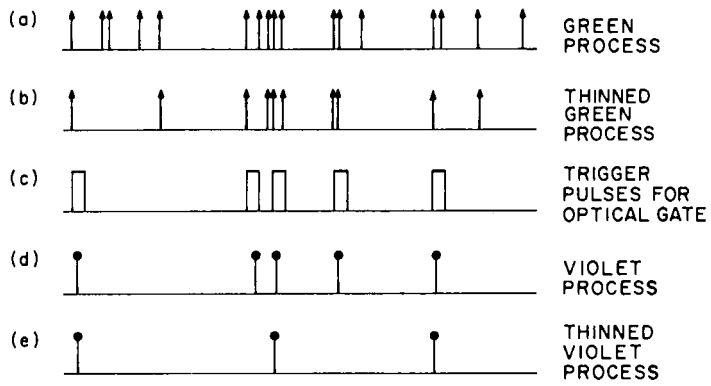


Fig. 6.4. Sample functions of the green and violet photon events for the scheme shown in fig. 6.3. The thinned violet process displayed in (e) represents a low-flux source of weakly sub-Poisson light. (After SALEH and TEICH [1985].)

Several representative sample functions of the photon events are presented in fig. 6.4. A simple picture of this kind assumes that the photon occurrences are sufficiently sparse so that their wavepackets do not overlap. This is equivalent to assuming that the degeneracy parameter $\delta = \mu\tau_p$ (where $\mu$ represents the photon rate and $\tau_p$ is the emission lifetime) is low, which is the condition under which such an experiment must be operated. The emission of the green photons from suitably excited calcium atoms may be represented as a Poisson point process (designated "green process" in row a). Some fraction of the green photons produces unitary events at the output of the green PMT (designated "thinned green process" in row b). As discussed in § 4, a Poisson photon process remains Poisson under Bernoulli random deletion, but with a rate that is reduced (TEICH and SALEH [1982], PEŘINA, SALEH and TEICH [1983]).

The thinned green events are then used to produce trigger pulses (of duration $\tau_g$) in accordance with a prespecified rule designed to render the trigger process sub-Poisson. As an example, a trigger pulse may be produced upon the registration of every $\mathcal{N}$th green photon. (This selective deletion rule is illustrated for $\mathcal{N} = 2$ in row c, designated "trigger pulses for optical gate".) This is the same rule denoted as decimation in fig. 1.1d. It is well known from renewal point-process theory that the selective deletion of every $\mathcal{N}$th event from a Poisson process (denoted a gamma-$\mathcal{N}$ process) leads to a counting process that becomes increasingly sub-Poisson as $\mathcal{N}$ increases, provided that the counting time $T$ is sufficiently long (see § 3.4.1 and TEICH, SALEH and PEŘINA [1984], eq. A24). Alternatively, another mechanism such as dead time can be used to

make the trigger pulses sub-Poisson (see § 3.4.1 and TEICH and VANNUCCI [1978]). The trick is that for each green photon, and therefore for each trigger pulse, there is a large probability that a violet companion photon is following closely behind (roughly within the intermediate-state lifetime $\tau_p = 5$ ns). The optical gate permits the violet photons to pass only during the times when it is open, and those times form a sub-Poisson counting process. Assuming for the moment that no violet photons are lost, row d illustrates the "violet process" which, in our example, is clearly also described by the gamma-$\mathcal{N}$ counting process. Of course, not all of the violet photons survive, so that what actually passes through the optical gate (designated "thinned violet process" in row e) is a randomly deleted version of the gamma-$\mathcal{N}$ photon-counting process. In accordance with the results presented in § 4, a randomly deleted sub-Poisson photon point process remains sub-Poisson but moves toward the Poisson barrier.

Using eq. (4.1), the Fano factor for a Bernoulli-deleted gamma-$\mathcal{N}$ photon-counting process is easily shown to be (SALEH and TEICH [1985])

$$F_n(T) = 1 - \eta_v\left(1 - \frac{1}{\mathcal{N}}\right), \tag{6.1}$$

where $\eta_v$ is an effective quantum efficiency for the violet photons. For an experimental configuration similar to that used by ASPECT, GRANGIER and ROGER [1981], the photon Fano factor is estimated to be $F_n(T) \approx 0.9990$. Folding in the violet-PMT quantum efficiency provides an estimated photoelectron Fano factor (SALEH and TEICH [1985]) $F_n(T) \approx 0.9999$, which is close to unity but should be measurable.

### 6.2.2. *Correlated photon pairs from parametric downconversion*

WALKER and JAKEMAN [1985a] recognized that a similar result can be achieved by using photon pairs generated by the process of spontaneous parametric downconversion (see also JAKEMAN and WALKER [1985] and JAKEMAN and JEFFERSON [1986]). This effect may be described as the splitting of a single photon into two (correlated) photons of lower frequency. The effect was first observed experimentally by BURNHAM and WEINBERG [1970]. The time uncertainty in the emission of the photon pairs can be short; it is determined by the inverse bandwidth of the detected light (HONG and MANDEL [1985], FRIBERG, HONG and MANDEL [1985]).

The first parametric downconversion experiment conducted by WALKER and JAKEMAN [1985b] used a configuration similar to that shown in fig. 6.2c.

M. C. Teich and B. E. A. Saleh, "Photon Bunching and Ant bunching," in Progress in Optics, vol. 26, edited by E. Wolf (North-Holland, Amsterdam, 1988), ch. 1, pp. 1-104.

One member of each correlated photon pair was detected. This event provided an electrical feedback signal, which controlled an optical shutter in the excitation beam. The optical shutter was closed for a fixed dead-time period $\tau_d$ following the detection of an event. Poisson photons obtained from a He–Cd laser operated at 325 nm served as the excitation process. This UV light was passed through an acousto-optic shutter (the control gate) and impinged on an ammonium dihydrogen phosphate (ADP) nonlinear crystal (the source), which produced red photon pairs by parametric downconversion. The signal light generated had an experimental second-order correlation function $g^{(2)}(\tau)$ that increased with $\tau$, as $\tau$ increased from 0. This indicates photon antibunching, in accordance with the positive-derivative definition provided in § 2.1.3. However, because $g^{(2)}(\tau)$ was always greater than unity, the light generated in this experiment was not sub-Poisson; this was attributed to long-term laser power fluctuations.

More recently, RARITY, TAPSTER and JAKEMAN [1987] succeeded in using this technique to produce sub-Poisson light. A block diagram of their apparatus is presented in fig. 6.5. The experimental arrangement is similar to that used in the antibunching experiment just described; fiber-optic light guiding and a single-photon-counting avalanche photodiode were added. The source of downconverted photons in this case was a potassium dihydrogen phosphate (KD*P) crystal, and the control gate acted on the signal channel rather than on the excitation channel so that the configuration is similar to that shown in fig. 6.2a rather than 6.2c. The observed effect was small but statistically significant; the postdetection Fano factor turned out to be F = 0.9998 with a photoelectron counting rate $\approx 30\ s^{-1}$ and a switching time $\approx 19\ \mu s$.

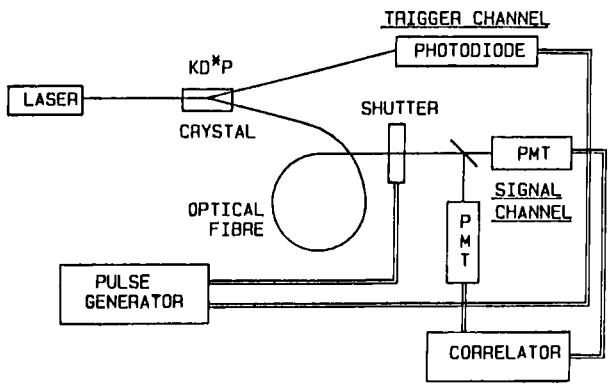


Fig. 6.5. Block diagram of the parametric downconversion experiment used by RARITY, TAPSTER and JAKEMAN [1987] to generate sub-Poisson light. (After RARITY, TAPSTER and JAKEMAN [1987].)

TAPSTER, RARITY and SATCHELL [1988] modified this experiment by using analog rate compensation of the pump power (see fig. 1.1f) provided by the control beam, using an electro-optic modulator. They generated $\sim 60$ pW of sub-Poisson light with a remarkably low Fano factor F = 0.78. This appears to be the lowest Fano factor yet reported for the direct generation of sub-Poisson light. However, the bandwidth over which the light was sub-Poisson was quite limited ($\sim 60$ Hz) and the overall quantum efficiency of the process was very low ($\sim 6 \times 10^{-11}$). Also recently, HEIDMANN, HOROWICZ, REYNAUD, GIACOBINO and FABRE [1987] used a two-mode optical parametric oscillator operating above threshold to generate high-intensity twin beams exhibiting strong quantum correlations.

A number of techniques have been suggested to enhance the nonclassical degree of the light (see, for example, WALKER [1986, 1987]). Suggestions have also been made for the use of other related schemes (YUEN [1986], STOLER and YURKE [1986], SRINIVASAN [1986b]), some of which are closely connected with overflow count deletion (MANDEL [1976a]), which is illustrated in fig. 1.1e.

### 6.2.3. *All-optical systems using correlated photon pairs*

In the examples discussed in the previous two subsections the feedback signal, although initiated by the photons in one of the twin beams, was carried electrically. This electrical signal was then used to control an optical beam. This external signal can also be carried optically (e.g., on an optical fiber) and used for direct optical control of the excitation or signal beams. The potential advantage in short-circuiting the electrical link is the high speed inherent in all-optical systems. A general block diagram of a system of this type is shown in fig. 6.6. The correlated photon-pair generator might be a parametric down-converter. The control signal is carried on an optical fiber to a nonlinear optical mechanism, which modifies the excitation in opposition to the control signal, that is, it provides negative feedback. Mechanisms that achieve this are second-harmonic generation and the photochromic effect (which is usually

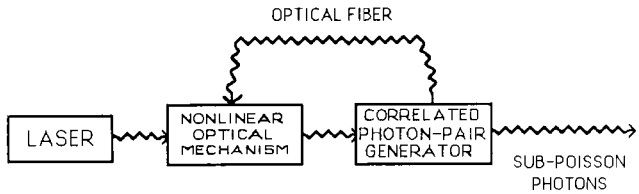


Fig. 6.6. Block diagram of a general all-optical system using correlated photon pairs, optical feedback, and a nonlinear optical mechanism that rate-compensates the excitation beam.

quite slow, however). Rate compensation can be used so that operation is not restricted to a single-file photon stream.

### 6.2.4. *Quantum-nondemolition measurements*

Quantum nondemolition (QND) measurements, in which an observable may be measured without perturbing its free motion, have been studied in the context of gravitational-wave detection and quantum optics (BRAGINSKY and VORONTSOV [1974], CAVES, THORNE, DREVER, SANDBERG and ZIMMERMAN [1980], BRAGINSKY and VYATCHANIN [1981, 1982], MILBURN and WALLS [1983]). IMOTO, HAUS and YAMAMOTO [1985] recently presented a theoretical treatment illustrating that a QND measurement of the photon number in a signal beam can be made, without photon destruction, by use of the lossless optical Kerr effect. In the proposed measurement scheme the phase of a probe wave passed through the Kerr medium provides information about the refractive-index change, which, in turn, is dependent on the signal photon number in the medium. Precision in the photon number measurement is provided at the expense of increased uncertainty in the canonically conjugate signal phase variable (CARRUTHERS and NIETO [1968]), subject to the minimum value provided by the Heisenberg uncertainty principle.

YAMAMOTO, IMOTO and MACHIDA [1986a] further proposed that the results of such a QND photon-flux measurement at the output of a semiconductor diode injection laser could be negatively fed back to control the rate of excitation of the laser, thereby producing sub-Poisson photons by rate compensation, in the manner shown in fig. 1.1f. They calculate that the phase noise of the signal beam is increased in an amount such that the number–phase minimum uncertainty product is preserved. Their scheme is illustrated in the block diagram of fig. 6.7. The (single) photon beam at the output of the laser gives rise, without loss of photons, to an electrical feedback signal that controls the laser excitation rate. The feedback signal is actually obtained from a probe laser in conjunction with a Kerr nonlinear interferometer, as is evident from fig. 6.7. More recently, YAMAMOTO and HAUS [1986] showed that under proper conditions a quasi-QND measurement of photon number, followed by a phase measurement, leads to a doubling of the noise associated with photon number and phase as required for the simultaneous measurement of two noncommuting variables.

A QND signal can also be obtained by means of other nonlinear optical processes, such as four-wave mixing (MILBURN and WALLS [1983]). The principle of QND detection has recently been verified by LEVENSON, SHELBY, REID and WALLS [1986].

M. C. Teich and B. E. A. Saleh, "Photon Bunching and Ant bunching," in Progress in Optics, vol. 26, edited by E. Wolf (North-Holland, Amsterdam, 1988), ch. 1, pp. 1-104.

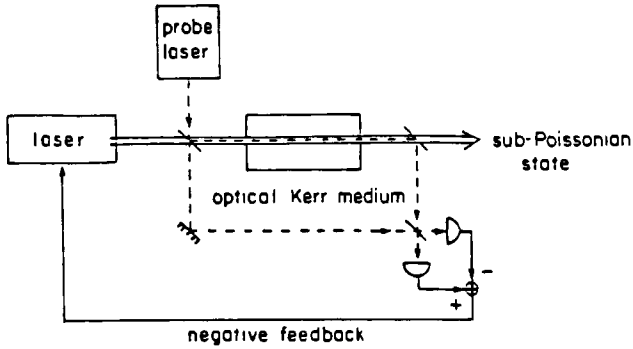


Fig. 6.7. Block diagram of the scheme proposed by YAMAMOTO, IMOTO and MACHIDA [1986a] for generating sub-Poisson (photon-number-squeezed) light. A quantum nondemolition (QND) measurement of the laser-output photon number is used to control the laser excitation rate. (After YAMAMOTO and HAUS [1986].)

### 6.3. LIMITATIONS OF PHOTON-FEEDBACK METHODS

As indicated in § 1, a useful source of sub-Poisson light will exhibit a photon Fano factor $F_n(T)$ that is substantially below unity and will produce a large photon flux $\Phi$ (corresponding to a large average photon number $\langle n \rangle$) with a reasonably large overall quantum efficiency $\bar{\eta}$. Ideally, the device should also be small in size and produce a directed output so that the light can be coupled to an optical fiber. The structure should be designed in such a way that light loss is minimized (see § 4).

Nonlinear optics methods (see § 6.1) generally employ a laser pump that emits Poisson-distributed photons. In such cases $F_n(T)$ and $\bar{\eta}$ will be the principal limiting factors in producing a useful source; they are determined by the efficiency with which pairs or clusters of photons can be separated from the pump beam. The photon flux will generally be unlimited and $\tau$ can be small, since it is determined by the intermediate state lifetime of the nonlinear process.

Methods employing correlated photon pairs (see § 6.2.1 to § 6.2.3) can, in principle, exhibit small values of $F_n(T)$, but $\Phi$, $\bar{\eta}$ and $T$ will be limited. The limitation on the photon flux arises from the use of dead-time and selective-deletion gating, which require single-file events for the technique to operate. Rate compensation is a preferable feedback mechanism from this point of view, but $\bar{\eta}$ will still be limited by the photon-pair generation mechanism. The photon flux may also be limited by the necessity of avoiding photon interference effects (thereby requiring that the degeneracy parameter not exceed unity). $T$ is limited

M. C. Teich and B. E. A. Saleh, "Photon Bunching and Ant bunching," in Progress in Optics, vol. 26, edited by E. Wolf (North-Holland, Amsterdam, 1988), ch. 1, pp. 1-104.

by the particular configuration: the intermediate-state lifetime for two-photon atomic emissions ($\tau_p \approx 5$ ns in $^{40}$Ca), the dead-time (gating time) in parametric downconversion with optical dead-time gating ($\tau_d \approx$ ns–μs); and the pair event-time difference in correlated photon-pair generation with optical-fiber feedback ($\tau < 0.1$ ns for parametric downconversion).

If the light is to be used in an application such as lightwave communications, the switching time (or symbol duration) $T$ should be able to be made small so that the device can be modulated at a high rate (SALEH and TEICH [1987]). However, $T$ must be sufficiently large in comparison with the characteristic response time of the system $\tau$ to ensure that the sub-Poisson character of the photons is captured in the counting time.

Although sub-Poisson light generated by photon feedback may not be useful for the transmission of information (see § 8), it should be pointed out that there are specialized applications in which the use of correlated photon pairs and post-detection processing (e.g., subtraction, correlation) are potentially useful (JAKEMAN and RARITY [1986]).

The limitations of QND techniques are not yet well understood. Outstanding questions include (1) the assumption of losslessness of the Kerr medium, (2) the role of signal/probe interference (self-phase modulation), (3) the characteristic time constant of the process, and (4) the achievable value of $F_n(T)$. Some of these questions have begun to be answered, as described by LEVENSON, SHELBY, REID and WALLS [1986].

It will become evident in § 7 that excitation-feedback methods are governed by a different set of constraints which are often less restrictive.

## § 7. Generation of Antibunched and Sub-Poisson Light by Excitation Feedback

We now consider excitation feedback, which is an alternative technique for generating sub-Poisson light. In this case the excitation process itself is rendered sub-Poisson by means of feedback, as illustrated schematically in fig. 7.1a (compare with fig. 6.1). Excitation-feedback methods provide the greatest promise for producing sources with small photon Fano factor, large photon flux, high overall efficiency, small size, and the capability of being modulated at high speeds (small $T$). Excitation feedback methods are also called "direct generation methods".

Excitation feedback methods effectively operate by permitting a sub-Poisson number of electrons to generate a sub-Poisson number of photons (one photon per electron); the photons may be viewed as representing a nondestructive

M. C. Teich and B. E. A. Saleh, "Photon Bunching and Ant bunching," in Progress in Optics, vol. 26, edited by E. Wolf (North-Holland, Amsterdam, 1988), ch. 1, pp. 1-104.

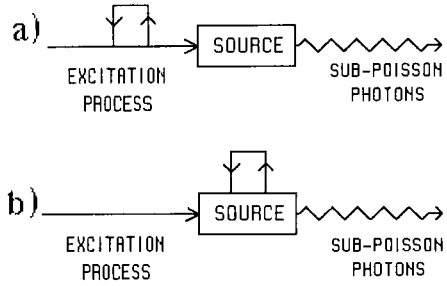


Fig. 7.1. Schematic diagram illustrating the generation of sub-Poisson light by means of excitation feedback: (a) feedback process intrinsic to physical excitation mechanism; (b) feedback process intrinsic to source. Excitation feedback can also be carried externally, as considered subsequently.

measurement of the electron number. This is to be distinguished from the QND configurations considered in § 6. There, a sub-Poisson number of photons generates an electrical current, which signals the photon number without destroying the photons (by means of a phase measurement). It is far easier to achieve a measurement of the electron number than the photon number because of the robustness (non-zero rest mass) of the electrons. Unlike photons, they are not destroyed by conventional measurement techniques.

A number of the limitations inherent in photon-feedback mechanisms, as discussed in the previous section, are avoided:

(1) Photons naturally gravitate toward Poisson-counting statistics and shot-noise fluctuations (SALEH, STOLER and TEICH [1983]). It is difficult for the nonlinear-optics methods to undo this natural Poisson photon noise. Electrons, on the other hand, are often governed by quieter thermal-noise fluctuations (MOULLIN [1938], WHINNERY [1959], LAMPERT and ROSE [1961]), thereby permitting $F_n(T)$ to be made smaller.

(2) Nonlinear-optics schemes in which Poisson photons are first generated (subject to a source power constraint) and subsequently converted into sub-Poisson photons cannot provide an enhancement of the channel capacity for applications such as lightwave communications as discussed in § 8 (SALEH and TEICH [1987]).

(3) Sub-Poisson electron-excitation configurations produce light by means of efficient single-photon transitions; high overall quantum efficiencies and large values for the photon flux are therefore readily achieved. Nonlinear-optics methods, on the other hand, rely on (relatively) inefficient multiple-photon transitions. Furthermore, they are subject to photon interference effects, which can limit the degeneracy parameter (and therefore the photon flux) to small values (SALEH and TEICH [1985]).

M. C. Teich and B. E. A. Saleh, "Photon Bunching and Ant bunching," in Progress in Optics, vol. 26, edited by E. Wolf (North-Holland, Amsterdam, 1988), ch. 1, pp. 1-104.

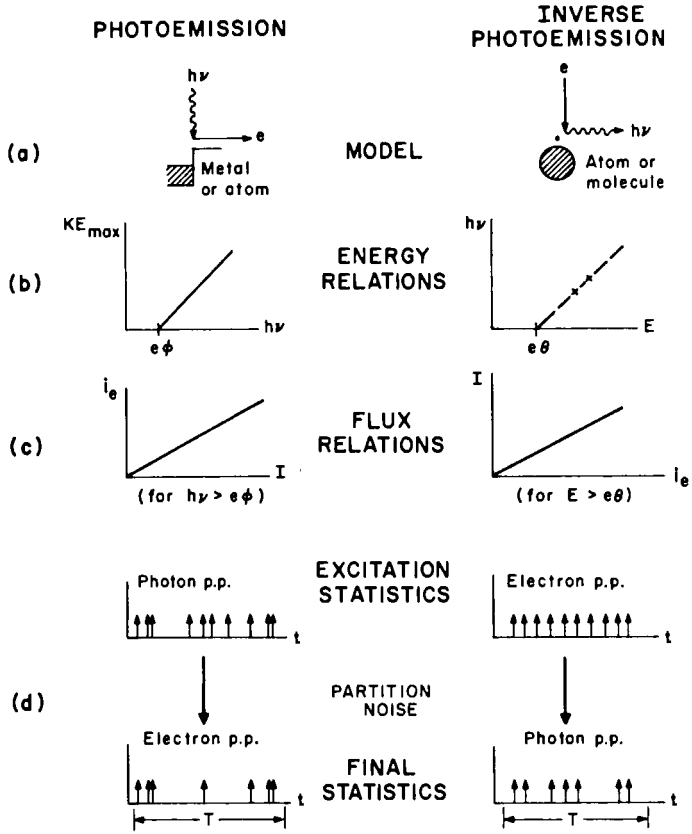


Fig. 7.2. Schematic representation of photoemission and inverse photoemission (illustrated by the Franck–Hertz effect). Energy relations and flux relatons are shown, as are sample functions of the excitation and final statistics; $i_e$ represents the average electron current and $I$ is the average light intensity (or photon flux). The generated photons behave like classical particles in a photon-counting paradigm, provided that the detector counting time and area are sufficiently large ($T \gg \tau_e, \tau_p$; $A \gg A_c$). (After TEICH and SALEH [1985].)

(4) Electron excitations, especially those mediated by physical processes (e.g., space charge), can attain a small characteristic response time $\tau_e$ so that fast switching can be achieved.

It is useful to view the conversion of electron excitations into single-photon emissions in terms of the process of inverse photoemission. A comparison between photoemission and inverse photoemission is schematically illustrated in fig. 7.2. For photoemission (fig. 7.2a) a photon impinges on a metal or atom and liberates an electron. The maximum kinetic energy of the electron ($KE_{max}$) is equal to the photon energy ($h\nu$) minus the work function of the material ($e\phi$)

in accordance with Einstein's photoelectric equation, as shown in fig. 7.2b. The flux relation displayed in fig. 7.2c demonstrates that the average photocurrent $i_e$ is proportional to the average light intensity or photon flux ($I$). Finally, sample functions of the photon point process (excitation statistics) and the resulting electron point process (final statistics) are represented in fig. 7.2d. They are related by a Bernoulli transform, which results from the non-unity quantum efficiency of the photodetector (partition noise), as discussed in § 4. The electrons liberated from the photocathode accurately sample the photon number, provided that the detector counting time $T$ and sampling area $A$ are properly adjusted (TEICH, SALEH and PEŘINA [1984]).

The processes are essentially reversed for inverse photoemission. For clarity we expressly consider the Franck–Hertz effect as an example. In fig. 7.2a an electron strikes an atom, loses its kinetic energy, and excites the atom. The atom then decays to a lower energy state and in the process emits a single photon by means of spontaneous emission. The energy of the emitted photon is equal to the energy supplied to the electron by an external field (E) less the cathode–emitter contact potential $e\Theta$, as shown in fig. 7.2b. Only electrons with kinetic energy corresponding to the discrete energy levels of the atom (indicated by crosses) are effective in producing photons. In fig. 7.2c we show that the average photon flux is proportional to the average electron current. Because this mechanism involves ordinary spontaneous (or stimulated) emission, it is a first-order optical process and can be expected to produce a high photon flux. Finally, in fig. 7.2d we illustrate the electron point process (excitation statistics). It is portrayed as quite regular because of the space-charge regularization. The photon point process (final statistics) is a Bernoulli-deleted version of the electron point process as a result of optical loss.

As in the case of sub-Poisson light generation by photon feedback, the feedback control signal may be intrinsic to the physical mechanism providing the excitation or it may be carried externally. Methods that make use of feedback intrinsic to a physical process, such as space-charge-limited excitations (in which the physical process is Coulomb repulsion), are considered in § 7.1. In § 7.1.1 we discuss the space-charge-limited Franck–Hertz experiment (TEICH and SALEH [1985]), which provided the first source of unconditionally sub-Poisson light. In § 7.1.2 we discuss a solid-state version of the Franck–Hertz experiment that should lead to sub-Poisson recombination radiation. This is followed, in § 7.1.3, by a discussion of the potential improvements to be realized by the cascading of sub-Poisson electron excitations and stimulated emissions.

M. C. Teich and B. E. A. Saleh, "Photon Bunching and Ant bunching," in Progress in Optics, vol. 26, edited by E. Wolf (North-Holland, Amsterdam, 1988), ch. 1, pp. 1-104.

Methods that make use of an external feedback signal are considered in § 7.2. The method reported in § 7.2.3 makes use of an in-loop auxiliary optical source, which emits light that effectively mimics the sub-Poisson electron current. External current stabilization schemes are discussed in § 7.2.4. Finally, a discussion of the limitations applicable to excitation-feedback methods is provided in § 7.3.

Although our attention is directed principally to excitation feedback, it is of interest to point out that there are other related schemes which may be useful. A schematic representation in which source feedback is used is shown in fig. 7.1b. For example, this mechanism could be used, at least in principle, to convert the sub-Poisson individual emissions observed by SHORT and MANDEL [1983] into a cw sub-Poisson source. As illustrated in fig. 5.3, the Poisson nature of the atomic entries into their apparatus (random source statistics) precludes the production of cw sub-Poisson light. However, if the source were a cold ion beam rather than an atomic beam, it could be rendered sub-Poisson by virtue of the ionic Coulomb repulsion. The source feedback could then be used to convert the sub-Poisson individual emissions into unconditionally sub-Poisson light provided, of course, that the emissions themselves were sufficiently sub-Poisson. The experiment carried out by DIEDRICH and WALTHER [1987], in which resonance fluoresence was observed from a single trapped ion, can be viewed as a degenerate example of source feedback.

## 7.1. METHODS USING FEEDBACK INTRINSIC TO A PHYSICAL PROCESS

We now consider several methods that make use of the sub-Poisson excitations inherent in an electric current. Current supplied from a dc source, such as a battery for example, is naturally sub-Poisson as a result of the intrinsic Coulomb repulsion of the electrons (the principal source of noise is Johnson noise). In such cases it suffices to drive an emitter operating by means of single-photon transitions with such a current. Thus, a simple LED driven by a constant current source should emit sub-Poisson photons.

Coulomb repulsion, which is the underlying physical feedback process for space-charge-limited current flow, is ubiquitous when excitations are achieved by means of charged particle beams. The single-photon emissions may be obtained in any number of ways. In § 7.1.1 they arise from spontaneous fluorescence emissions in mercury vapor, in § 7.1.2 they represent spontaneous recombination photons in a semiconductor, and in § 7.1.3 they are stimulated

M. C. Teich and B. E. A. Saleh, "Photon Bunching and Ant bunching," in Progress in Optics, vol. 26, edited by E. Wolf (North-Holland, Amsterdam, 1988), ch. 1, pp. 1-104.

recombination photons. These methods all operate by transferring the anti-clustering properties of the electrons, ultimately arising from Coulomb repulsion, directly to the photons.

### 7.1.1. *Space-charge-limited Franck–Hertz experiment*

Unconditionally sub-Poisson ultraviolet photons have been generated by the use of a space-charge-limited Franck–Hertz experiment (TEICH and SALEH [1983, 1985], TEICH, SALEH and STOLER [1983], TEICH, SALEH and LARCHUK [1984]). The essential element of the experiment was a collection of mercury atoms excited by inelastic collisions with a low-energy space-charge-limited (quiet) electron beam. The space-charge reduction of the usual shot noise associated with thermionically emitted electrons can be substantial (MOULLIN [1938], THOMPSON, NORTH and HARRIS [1940, 1941], WHINNERY [1959], SRINIVASAN [1965, 1986a]). Fano factors for the electron stream with values $F_e < 0.1$ are typical, and values as low as 0.01 are possible. After excitation each atom emits a (sub-Poisson) single photon by means of the Franck–Hertz (FH) effect (FRANCK and HERTZ [1914], FRANCK and JORDAN [1926]). This scheme is of the form represented in fig. 7.1a.

A block diagram of apparatus used in the experiment is shown in fig. 7.3. The light was generated in a specially constructed 25 mm-diameter UV-transmitting Franck–Hertz tube, filled with 0.75 g Hg. The radiation impinged on a

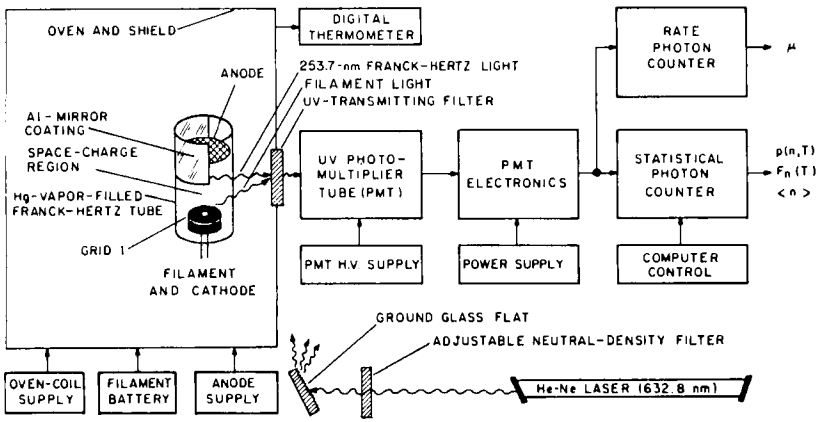


Fig. 7.3. Block diagram of the space-charge-limited Franck–Hertz experiment that produced unconditionally sub-Poisson light at 253.7 nm. (After TEICH, SALEH and LARCHUK [1984] and TEICH and SALEH [1985].)

M. C. Teich and B. E. A. Saleh, "Photon Bunching and Ant bunching," in Progress in Optics, vol. 26, edited by E. Wolf (North-Holland, Amsterdam, 1988), ch. 1, pp. 1-104.

UV-photon-counting photomultiplier tube (PMT) in a special base that provided preamplification, discrimination, and pulse shaping. The output of this circuitry was fed to electronic photon-counting equipment, which measured the probability distribution $p(n, T)$ for the detection of $n$ photoelectrons in the time $T$. The mean count $\langle n \rangle$ and the Fano factor $F_n(T)$ were calculated from $p(n, T)$. The details of the experiment have been described by TEICH, SALEH and LARCHUK [1984] and by TEICH and SALEH [1985].

A representative set of raw data for the post-detection Fano factor $F_n(T)$ (the average for a set of experiments) versus the detected photon count rate $\mu$ (kilocounts/s) is shown in fig. 7.4. Data are presented for Poisson filament light

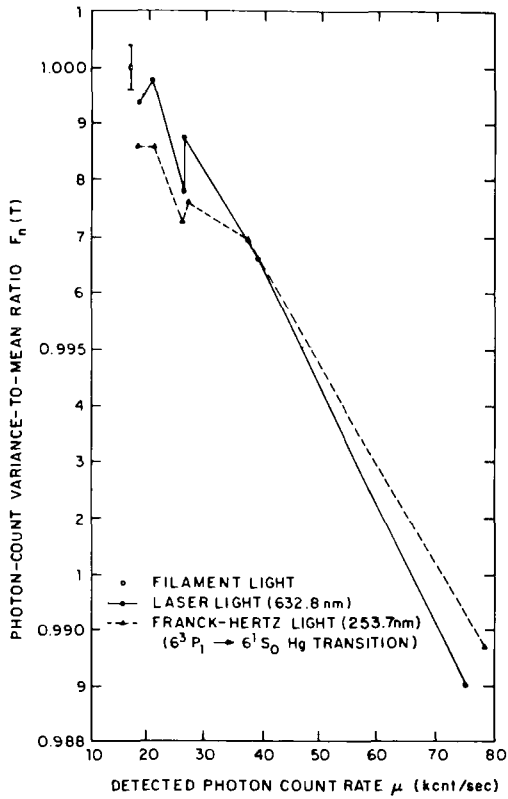


Fig. 7.4. Average post-detection photon-count variance-to-mean ratio (Fano factor) $F_n(T)$ versus detected photon count rate $\mu$ (kilocounts/s), for $T = 1.0$ μs. The error bracket ($\pm 0.0004$) is the same for all data points. The Fano factor for Franck–Hertz light lies below that for Poisson light for several (sufficiently small) values of the count rate $\mu$. The overall negative slope of the data is a result of dead time in the photon-counting apparatus. (After TEICH, SALEH and LARCHUK [1984] and TEICH and SALEH [1985].)

M. C. Teich and B. E. A. Saleh, "Photon Bunching and Ant bunching," in Progress in Optics, vol. 26, edited by E. Wolf (North-Holland, Amsterdam, 1988), ch. 1, pp. 1-104.

(open circle), Poisson filament-plus-laser light (solid circles and solid-line segments), and sub-Poisson Franck–Hertz-plus-filament light (triangles and dashed-line segments). Because of afterpulsing and dead-time effects in the measuring apparatus, the experimental results for the FH light must be compared with those for Poisson light (rather than with a theoretical Poisson distribution) at each value of $\mu$. The filament-plus-laser light provided an excellent Poisson photoelectron distribution because of the short counting time ($T = 1$ μs) and the extremely low value of the PMT quantum efficiency for light at these wavelengths. The standard deviation (SD) for a measurement of $F_n(T)$ that consists of $L = 10^7$ samples turned out to be $\approx (2/L)^{1/2} \approx 0.0004$. This calculated value for the SD was experimentally verified by carrying out many series of runs and is the same for all data points.

In the range $\mu < 30$ kilocounts/s ($\langle n \rangle < 0.03$), values of the Fano factor for the Franck–Hertz light were below those of the Poisson light by between 2 and 3 standard deviations (depending on the details of how the estimates are made). A number of corrections (PMT afterpulsing, PMT cosmic-ray events, dead time in the photon-counting system, and Poisson filament background counts) were applied to the raw data to obtain an absolute experimental estimate of the post-detection Fano factor $F_n(T)$ for the Franck–Hertz light, which turned out to be $\approx 0.998$ at $T = 1$ μs. At higher count rates the Franck–Hertz light was consistently noisier than the Poisson light. There are several possible explanations for this observation; these include the diminished role that dead time may play for sub-Poisson processes, the increase in the degeneracy parameter of the light, and the possibility of stimulated photoluminescence.

The theoretical Fano factor was calculated from eq. (4.2). Using appropriate estimates for the experimental arrangement ($\eta \approx 0.0025$, $\beta \approx 0.3$, and $F_e \approx 0.1$) provides an expected Fano factor $F_n(T) = 0.999$, in good accord with the observed value. The small degree of sub-Poisson behavior is principally the result of optical losses in the experimental apparatus.

### 7.1.2. *Space-charge-limited excitation of recombination radiation*

As indicated earlier a useful source of sub-Poisson light should exhibit a photon Fano factor that is substantially below unity while producing a large photon flux with high efficiency, preferably in a directed beam. It should also be small in size and rapidly switchable.

This has led to a proposal for a semiconductor device structure in which sub-Poisson electron excitations are attained through space-charge-limited current flow, and single-photon emissions are achieved by means of recombi-

M. C. Teich and B. E. A. Saleh, "Photon Bunching and Ant bunching," in Progress in Optics, vol. 26, edited by E. Wolf (North-Holland, Amsterdam, 1988), ch. 1, pp. 1-104.

nation radiation (TEICH, CAPASSO and SALEH [1987]). Again, this scheme is of the form represented in fig. 7.1a. A device of this nature will emit sub-Poisson recombination radiation. The energy-band diagram for such a space-charge-limited light-emitting device (SCL-LED) is illustrated in fig. 7.5. Sub-Poisson electrons are directly converted into sub-Poisson photons, as in the space-charge-limited Franck–Hertz experiment, but these are now recombination photons in a semiconductor. In designing such a device, carrier and photon confinement should be optimized and optical losses should be minimized. The basic structure of the device is that of a $p^+$–i–$n^+$ diode. Near-infrared recombination radiation is emitted from the LED-like region.

The current noise in such a space-charge-limited diode (SZE [1969]) can be low. It has a thermal (rather than shot-noise) character (LAMPERT and ROSE [1961], NICOLET, BILGER and ZIJLSTRA [1975a,b]). The current noise spectral density $S_e(\omega)$ for a device in which only electrons participate in the conduction process is given by (TEICH, CAPASSO and SALEH [1987])

$$\frac{S_e(\omega)}{2e\langle i_e\rangle} = \frac{8k\theta}{e\langle V_e\rangle}, \tag{7.1}$$

where $\langle i_e\rangle$ is the average forward current in the device. $\langle V_e\rangle$ is the applied forward-bias voltage, $k$ is Boltzmann's constant, $\theta$ is the device temperature in K, $\omega$ is the circular frequency, and $e$ is the electronic charge.

Using eqs. (4.1) and (4.5), the degree of sub-Poisson behavior of the detected photons is then expected to be (TEICH, CAPASSO and SALEH [1987])

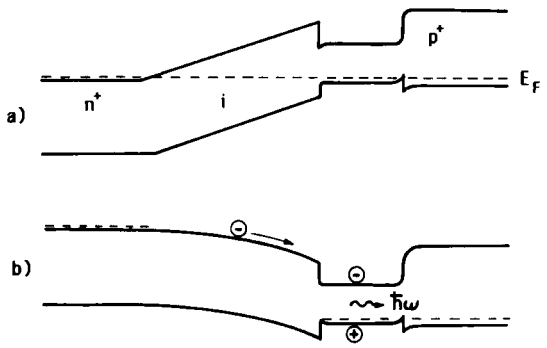


Fig. 7.5. Energy-band diagram of a specially constructed, solid-state space-charge-limited light-emitting device under (a) equilibrium conditions and (b) strong forward-bias conditions. The curvature of the intrinsic region under forward-bias conditions indicates the space-charge potential. (After TEICH, CAPASSO and SALEH [1987].)

$$F_n(T) = 1 + \eta\left(\frac{8k\theta}{e\langle V_e\rangle} - 1\right), \tag{7.2}$$

provided that background light is absent ($\beta = 1$). For a space-charge-limited diode, such as that shown in fig. 7.5, it is estimated that $8k\theta/e\langle V_e\rangle \approx 0.1$ when $\theta = 300$ K and $\langle V_e\rangle = 2$ V (corresponding to $\langle i_e\rangle \approx 33$ mA). This ratio can be further reduced by cooling the device. If a dome-shaped surface-emitting GaAs/GaAlAs configuration and a Si p–i–n photodetector are used, the overall quantum efficiency is estimated to be $\eta \approx 0.1125$, yielding an overall estimated post-detection Fano factor $F_n(T) \approx 0.899$. A commercially available standard LED should provide $F_n(T) \approx 0.973$. In both cases $T$ can be as short as $\approx 1$ ns.

The space-charge-limited light-emitting device therefore promises sub-Poisson light with properties that are significantly superior to those of the mercury-vapor space-charge-limited Franck–Hertz source discussed in the previous subsection ($F_n(T) \approx 0.998$ with $T \approx 1$ μs). Indeed, the degree of sub-Poisson behavior of the recombination radiation from the SCL-LED is limited essentially only by the geometrical collection efficiency.

### 7.1.3. *Sub-Poisson excitations and stimulated emissions*

The properties of the light generated by the SCL-LED might be subject to improvement if stimulated emissions are permitted. These include improved beam directionality, switching speed, spectral properties, and coupling to an optical fiber. This could be achieved by the use of an edge-emitting (rather than surface-emitting) LED configuration, with its waveguiding geometry and superfluorescence properties (single-pass stimulated emission). Although eqs. (4.1) and (4.5) were explicitly derived for independent photon emissions, they will apply even if the photon emissions are not independent, as is the case when stimulated emission plays a role, provided that $T \gg \tau_e, \tau_c$; $A \gg A_c$, where $\tau_c$ and $A_c$ are now the coherence time and coherence area of the superfluorescent emission, respectively. The effect of the stimulated emissions is to extend $\tau_p$ into $\tau_c$ and to reduce the coherence area $A_c$. From a physical point of view the photons still behave as classical particles in this regime, since each electron gives rise to a single photon and there is no memory beyond the counting interval $T$.

There will likely be further advantage in combining space-charge-limited current injection with a semiconductor laser structure rather than with a LED structure. This method would provide increased emission efficiency as well as additional improvement in beam directionality, switching speed, spectral

M. C. Teich and B. E. A. Saleh, "Photon Bunching and Ant bunching," in Progress in Optics, vol. 26, edited by E. Wolf (North-Holland, Amsterdam, 1988), ch. 1, pp. 1-104.

properties, and coupling. This will be beneficial when the laser can be drawn into a realm of operation in which it produces a state more akin to a number state than a coherent state (the coherent state has Poisson photon-number fluctuations and minimal phase fluctuations) (FILIPOWICZ, JAVANAINEN and MEYSTRE [1986], YAMAMOTO, MACHIDA and NILSSON [1986], YAMAMOTO, IMOTO and MACHIDA [1986b], YAMAMOTO and MACHIDA [1987]). MACHIDA, YAMAMOTO and ITAYA [1987] have shown that this mode of operation can be attained in a semiconductor laser oscillator, within the cavity bandwidth and at high photon-flux levels, if the pump fluctuations are suppressed below the shot-noise level, using external feedback to achieve the pump quieting (see § 7.2.4). Related suggestions have been made by SMIRNOV and TROSHIN [1985] and by CARROLL [1986].

## 7.2. METHODS USING EXTERNAL FEEDBACK

A number of external-feedback mechanisms can be used to ensure that the *current* flowing in a circuit is sub-Poisson. These include both opto-electronic and current-stabilization schemes. In § 7.2.1 we discuss the use of two negative-feedback schemes that rely on the use of a light source and detector in a feedback loop. However, under ordinary conditions the use of a beamsplitter to extract a portion of these in-loop photons is not useful for producing nonclassical light, as discussed in § 7.2.2.

In § 7.2.3 we discuss the possibility of generating sub-Poisson photons from sub-Poisson electrons by making use of external excitation feedback and an in-loop auxiliary optical source. Sub-Poisson electrons flow through the auxiliary source and produce sub-Poisson photons en route. The photon number represents a nondestructive measurement of the *electron* number. The robustness of the electrons permits them to emit recombination photons without being destroyed. In this sense this configuration is like the Franck–Hertz experiment in which we begin with atoms and electrons and end with atoms, electrons and photons. The QND measurement discussed in § 6.2.4, on the other hand, begins with atoms and photons and ends with atoms, photons and electrons, which is a more difficult process to achieve.

Finally, in § 7.2.4 we discuss the generation of sub-Poisson electrons by means of an electronic scheme, namely, external current stabilization.

### 7.2.1. *Opto-electronic generation of sub-Poisson electrons*

Sub-Poisson excitations can be generated by the use of external feedback. Two opto-electronic experiments incorporating external feedback have been

M. C. Teich and B. E. A. Saleh, "Photon Bunching and Ant bunching," in Progress in Optics, vol. 26, edited by E. Wolf (North-Holland, Amsterdam, 1988), ch. 1, pp. 1-104.

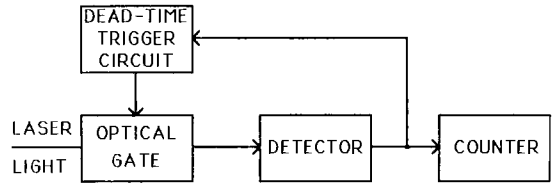


Fig. 7.6. Generation of antibunched and sub-Poisson *electrons* by external feedback, as studied by WALKER and JAKEMAN [1985a].

used to generate sub-Poisson *electrons*. One of these experiments was carried out by WALKER and JAKEMAN [1985a] (see also BROWN, JAKEMAN, PIKE, RARITY and TAPSTER [1986]) and the other by MACHIDA and YAMAMOTO [1986] (see also YAMAMOTO, IMOTO and MACHIDA [1986a]). The simplest form of the experiment carried out by WALKER and JAKEMAN [1985a] is illustrated in fig. 7.6. The registration of a photoevent at the detector operates a trigger circuit, which causes an optical gate to be closed for a fixed period of time $\tau_d$ following the time of registration. During this period, the power $P_t$ of the (He–He) laser illuminating the detector is set precisely equal to zero so that no photoevents are registered. This is the dead-time optical gating scheme shown schematically in fig. 1.1b and discussed in § 6.2.2. Sub-Poisson photoelectrons were observed.

MACHIDA and YAMAMOTO'S [1986] experiment (fig. 7.7) has a similar thrust, although it is based on rate compensation (see fig. 1.1f). They used a single-longitudinal-mode GaAs/AlGaAs semiconductor injection laser diode (LD) to generate light and a Si p–i–n photodiode (PD) to detect it, as shown in fig. 7.7a. Negative electrical feedback from the detector was provided to the current driving the laser diode. A sub-shot-noise spectrum and sub-Poisson photoelectron counts were observed.

The similarity in the experimental results reported by WALKER and JAKEMAN [1985a] and by MACHIDA and YAMAMOTO [1986] can be understood from a physical point of view. In the configuration used by the latter authors, the injection-laser current (and therefore the injection-laser light output) is reduced in response to peaks of the in-loop photodetector current $i_t$. This rate compensation is essentially the same effect as that produced in the Walker–Jakeman experiment where the He–Ne laser light output is reduced (in their case to zero) in response to photoevent registrations at the in-loop photodetector. The feedback acts like a dead time, suppressing the emission of light in a manner that is correlated with photoevent occurrences at the in-loop detector.

M. C. Teich and B. E. A. Saleh, "Photon Bunching and Ant bunching," in Progress in Optics, vol. 26, edited by E. Wolf (North-Holland, Amsterdam, 1988), ch. 1, pp. 1-104.

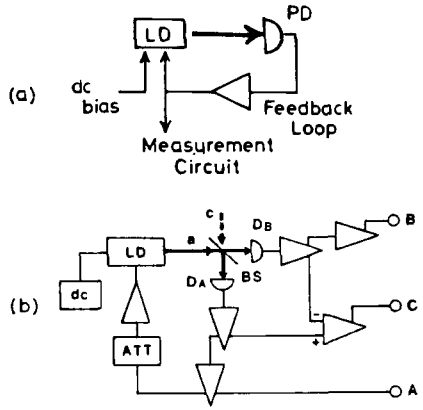


Fig. 7.7. (a) Generation of antibunched and sub-Poisson *electrons* by external feedback using rate compensation, as investigated by MACHIDA and YAMAMOTO [1986]. (b) The removal of in-loop photons by a beamsplitter leads to super-Poisson light at the out-of-loop detector ($D_B$), as understood from the arguments of WALKER and JAKEMAN [1985a] and SHAPIRO, TEICH, SALEH, KUMAR and SAPLAKOGLU [1986]. (After MACHIDA and YAMAMOTO [1986].)

### 7.2.2. *Extraction of in-loop photons by a beamsplitter*

Unfortunately, these simple configurations cannot generate usable sub-Poisson *photons*, since the feedback current controlling the source is generated from the annihilation of the in-loop photons. Indeed, any ordinary attempt to remove in-loop photons by means of a beamsplitter, such as that made by MACHIDA and YAMAMOTO [1986], as illustrated in fig. 7.7b, will lead to super-Poisson light. This result can be understood in terms of the arguments of WALKER and JAKEMAN [1985a], SHAPIRO, TEICH, SALEH, KUMAR and SAPLAKOGLU [1986], and SHAPIRO, SAPLAKOGLU, HO, KUMAR, SALEH and TEICH [1987].

A heuristic explanation for this phenomenon is as follows. The point process registered at the in-loop detector ($D_A$) is a self-exciting point process (SEPP), providing sub-Poisson counts. Because there is no feedback from the out-of-loop detector ($D_B$), however, it registers a doubly stochastic Poisson point process (DSPP). The laser-diode current fluctuations, regulated by the events at the in-loop detector, provide a form of asynchronous modulation of the light power seen by the out-of-loop detector, thereby leading to a photocount variance that is greater than the photocount mean. The result is confirmed by the experiments of WALKER and JAKEMAN [1985a].

From a quantum-mechanical point of view, the culprit is the open port of the

beamsplitter used for the extraction of light. It is possible, at least in principle, to use a beamsplitter to extract sub-Poisson photons if the open port of the beamsplitter is filled with squeezed-vacuum radiation (CAVES [1987]).

When components other than beamsplitters are used, the electrical feedback technique can be useful in generating sub-Poisson light. Two examples involving photon feedback have already been cited: the use of correlated photon pairs (as discussed in § 6.2.1 to § 6.2.3) and when a QND measurement may be made (as discussed in § 6.2.4).

### 7.2.3. *Use of an in-loop auxiliary optical source*

One of the more direct ways of producing antibunched and sub-Poisson light from a system making use of external feedback is to insert an auxiliary optical source in the path of the sub-Poisson electron stream, as suggested by CAPASSO and TEICH [1986]. Two alternative configurations are shown in fig. 7.8. The character of the photon emitter is immaterial; it has been chosen to be a light-emitting diode (LED) for simplicity, but it could be a laser. In fig. 7.8a the photocurrent derived from the detection of light is negatively fed back to the LED input. It has been established both experimentally (MACHIDA and YAMAMOTO [1986]) and theoretically (SHAPIRO, TEICH, SALEH, KUMAR and SAPLAKOGLU [1986]) that, in the absence of the block labeled "source", sub-Poisson electrons (i.e., a sub-shot-noise photocurrent) will flow in a circuit such as this. This conclusion is also valid in the presence of this block, which in this case acts simply as an added impedance to the electron flow.

Incorporating this element into the system offers access to the loop and permits the sub-Poisson electrons flowing in the circuit to be converted into sub-Poisson photons by means of dipole electronic transitions. This process is achieved by replacing the detector used in the feedback configurations of MACHIDA and YAMAMOTO [1986] and WALKER and JAKEMAN [1985a] with a structure that acts simultaneously as a detector and a source. The sub-Poisson electrons emit sub-Poisson photons and continue on their way. The configuration presented in fig. 7.8b is similar, except that the (negative) feedback current gates the light intensity at the output of the LED in the manner of Walker and Jakeman, rather than the current at its input in the manner of Machida and Yamamoto. Any similar scheme, such as selective deletion (SALEH and TEICH [1985]) could be used as well.

Two possible solid-state detector/source configurations have been suggested (CAPASSO and TEICH [1986]). The scheme shown in fig. 7.9a makes use of sequential resonant tunneling (CAPASSO, MOHAMMED and CHO [1986]) and

M. C. Teich and B. E. A. Saleh, "Photon Bunching and Ant bunching," in Progress in Optics, vol. 26, edited by E. Wolf (North-Holland, Amsterdam, 1988), ch. 1, pp. 1-104.

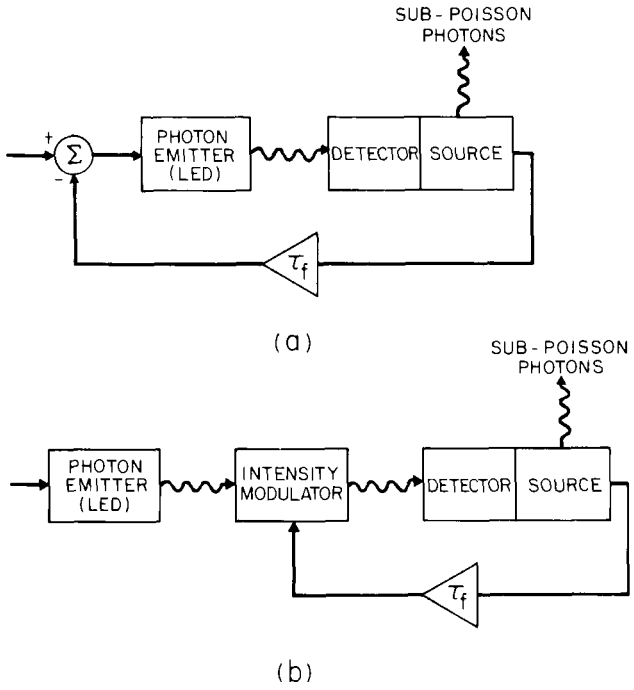


Fig. 7.8. Generation of antibunched and sub-Poisson photons by insertion of an auxiliary source into the path of a sub-Poisson electron stream, as proposed by CAPASSO and TEICH [1986]. Wavy lines represent photons; solid lines represent the electron current; $\tau_f$ signifies the feedback time constant. The schemes represented in (a) and (b) make use of the sub-Poisson electron production methods illustrated in figs. 7.7 and 7.6, respectively. (After CAPASSO and TEICH [1986].)

single-photon electronic dipole transitions between the energy levels of a quantum-well heterostructure. The device consists of a reverse-biased $p^+$–i–$n^+$ diode, where the $p^+$ and $n^+$ heavily doped regions have a wider bandgap than the high-field, light-absorbing/emitting i region. This arrangement ensures both high quantum efficiency at the incident photon wavelength (to which the $p^+$ window layer is transparent) and high collection efficiency (due to the waveguide geometry) for the light generated by the electrons drifting in the i layer. An edge-emitting geometry is therefore appropriate. To maximize the collection efficiency, some of the facets of the device could be reflectively coated. The scheme shown in fig. 7.9b is similar, except that it uses the impact excitation of electroluminescent centers in the i region by drifting electrons. Of course, the ability of configurations such as these to generate sub-Poisson light requires a number of interrelations among various characteristic times associated with the system, much as those represented in eq. (4.1).

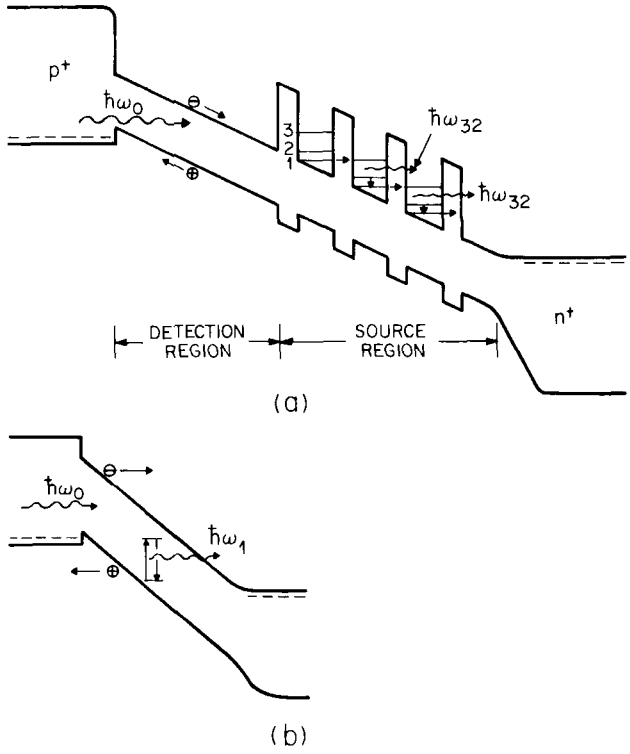


Fig. 7.9. (a) Representative energy-band diagram of a quantum-well detector/source device (see fig. 7.8). The energy of the incident photon emitted by the LED is denoted $\hbar\omega_0$. Detection and source regions are shown. Photons of energy $\hbar\omega_{32}$ are emitted by means of electronic quantum-well transitions. (b) Representative energy-band diagram of a detector/source device with electroluminescent centers impact-excited by energetic photoelectrons, emitting photons with energy $\hbar\omega_1$. (After CAPASSO and TEICH [1986].)

An estimate of the degree to which this mechanism will give rise to sub-Poisson light is, of course, provided by the Fano factor. The relevant relations are similar to those for the Franck–Hertz source, since the emissions are independent. However, in this situation a single electron may give rise to multiple photons, since there is a number of stages in the device. We consider a sub-Poisson electron counting process e, each event of which independently generates a random number of photons $\alpha$ in the source. The overall photon-number Fano factor $F_n(T)$ can then be represented in terms of the Fano factor for the electron number $F_e(T)$ and the Fano factor for the source random variable $F_\alpha(T)$. From eq. (3.48), the relationship is

$$F_n = \langle \alpha \rangle F_e + F_\alpha , \tag{7.3}$$

where $\langle \alpha \rangle$ is the average number of photons generated in the source by each electron.

For the case at hand it is reasonable to assume that the source random variable is Bernoulli distributed in each stage of the device, with the probability that an electron gives rise to a photon denoted $\eta_r$. No generality is lost by considering the multilayer superlattice case, which consists of $u$ independent stages. The source statistics will then be described by a binomial random variable with $\langle \alpha \rangle = u\eta_r$ and $\mathrm{Var}(\alpha) = u\eta_r(1 - \eta_r)$. In the presence of random deletion arising from other factors (e.g., finite geometrical photon-collection efficiency, absorption, external detection) and background or dark photons, these results remain valid if $\eta_r$ is replaced by the quantity $\eta\beta$, where $\eta$ is the overall quantum efficiency from electrons to detected photons and $\beta$ is the factor representing the admixture of independent dark and/or background events (see § 4.2). Equation (7.3) then gives rise to

$$[F_n - 1] = \eta\beta[uF_e - 1], \tag{7.4}$$

which differs from eq. (4.2) in that it depends on $u$. It is evident that sub-Poisson behavior is achieved when $F_e < 1/u$. The lowest Fano factor at the output is achieved when $u = 1$. In this case the photon counting process is simply a randomly deleted version of the electron counting process so that eq. (7.4) reduces to eq. (4.2).

Assuming that $\beta \approx 1$, numerical estimates for the Fano factor turn out to be similar for both structures illustrated in fig. 7.9, viz. $F_n \approx 0.968$ (under the assumption that the photodetector has an external quantum efficiency of 0.8). This provides a substantial potential improvement over the value observed in the space-charge-limited Franck–Hertz experiment. However, the Fano factor is not as low as that attainable by the SCL-LED, principally because of low radiative efficiency in the tunneling scheme. Furthermore the external feedback mechanism is likely to be slower than the internal feedback scheme of the SCL-LED.

### 7.2.4. *Use of a current source with external compensation*

Probably the simplest way of achieving sub-Poisson electron counting statistics and single-photon emissions is by discharging a capacitor $C$ through a circuit containing a photon emitter such as a light-emitting diode (LED). The current waveform then will be a nonstationary pulse with time constant $\tau_{RC} = RC$ (where $R$ is the resistance of the circuit). Steady-state current stabilization can be achieved by the use of a constant voltage source in series

M. C. Teich and B. E. A. Saleh, "Photon Bunching and Ant bunching," in Progress in Optics, vol. 26, edited by E. Wolf (North-Holland, Amsterdam, 1988), ch. 1, pp. 1-104.

with a sufficiently large external resistor $R$ (YAMAMOTO, MACHIDA and NILSSON [1986], YAMAMOTO and MACHIDA [1987]), or in series with some other optoelectronic component with suitable $I-V$ characteristic.

Strong sub-Poisson light has recently been generated in two experiments that make use of external compensation. TAPSTER, RARITY and SATCHELL [1987] carried out an elegantly simple experiment, using a high-efficiency commercial GaAs LED fed by a Johnson-noise-limited high-impedance current source. They achieved a Fano factor $F_n \approx 0.96$ over a bandwidth of about 100 kHz, with a current transfer efficiency $\eta$ in excess of 11%. MACHIDA, YAMAMOTO and ITAYA [1987] fed a InGaAsP/InP single-longitudinal-mode distributed-feedback laser oscillator, operating at a wavelength of 1.56 μm, with a current source whose fluctuations were suppressed by the use of an external high-impedance element. These authors obtained an average Fano factor $F_n \approx 0.96$ over a bandwidth of about 100 MHz, with a minimum Fano factor $F_n \approx 0.93$. They calculate that the radiation produced by their device is in a near number–phase minimum-uncertainty state (JACKIW [1968]), in the frequency range below the cavity bandwidth (which is in excess of 100 GHz for a typical semiconductor laser). These results are impressive. It should be kept in mind, however, that the characteristic electron anticorrelation time $\tau_f$ in external feedback circuits such as these is likely to be larger than $\tau_e$ for space-charge-limited electron excitations, as pointed out earlier.

### 7.3. LIMITATIONS OF EXCITATION-FEEDBACK METHODS

We have shown that the generation of sub-Poisson light is best achieved by the use of sub-Poisson electron excitations, mediated by a physical mechanism such as space charge, and a single photon emission for each excitation. This method is in general superior to nonlinear-optics methods. A space-charge-limited light-emitting structure that operates in this manner has been discussed.

In all cases using external feedback, the characteristic anticorrelation time of the excitations $\tau_e$ is determined by the feedback time constant of the loop $\tau_f$. A lower limit on the feedback time constant is imposed by the response time and transit time of carriers through the device and by the $RC$ characteristics of the feedback circuitry. In general, an internal feedback process such as space charge will provide a more effective means of providing sub-Poisson excitations than external feedback. This is because an internal physical process is likely to result in a smaller value of $\tau_e$ than will external electronic circuitry. Configurations making use of space-charge-limited excitations will therefore have the capacity of being switched faster than those making use of external

M. C. Teich and B. E. A. Saleh, "Photon Bunching and Ant bunching," in Progress in Optics, vol. 26, edited by E. Wolf (North-Holland, Amsterdam, 1988), ch. 1, pp. 1-104.

feedback, although this distinction is not likely to be important if external switching can be used.

## § 8. Information Transmission using Sub-Poisson Light

Sub-Poisson light may find use in the study of optical interactions in various disciplines, ranging from the behavior of the human visual system at the threshold of seeing (TEICH, PRUCNAL, VANNUCCI, BRETON and MCGILL [1982]) to optical precision measurement (JAKEMAN and RARITY [1986]). In this section we consider the potential use of sub-Poisson light in direct-detection lightwave communication systems and other information carrying applications. Systems of this kind that have been developed to date make use of Poisson or super-Poisson light (GAGLIARDI and KARP [1976], HELSTROM [1976], SALEH [1978], KOGELNIK [1985], HENRY [1985], SENIOR [1985]).

There are essentially two classes of mechanisms by means of which unconditionally sub-Poisson photons may be generated. Sub-Poisson photons can be produced from a beam of initially Poisson (or super-Poisson) photons, represented by the photon-feedback examples of § 6 (see fig. 1.1). Alternatively, unconditionally sub-Poisson photons may be directly generated from sub-Poisson excitations, as represented by the examples of § 7.

In §§ 8.1 and 8.2 we discuss the channel capacity of a lightwave communication system based on the observation of the photoevent *point process*, demonstrating that it *cannot* in principle be increased by the use of sub-Poisson light. In § 8.3, on the other hand, we show that the channel capacity of a *photon-counting* system *can* be increased by the use of sub-Poisson light (SALEH and TEICH [1987]). The channel capacity is the maximum rate of information that can be transmitted through a channel without error. The capacity of the photon channel has been the subject of a number of studies over the years (STERN [1960], GORDON [1962], PIERCE, POSNER and RODEMICH [1981], YAMAMOTO and HAUS [1986]). In § 8.4, we provide an example in which the use of sub-Poisson light produced from Poisson light either degrades or enhances the *error performance* of a simple binary ON–OFF keying photon-counting system, depending on where the average power constraint is placed. Finally, in § 8.5, we conclude with a discussion pertaining to some limitations on direct-detection communications using sub-Poisson light.

M. C. Teich and B. E. A. Saleh, "Photon Bunching and Ant bunching," in Progress in Optics, vol. 26, edited by E. Wolf (North-Holland, Amsterdam, 1988), ch. 1, pp. 1-104.

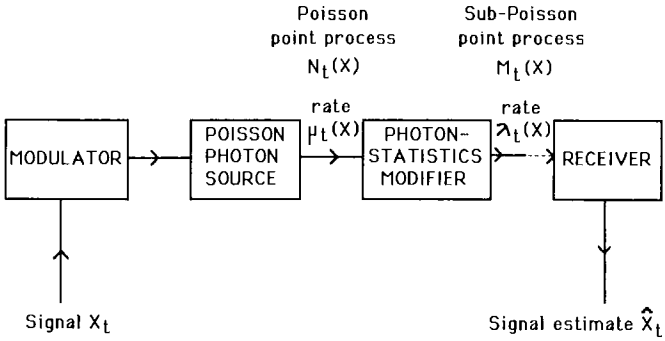


Fig. 8.1. Idealized lightwave communication system employing a Poisson photon source and a photon-statistics modifier.

## 8.1. COMMUNICATING WITH MODIFIED POISSON PHOTONS

Consider the transformation of a Poisson beam of photons (represented by a Poisson point process $N_t$ of rate $\mu_t$) into a sub-Poisson beam of photons represented by a point process $M_t$ of rate $\lambda_t$, as illustrated in fig. 8.1. The events of the initial process $N_t$ are assumed to be observable (e.g., by the use of correlated photon beams or a QND measurement) and their registrations used to operate a mechanism which, in accordance with a specified rule, leads to the events of the transformed photon process $M_t$. The rate $\lambda_t$ of the process $M_t$ is thereby rendered a function of the realizations of the initial point process $N_t$ at prior times, i.e., $\lambda_t = \lambda_t(N_{t'};\ t' \leqslant t)$.

Several examples of transformations of this kind that have been suggested for use in quantum optics have been discussed earlier and were illustrated in fig. 1.1. They include dead-time deletion, coincidence decimation, decimation, and overflow count deletion. We proceed to illustrate that none of these modifications can increase the channel capacity $C$ of a communication system based on photoevent point-process observations.

If a constraint is placed on the rate of the initial Poisson process $\mu_t \leqslant \mu_{\max}$, then it is obvious that $C$ cannot be increased by the modification $N_t \rightarrow M_t$. This is simply a consequence of the definition of channel capacity: it is the rate of information carried by the system without error, maximized over all coding, modulation, and *modification* schemes. Can the modification $N_t \rightarrow M_t$ increase the channel capacity if the constraint is instead placed on the rate of the modified process $\lambda_t$ (i.e., $\lambda_t \leqslant \lambda_{\max}$)? We address this question for an arbitrary self-exciting point process in the next section.

M. C. Teich and B. E. A. Saleh, "Photon Bunching and Ant bunching," in Progress in Optics, vol. 26, edited by E. Wolf (North-Holland, Amsterdam, 1988), ch. 1, pp. 1-104.

## 8.2. COMMUNICATING WITH SUB-POISSON PHOTONS DESCRIBED BY A SELF-EXCITING POINT PROCESS

Consider a self-exciting point process $M_t$ of rate $\lambda_t(M_{t'};\ t' \leqslant t)$. This is a process that contains an inherent feedback mechanism in which present event occurrences are affected by the previous event occurrences of the same point process. Of course, the modified Poisson processes $N_t \to M_t$ introduced above are special cases of self-exciting point processes.

An example of a system that generates a self-exciting point process is that of rate compensation (by linear feedback) of a source which, without feedback, would produce a Poisson process. Let each photon registration at time $t_i$ cause the rate of the process to be modulated by a factor $h(t - t_i)$ (which vanishes for $t < t_i$). In linear negative feedback the rate is $\lambda_t = \lambda_0 - \sum_i h(t - t_i)$, where $\lambda_0$ is a constant. If the instantaneous photon registration rate happens to be above the average then it is reduced, and vice versa. This process is schematically illustrated in fig. 1.1f for two adjacent sub-intervals $T_1$ and $T_2$.

Now consider a communication system that uses a point process $M_t(X)$ whose rate $\lambda_t(X)$ is modulated by a signal $X_t$. The process $M_t(X)$ can be an arbitrary self-exciting point process (e.g., it can be sub-Poisson) which includes processes obtained by the feedforward- or feedback-modification of an otherwise Poisson process. Neither feedforward nor feedback transformations can increase the capacity of this channel, as provided by Kabanov's theorem (KABANOV [1978]), and its extensions (DAVIS [1980], LAZAR [1980]):

**Kabanov's theorem.** *The capacity of the point-process channel cannot be increased by feedback.* Under the constraint $\lambda_0 \leqslant \lambda_t \leqslant \lambda_{\max}$, the channel capacity $C$ is

$$C = \lambda_0\left[\frac{1}{\mathrm{e}}\left(1 + \frac{s}{\lambda_0}\right)^{1 + \lambda_0/s} - \left(1 + \frac{\lambda_0}{s}\right)\ln\left(1 + \frac{s}{\lambda_0}\right)\right], \tag{8.1}$$

where $s = \lambda_{\max} - \lambda_0$. When $\lambda_0 = 0$ (no dark counts), this expressions reduces to

$$C = \frac{\lambda_{\max}}{\mathrm{e}}. \tag{8.2}$$

When the capacity is achieved, the output of the zero-dark-count point-process channel is a Poisson process with rate $\lambda_t = \lambda_{\max}/\mathrm{e}$ (the base e has been used for simplicity). The channel capacity has also been determined under added constraints on the mean rate. A coding theorem has also been proved. Kabanov's theorem is analogous to the well-known result that the capacity of

the white Gaussian channel cannot be increased by feedback (KADOTA, ZAKAI and ZIV [1971]).

In summary, no increase in the channel capacity of a point-process lightwave communication system may be achieved by using photons that are first generated with Poisson statistics and subsequently converted into sub-Poisson statistics regardless of whether the power constraint is placed at the Poisson photon source or at the output of the conversion process. Nor may an increase in channel capacity be achieved by using feedback to generate a self-exciting point process.

### 8.3. COMMUNICATING WITH SUB-POISSON PHOTON COUNTS

The conclusions of §§ 8.1 and 8.2 are valid only when there are no restrictions on the receiver structure. The conclusion is different if the receiver is operated in the photon-*counting* regime, in which information is carried by a random variable $n$ representing the number of photoevents registered in time intervals of prescribed duration $T$ (rather than by the photon occurrence times).

The capacity of the photon-counting channel is given by (GORDON [1962])

$$C = B\left[\langle n\rangle \ln\left(1 + \frac{1}{\langle n\rangle}\right) + \ln(1 + \langle n\rangle)\right], \tag{8.3}$$

where $\langle n\rangle$ is the mean number of counts in $T$ and $B = 1/T$. Two limiting expressions emerge:

$$C = B\langle n\rangle \ln\left(\frac{1}{\langle n\rangle}\right), \quad \langle n\rangle \ll 1,$$

$$C = B\ln(\langle n\rangle), \qquad \langle n\rangle \gg 1. \tag{8.4}$$

If an added constraint is applied to the photon counts, such that they must obey the Poisson counting distribution, the capacity is further reduced. In that case, the limiting results analogous to eq. (8.4) are

$$C = B\langle n\rangle \ln\left(\frac{1}{\langle n\rangle}\right), \quad \langle n\rangle \ll 1,$$

$$C = \tfrac{1}{2}B\ln(\langle n\rangle), \qquad \langle n\rangle \gg 1. \tag{8.5}$$

In the case of photon counting, therefore, an increase in the channel capacity can in principle be realized by using sub-Poisson light. However, in the small

M. C. Teich and B. E. A. Saleh, "Photon Bunching and Ant bunching," in Progress in Optics, vol. 26, edited by E. Wolf (North-Holland, Amsterdam, 1988), ch. 1, pp. 1-104.

mean-count limit $\langle n \rangle \ll 1$ (very short $T$), the capacity of the Poisson counting channel approaches that of the unrestricted counting channel, and the advantage of sub-Poisson light disappears. This is not unexpected in view of the result obtained from Kabanov's theorem for the point-process channel.

### 8.4. PERFORMANCE OF A SUB-POISSON PHOTON-COUNTING RECEIVER

The channel capacity provides a limit on the maximum rate of error-free information transmission for all codes, modulation formats, and receiver structures. As such, it does not specify the performance (error probability) achievable by a communication system with prescribed coding, modulation, and receiver structure.

It is therefore of interest to examine the performance of a system with specified structure. We consider a binary ON–OFF keying (OOK) photon-counting system (GAGLIARDI and KARP [1976], HELSTROM [1976], SALEH [1978], KOGELNIK [1985], HENRY [1985], SENIOR [1985]). The information is transmitted by selecting one of two values for the photon rate $\lambda_r$, in time slots of (pulse) duration $T$. The receiver operates by counting the number of photons received during the time interval $T$ and then deciding which rate was transmitted in accordance with a likelihood-ratio decision rule (threshold test). For simplicity, it is assumed that background light, dark noise, and thermal noise are absent so that photon registrations are not permitted when the keying is OFF (i.e., false alarms are not possible). Furthermore, the detector quantum efficiency is initially taken to be unity so that system performance is limited only by the quantum fluctuations of the light.

A measure of performance for a digital system such as this is the error probability $P_e$. In the simplified system described above, errors are possible only when the keying is ON and 0 photons are received (a miss). For a Poisson transmitter, with equal a priori probabilities for ON and OFF, $P_e$ is (HENRY [1985])

$$P_e(\text{Poisson}) = \tfrac{1}{2} \exp(-\langle n \rangle), \tag{8.6}$$

where $\langle n \rangle$ denotes the mean number of photons in the time $T$ (that is, the number of photons/pulse). To minimize $P_e$, $\langle n \rangle$ is made equal to its maximum allowed value $\langle n \rangle_{\max}$. This result is now compared with those obtained for sub-Poisson light derived from an initially Poisson source. The outcome will depend on where the mean photon-number constraint is placed. Two transformations are explicity considered: dead-time deletion and decimation.

M. C. Teich and B. E. A. Saleh, "Photon Bunching and Ant bunching," in Progress in Optics, vol. 26, edited by E. Wolf (North-Holland, Amsterdam, 1988), ch. 1, pp. 1-104.

It will become evident from these examples that system performance can be enhanced by using sub-Poisson light, provided that the power constraint is applied to the sub-Poisson light. No enhancement of system performance emerges in converting Poisson photons into sub-Poisson photons when the average power constraint is at the Poisson source.

### 8.4.1. *Dead-time-modified-Poisson photon counts*

For a nonparalyzable dead-time modifier that is always *blocked* for a dead time period $\tau_d$ at the beginning of the counting interval $T$, the passage of 0 photons arises from the emission of 0 photons in the time $T - \tau_d$, independent of the number of emissions during $\tau_d$. The error probability for this system is therefore

$$P_e(\text{dead-time}) = \tfrac{1}{2}\exp\left[-\langle n\rangle\left(1 - \frac{\tau_d}{T}\right)\right]. \tag{8.7}$$

To minimize error under the constraint $\langle n\rangle \leqslant \langle n\rangle_{max}$, we take $\langle n\rangle = \langle n\rangle_{max}$. The error probability is obviously larger than that for the Poisson channel (eq. 8.6) so no performance enhancement can be achieved by use of this modifier with this constraint.

If, instead, the dead-time modifier is always *unblocked* at the beginning of each bit then the passage of 0 photons can arise only from the emission of 0 photons in the time $T$, and the dead-time has no effect on the error rate in this simple system. Calculations for the unblocked counter in the presence of false alarms, however, demonstrate that the presence of dead time always does, in fact, degrade system performance with such a constraint (TEICH and CANTOR [1978]). Although these detailed calculations were carried out for electrical dead time, the results are also applicable for optical dead time when the photon detection efficiency $\eta = 1$.

On the other hand, if the constraint is placed on the mean photon count $\langle m\rangle$ after dead-time modification ($\langle m\rangle \leqslant \langle m\rangle_{max}$), it can be shown that there exists a value of $\langle m\rangle_{max}$ below which performance is degraded, and above which performance is improved, relative to the Poisson channel.

### 8.4.2. *Decimated-Poisson photon counts*

We assume that the decimation parameter $\mathcal{M} = 2$ (i.e., every other photon of a Poisson sequence of events is selected) and that the decimation process is reset at the beginning of each bit (i.e., the first photon in each bit is not selected).

M. C. Teich and B. E. A. Saleh, "Photon Bunching and Ant bunching," in Progress in Optics, vol. 26, edited by E. Wolf (North-Holland, Amsterdam, 1988), ch. 1, pp. 1-104.

The error probability is then

$$P_e(\text{decimation}) = \tfrac{1}{2}(1 + \langle n \rangle) \exp(-\langle n \rangle), \tag{8.8}$$

which again represents a degradation of performance in comparison with the Poisson channel (under a constraint $\langle n \rangle \leqslant \langle n \rangle_{max}$). In this case, the error rate is increased because there are two ways for the passage of 0 photons to arise in the time $T$: from the emission of 0 photons or from the emission of 1 photon.

However, if the constraint is placed on the modified process then, once again, there exists a value of $\langle m \rangle_{max}$ below which performance is degraded and above which it is improved, relative to the Poisson channel.

8.4.3. *Binomial photon counts*

We conclude by considering the effects of photon deletion. We do this in the context of an ideal sub-Poisson source that generates a deterministic photon number. This is an important consideration because random photon deletion is inevitable; it results from absorption, scattering, and the finite quantum efficiency of the detector, as discussed in § 4. It is well known that such deletions will transform a deterministic photon number into a binomial photon number (MANDEL [1976a]), which always remains sub-Poisson but approaches the Poisson boundary as the photon-survival probability $\eta$ decreases (TEICH and SALEH [1982]). MANDEL [1976a] has shown that the information rate per symbol carried by such a counting channel will be greater than that for the Poisson channel, but will approach the latter as $\eta$ approaches 0. A source that emits a binomial photon number at the outset (STOLER, SALEH and TEICH [1985], DATTOLI, GALLARDO and TORRE [1987]) retains its binomial form, but exhibits a reduced mean, in the presence of random deletion (TEICH and SALEH [1982]).

The performance of such a binary OOK photon-counting receiver, in the absence of background, is limited by the binomial fluctuations of the detected photons. In this case, it is easily shown from the binomial distribution that

$$P_e(\text{binomial}) = \tfrac{1}{2} F_n^{[2\langle n' \rangle/(1 - F_n)]}, \tag{8.9}$$

where $F_n = 1 - \eta$ is the Fano factor of the photon-counting distribution and where $\langle n' \rangle$ represents the mean number of photons/bit ($2\langle n' \rangle = \langle n \rangle$ since there are 2 bits per pulse in OOK). The Poisson result in eq. (8.6) is recovered as $F_n \to 1$. The probability of error represented by eq. (8.9) is plotted as a function of the mean number of photons per bit $\langle n' \rangle$, with the Fano factor $F_n$ as a parameter, in fig. 8.2. System performance improves as $F_n$ decreases.

M. C. Teich and B. E. A. Saleh, "Photon Bunching and Ant bunching," in Progress in Optics, vol. 26, edited by E. Wolf (North-Holland, Amsterdam, 1988), ch. 1, pp. 1-104.

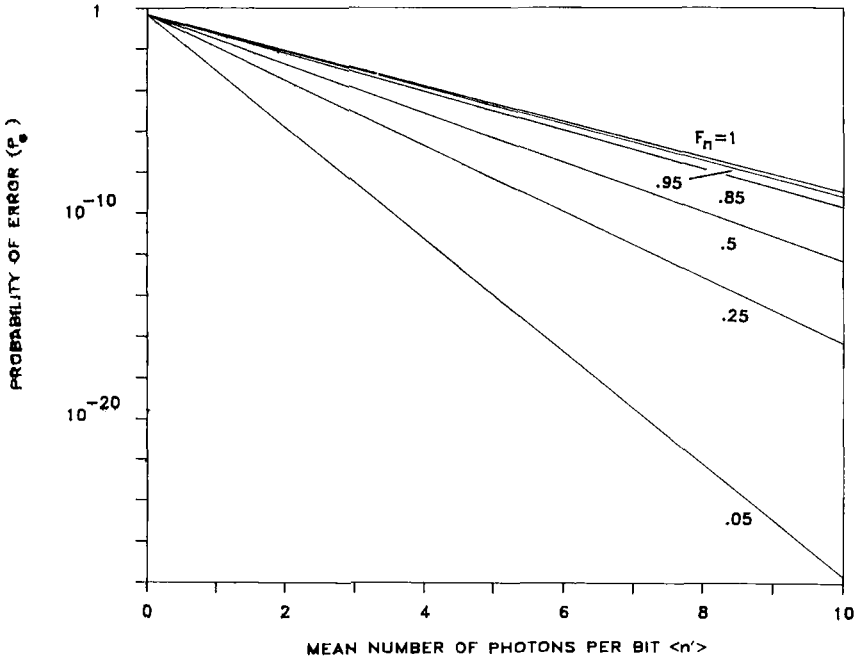


Fig. 8.2. Error probability ($P_e$) versus mean number of photons per bit $\langle n' \rangle$ for the binomial channel, with the Fano factor $F_n$ as a parameter. System performance clearly improves as $F_n$ decreases below unity.

Solving eq. (8.9) for the mean number of photons per bit $\langle n' \rangle$ provides

$$\langle n' \rangle = \tfrac{1}{2}\left[\frac{(1 - F_n)}{\ln(1/F_n)}\right] \ln\left(\frac{1}{2P_e}\right), \tag{8.10}$$

which leads to a direct-detection quantum limit that is $< 10$ photons/bit ($< 20$ photons/pulse) for OOK, if $F_n < 1$ and $P_e = 10^{-9}$. The mean number of photons per bit $\langle n' \rangle$ is plotted as a function of $F_n$ in fig. 8.3. The usual quantum limit ($\langle n' \rangle = 10$ photons/bit) emerges in the limit $F_n = 1$ where the binomial distribution goes over to the Poisson.

## 8.5. LIMITATIONS ON COMMUNICATING WITH SUB-POISSON LIGHT

Sub-Poisson light sources can, in principle, be useful in lightwave communications systems. However, their use will only be practical if they can be made to exhibit high photon flux, low Fano factor, and a short feedback time constant, and if losses in the system as a whole are minimized. Fortunately, photomultiplier tubes and even avalanche photodiodes can (at least in principle)

M. C. Teich and B. E. A. Saleh, "Photon Bunching and Ant bunching," in Progress in Optics, vol. 26, edited by E. Wolf (North-Holland, Amsterdam, 1988), ch. 1, pp. 1-104.

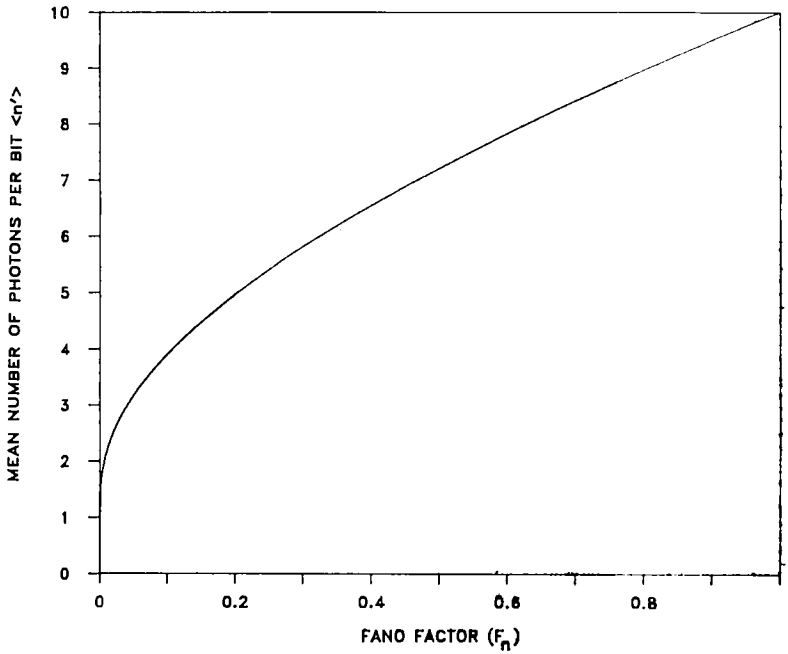


Fig. 8.3. Mean number of photons per bit $\langle n' \rangle$ as a function of the Fano factor $F_n$ for the binomial channel. The well-known "quantum limit" (10 photons/bit) emerges as the binomial distribution goes over to the Poisson distribution ($F_n \to 1$).

detect sub-Poisson light in an essentially noise-free manner (TEICH, MATSUO and SALEH [1986]). The short feedback time constant permits the signaling rate to be high. In conventional systems (i.e., those using Poisson light) this rate is determined by the time character of the source and receiver, subject to there being a sufficiently large number of photons per bit (HENRY [1985]). However, for systems using sub-Poisson photons, the symbol duration $T$ must exceed the anticorrelation time of the photons ($\tau_e$ or $\tau_r$) so that the sub-Poisson nature of the signal is captured (see § 7). Solid-state implementations of single-photon emission devices driven by sub-Poisson currents should therefore be constructed in such a way that $\tau_e$ is made as small as possible (TEICH, CAPASSO and SALEH [1987]).

## References

ANDREWS, L.C., and R.L. PHILLIPS, 1986, J. Opt. Soc. Am. A **3**, 1912.
ARECCHI, F.T., E. GATTI and A. SONA, 1966, Phys. Lett. **20**, 27.
ASPECT, A., 1986, private communication.
ASPECT, A., P. GRANGIER and G. ROGER, 1981, Phys. Rev. Lett. **47**, 460.
ASPECT, A., J. DALIBART and G. ROGER, 1982, Phys. Rev. Lett. **49**, 1804.
ASPECT, A., P. GRANGIER and G. ROGER, 1982, Phys. Rev. Lett. **49**, 91.
BARAKAT, R., 1974, Opt. Acta **21**, 903.

M. C. Teich and B. E. A. Saleh, "Photon Bunching and Ant bunching," in Progress in Optics, vol. 26, edited by E. Wolf (North-Holland, Amsterdam, 1988), ch. 1, pp. 1-104.

BARAKAT, R., 1976, J. Opt. Soc. Am. **66**, 211.
BARAKAT, R., and J. BLAKE, 1976, Phys. Rev. A **13**, 1122.
BARAKAT, R., and J. BLAKE, 1980, Phys. Rep. **60**, 255.
BERAN, M.J., and G.B. PARRENT JR, 1964, Theory of Partial Coherence (Prentice Hall, Englewood Cliffs, NJ).
BORN, M., and E. WOLF, 1980, Principles of Optics, 6th Ed. (Pergamon, Oxford).
BRAGINSKY, V.B., and YU.I. VORONTSOV, 1974, Usp. Fiz. Nauk. **114**, 41 [1975, Sov. Phys.-Usp. **17**, 644].
BRAGINSKY, V.B., and S.P. VYATCHANIN, 1981, Dokl. Akad. Nauk SSSR **259**, 570 [Sov. Phys.-Dokl. **26**, 686].
BRAGINSKY, V.B., and S.P. VYATCHANIN, 1982, Dokl. Akad. Nauk SSSR **264**, 1136 [Sov. Phys.-Dokl. **27**, 478].
BROWN, R.G.W., E. JAKEMAN, E.R. PIKE, J.G. RARITY and P.R. TAPSTER, 1986, Europhys. Lett. **2**, 279.
BURGESS, R.E., 1961, J. Phys. & Chem. Solids **22**, 371.
BURNHAM, D.C., and D.L. WEINBERG, 1970, Phys. Rev. Lett. **25**, 84.
CANTOR, B.I., and M.C. TEICH, 1975, J. Opt. Soc. Am. **65**, 786.
CAPASSO, F., and M.C. TEICH, 1986, Phys. Rev. Lett. **57**, 1417.
CAPASSO, F., K. MOHAMMED and A.Y. CHO, 1986, Appl. Phys. Lett. **48**, 478.
CARMICHAEL, H.J., and D.F. WALLS, 1976a, J. Phys. B **9**, L43.
CARMICHAEL, H.J., and D.F. WALLS, 1976b, J. Phys. B **9**, 1199.
CARMICHAEL, H.J., P. DRUMMOND, P. MEYSTRE and D.F. WALLS, 1978, J. Phys. A **11**, L121.
CARROLL, J.E., 1986, Opt. Acta **33**, 909.
CARRUTHERS, P., and M.M. NIETO, 1968, Rev. Mod. Phys. **40**, 411.
CAVES, C.M., 1986, Amplitude and phase in quantum optics, in: Coherence, Cooperation, and Fluctuations, eds F. Haake, L.M. Narducci and D.F. Walls (Cambridge Univ. Press, Cambridge).
CAVES, C.M., 1987, Opt. Lett. **12**, 971.
CAVES, C.M., K.S. THORNE, R.W.P. DREVER, V.D. SANDBERG and M. ZIMMERMAN, 1980, Rev. Mod. Phys. **52**, 341.
CHANDRA, N., and H. PRAKASH, 1970, Phys. Rev. A **1**, 1696.
CHEN, S.H., and P. TARTAGLIA, 1972, Opt. Commun. **6**, 119.
COOK, R.J., 1980, Opt. Commun. **35**, 347.
COOK, R.J., 1981, Phys. Rev. A **23**, 1243.
COX, D.R., 1955, J. R. Stat. Soc. B **17**, 129.
COX, D.R., 1962, Renewal Theory (Methuen, London).
CRESSER, J.D., J. HÄGER, G. LEUCHS, F.-M. RATEIKE and H. WALTHER, 1982, Resonance fluorescence of atoms in strong monochromatic laser fields, in: Dissipative Systems in Quantum Optics, Topics in Current Physics, Vol. 27, eds R. Bonifacio and L.A. Lugiato (Springer, Berlin) p. 21.
DAGENAIS, M., and L. MANDEL, 1978, Phys. Rev. A **18**, 2217.
DATTOLI, G., J. GALLARDO and A. TORRE, 1987, J. Opt. Soc. Am. B **4**, 185.
DAVIS, M.H.A., 1980, IEEE Trans. Inf. Theory **IT-26**, 710.
DIEDRICH, F., and H. WALTHER, 1987, Phys. Rev. Lett. **58**, 203.
EBELING, K.J., 1980, Opt. Commun. **35**, 323.
EINSTEIN, A., 1909, Phys. Z. **10**, 185.
EVERY, I.M., 1975, J. Phys. A **8**, L69.
FANO, U., 1947, Phys. Rev. **72**, 26.
FILIPOWICZ, P., J. JAVANAINEN and P. MEYSTRE, 1986, Phys. Rev. A **34**, 3077.
FORRESTER, A.T., 1972, J. Opt. Soc. Am. **62**, 654.
FRANCK, J., and G. HERTZ, 1914, Verhandl. Deutsch. Phys. Ges. (Berlin) **16**, 512.
FRANCK, J., and P. JORDAN, 1926, Anregung von Quantensprüngen durch Stöße, in: Struktur der Materie in Einzeldarstellungen, III (Springer, Berlin).

M. C. Teich and B. E. A. Saleh, "Photon Bunching and Ant bunching," in Progress in Optics, vol. 26, edited by E. Wolf (North-Holland, Amsterdam, 1988), ch. 1, pp. 1-104.

FRIBERG, S., C.K. HONG and L. MANDEL, 1985, Phys. Rev. Lett. **54**, 2011.
GABOR, D., 1946, J. Inst. Electron. Eng. **93**, 429.
GAGLIARDI, R.M., and S. KARP, 1976, Optical Communications (Wiley, New York).
GHIELMETTI, F., 1976, Nuovo Cimento B **35**, 243.
GILBERT, E.N., and H.O. POLLAK, 1960, Bell Syst. Tech. J. **39**, 333.
GLAUBER, R.J., 1963a, Phys. Rev. **130**, 2529.
GLAUBER, R.J., 1963b, Phys. Rev. **131**, 2766.
GOODMAN, J., 1985, Statistical Optics (Wiley, New York).
GORDON, J.P., 1962, Proc. IRE **50**, 1898.
GRANGIER, P., G. ROGER and A. ASPECT, 1986, Europhys. Lett. **1**, 173.
GRANGIER, P., G. ROGER, A. ASPECT, A. HEIDMANN and S. REYNAUD, 1986, Phys. Rev. Lett. **57**, 687.
HANBURY-BROWN, R., 1974, The Intensity Interferometer (Taylor and Francis, London).
HANBURY-BROWN, R., and R.Q. TWISS, 1956a, Nature **177**, 27.
HANBURY-BROWN, R., and R.Q. TWISS, 1956b, Nature **178**, 1046.
HEIDMANN, A., R.J. HOROWICZ, S. REYNAUD, E. GIACOBINO and C. FABRE, 1987, Phys. Rev. Lett. **59**, 2555.
HELSTROM, C.W., 1976, Quantum Detection and Estimation Theory (Academic, New York).
HENRY, P.S., 1985, IEEE J. Quantum Electron. **QE-21**, 1862.
HOENDERS, B.J., E. JAKEMAN, H.P. BALTES and B. STEINLE, 1979, Opt. Acta **26**, 1307.
HONG, C.K., and L. MANDEL, 1985, Phys. Rev. A **31**, 2409.
HONG, C.K., and L. MANDEL, 1986, Phys. Rev. Lett. **56**, 58.
IMOTO, N., H.A. HAUS and Y. YAMAMOTO, 1985, Phys. Rev. A **32**, 2287.
JACKIW, R., 1968, J. Math. Phys. **9**, 339.
JAKEMAN, E., 1980a, Proc. Soc. Photo-Opt. Instrum. Eng. **243**, 9.
JAKEMAN, E., 1980b, J. Phys. A **13**, 31.
JAKEMAN, E., 1982, J. Opt. Soc. Am. **72**, 1034.
JAKEMAN, E., 1983, Opt. Acta **30**, 1207.
JAKEMAN, E., 1986, The use of photo-event triggered optical shutters to generate sub-Poissonian photo-electron statistics, in: Frontiers in Quantum Optics (Adam Hilger, London) p. 342.
JAKEMAN, E., and B.J. HOENDERS, 1982, Opt. Acta **29**, 1598.
JAKEMAN, E., and J.H. JEFFERSON, 1986, Opt. Acta **33**, 557.
JAKEMAN, E., and P.N. PUSEY, 1976, IEEE Trans. Antennas & Propag. **24**, 806.
JAKEMAN, E., and P.N. PUSEY, 1978, Phys. Rev. Lett. **40**, 546.
JAKEMAN, E., and J.G. RARITY, 1986, Opt. Commun. **59**, 219.
JAKEMAN, E., and J.G. WALKER, 1985, Opt. Commun. **55**, 219.
JAKEMAN, E., E.R. PIKE, P.N. PUSEY and J.M. VAUGHAN, 1977, J. Phys. A **10**, L257.
KABANOV, YU.M., 1978, Theory Probab. & Appl. **23**, 143.
KADOTA, T.T., M. ZAKAI and I. ZIV, 1971, IEEE Trans. Inf. Theory **IT-17**, 368.
KARP, S., 1975, J. Opt. Soc. Am. **65**, 421.
KARP, S., R.M. GAGLIARDI and I.S. REED, 1968, Proc. IEEE **56**, 1704.
KELLEY, P.L., and W.H. KLEINER, 1964, Phys. Rev. A **136**, 316.
KIMBLE, H.J., and L. MANDEL, 1976, Phys. Rev. A **13**, 2123.
KIMBLE, H.J., M. DAGENAIS and L. MANDEL, 1977, Phys. Rev. Lett. **39**, 691.
KIMBLE, H.J., M. DAGENAIS and L. MANDEL, 1978, Phys. Rev. A **18**, 201.
KOGELNIK, H., 1985, Science **228**, 1043.
LAMPERT, M.A., and A. ROSE, 1961, Phys. Rev. **121**, 26.
LAX, M., and M. ZWANZIGER, 1973, Phys. Rev. A **7**, 750.
LAZAR, A.A., 1980, On the capacity of the Poisson-type channel, in: Proc. 14th Ann. Conf. on Information Sciences and Systems, March 26–28, 1980 (Princeton, NJ).
LENSTRA, D., 1982, Phys. Rev. A **26**, 3369.
LEVENSON, M.D., R.M. SHELBY, M. REID and D.F. WALLS, 1986, Phys. Rev. Lett. **57**, 2473.
LOUDON, R., 1976, Phys. Bull. **27**, 21.

M. C. Teich and B. E. A. Saleh, "Photon Bunching and Ant bunching," in Progress in Optics, vol. 26, edited by E. Wolf (North-Holland, Amsterdam, 1988), ch. 1, pp. 1-104.

LOUDON, R., 1980, Rep. Prog. Phys. **43**, 913.
LOUDON, R., 1983, The Quantum Theory of Light, 2nd Ed. (Clarendon, Oxford).
LOUDON, R., and P.L. KNIGHT, 1987, J. Mod. Opt. (Opt. Acta) **34**, 709.
LOUDON, R., and T.J. SHEPHERD, 1984, Opt. Acta **31**, 1243.
LOUISELL, W.H., A. YARIV and A.E. SIEGMAN, 1961, Phys. Rev. **124**, 1646.
MACHIDA, S., and Y. YAMAMOTO, 1986, Opt. Commun. **57**, 290.
MACHIDA, S., Y. YAMAMOTO and Y. ITAYA, 1987, Phys. Rev. Lett. **58**, 1000.
MAEDA, M.W., P. KUMAR and J.H. SHAPIRO, 1987, Opt. Lett. **12**, 161.
MANDEL, L., 1958, Proc. Phys. Soc. (London) **72**, 1037.
MANDEL, L., 1959a, Proc. Phys. Soc. (London) **74**, 233.
MANDEL, L., 1959b, Br. J. Appl. Phys. **10**, 233.
MANDEL, L., 1963, Fluctuations of light beams, in: Progress in Optics, Vol. 2, ed. E. Wolf (North-Holland, Amsterdam) p. 181.
MANDEL, L., 1976a, J. Opt. Soc. Am. **66**, 968.
MANDEL, L., 1976b, The case for and against semiclassical radiation theory, in: Progress in Optics, Vol. 13, ed. E. Wolf (North-Holland, Amsterdam) p. 27.
MANDEL, L., 1979, Opt. Lett. **4**, 205.
MANDEL, L., 1983, Phys. Rev. A **28**, 929.
MANDEL, L., and E. WOLF, 1965, Rev. Mod. Phys. **37**, 231.
MATSUO, K., M.C. TEICH and B.E.A. SALEH, 1983, Appl. Opt. **22**, 1898.
MIDDLETON, D., 1967a, IEEE Trans. Inf. Theory **13**, 372.
MIDDLETON, D., 1967b, IEEE Trans. Inf. Theory **13**, 393.
MILBURN, G.J., and D.F. WALLS, 1983, Phys. Rev. A **28**, 2065.
MILLER, M.M., and E.A. MISHKIN, 1967, Phys. Lett. A **24**, 188.
MITCHELL, R.L., 1968, J. Opt. Soc. Am. **58**, 1267.
MOLLOW, B.R., and R.J. GLAUBER, 1967a, Phys. Rev. **160**, 1076.
MOLLOW, B.R., and R.J. GLAUBER, 1967b, Phys. Rev. **160**, 1097.
MORGAN, B.L., and L. MANDEL, 1966, Phys. Rev. Lett. **16**, 1012.
MOULLIN, E.B., 1938, Spontaneous Fluctuations of Voltage due to Brownian Motions of Electricity, Shot Effect, and Kindred Phenomena (Oxford Univ. Press, Oxford) p. 241.
MÜLLER, J.W., 1974, Nucl. Instrum. & Methods **117**, 401.
NICOLET, M.A., H.R. BILGER and R.J.J. ZIJLSTRA, 1975a, Phys. Status Solidi b **70**, 9.
NICOLET, M.A., H.R. BILGER and R.J.J. ZIJLSTRA, 1975b, Phys. Status Solidi b **70**, 415.
O'DONNELL, K.A., 1982, J. Opt. Soc. Am. **72**, 1459.
OLIVER, C.J., 1984, Opt. Acta **31**, 701.
PAPOULIS, A., 1984, Probability, Random Variables and Stochastic Processes, 2nd Ed. (McGraw-Hill, New York).
PARRY, G., and P.N. PUSEY, 1979, J. Opt. Soc. Am. **69**, 796.
PARZEN, E., 1962, Stochastic Processes (Holden-Day, San Francisco, CA).
PAUL, H., 1966, Fortschr. Phys. **145**, 141.
PAUL, H., 1982, Rev. Mod. Phys. **54**, 1061.
PEŘINA, J., 1984, Quantum Statistics of Linear and Nonlinear Optical Phenomena (Reidel, Dordrecht).
PEŘINA, J., 1985, Coherence of Light, 2nd Ed. (Reidel, Dordrecht).
PEŘINA, J., B.E.A. SALEH and M.C. TEICH, 1983, Opt. Commun. **48**, 212.
PEŘINA, J., V. PEŘINOVÁ and J. KOĎOUSEK, 1984, Opt. Commun. **49**, 210.
PICINBONO, B., C. BENDJABALLAH and J. POUGET, 1970, J. Math. Phys. **11**, 2166.
PIERCE, J.R., E.C. POSNER and E.R. RODEMICH, 1981, IEEE Trans. Inf. Theory **IT-27**, 61.
PUSEY, P.N., D.W. SCHAEFER and D.E. KOPPEL, 1974, J. Phys. A **7**, 530.
RARITY, J.G., P.R. TAPSTER and E. JAKEMAN, 1987, Opt. Commun. **62**, 201.
REID, M.D., and D.F. WALLS, 1984, Phys. Rev. Lett. **53**, 955.
RICCIARDI, L.M., and F. ESPOSITO, 1966, Kybernetik (Biol. Cybern.) **3**, 148.

M. C. Teich and B. E. A. Saleh, "Photon Bunching and Ant bunching," in Progress in Optics, vol. 26, edited by E. Wolf (North-Holland, Amsterdam, 1988), ch. 1, pp. 1-104.

RICE, S.O., 1944, Mathematical analysis of random noise, Bell. Syst. Tech. J. **23**, 1; reprinted 1954, in: Selected Papers on Noise and Stochastic Processes, ed. N. Wax (Dover, New York) p. 133.
SALEH, B.E.A., 1978, Photoelectron Statistics (Springer, Berlin).
SALEH, B.E.A., and M.C. TEICH, 1982, Proc. IEEE **70**, 229.
SALEH, B.E.A., and M.C. TEICH, 1983, IEEE Trans. Inf. Theory **29**, 939.
SALEH, B.E.A., and M.C. TEICH, 1985, Opt. Commun. **52**, 429.
SALEH, B.E.A., and M.C. TEICH, 1987, Phys. Rev. Lett. **58**, 2656.
SALEH, B.E.A., J. TAVOLACCI and M.C. TEICH, 1981, IEEE J. Quantum Electron. **17**, 2341.
SALEH, B.E.A., D. STOLER and M.C. TEICH, 1983, Phys. Rev. A **27**, 360.
SARGENT III, M., M.O. SCULLY and W.E. LAMB JR, 1974, Laser Physics (Addison-Wesley, Reading, MA).
SCHAEFER, D.W., 1975, in: Laser Applications to Optics and Spectroscopy: Physics of Quantum Electronics, Vol. 2, eds S.F. Jacobs, M. Sargent, J.F. Scott and M.O. Scully (Addison-Wesley, Reading, MA) p. 245.
SCHAEFER, D.W., and P.N. PUSEY, 1972, Phys. Rev. Lett. **29**, 843.
SCHAWLOW, A.L., and C.H. TOWNES, 1958, Phys. Rev. **112**, 1940.
SCHLEICH, W., and J.A. WHEELER, 1987, J. Opt. Soc. Am. B **4**, 1715.
SCHUBERT, M., and B. WILHELMI, 1980, The mutual dependence between coherence properties of light and nonlinear optical processes, in: Progress in Optics, Vol. 17, ed. E. Wolf (North-Holland, Amsterdam) p. 163.
SCHUBERT, M., and B. WILHELMI, 1986, Nonlinear Optics and Quantum Electronics (Wiley, New York).
SENIOR, J., 1985, Optical Fiber Communications (Prentice-Hall, Englewood Cliffs, NJ).
SHAPIRO, J.H., 1985, IEEE J. Quantum Electron. **QE-21**, 237.
SHAPIRO, J.H., H.P. YUEN and J.A. MACHADO MATA, 1979, IEEE Trans. Inf. Theory **IT-25**, 179.
SHAPIRO, J.H., M.C. TEICH, B.E.A. SALEH, P. KUMAR and G. SAPLAKOGLU, 1986, Phys. Rev. Lett. **56**, 1136.
SHAPIRO, J.H., G. SAPLAKOGLU, S.-T. HO, P. KUMAR, B.E.A. SALEH and M.C. TEICH, 1987, J. Opt. Soc. Am. B **4**, 1604.
SHELBY, R.M., M.D. LEVENSON, S.H. PERLMUTTER, R.G. DEVOE and D.F. WALLS, 1986, Phys. Rev. Lett. **57**, 691.
SHOCKLEY, W., and J.R. PIERCE, 1938, Proc. IRE **26**, 321.
SHORT, R., and L. MANDEL, 1983, Phys. Rev. Lett. **51**, 384.
SHORT, R., and L. MANDEL, 1984, Sub-Poissonian photon statistics in resonance fluorescence, in: Coherence and Quantum Optics V, eds L. Mandel and E. Wolf (Plenum, New York) p. 671.
SIEGERT, A.J.F., 1954, IRE Prof. Group Inf. Theory **3**, 4.
SIMAAN, H.D., and R. LOUDON, 1975, J. Phys. A **8**, 539.
SLUSHER, R.E., L.W. HOLLBERG, B. YURKE, J.C. MERTZ and J.F. VALLEY, 1985, Phys. Rev. Lett. **55**, 2409.
SMIRNOV, D.F., and A.S. TROSHIN, 1985, Opt. & Spektrosk. **59**, 3 [Opt. & Spectrosc. **59**, 1].
SNYDER, D.L., 1975, Random Point Processes (Wiley, New York).
SRINIVASAN, S.K., 1965, Nuovo Cimento **38**, 979.
SRINIVASAN, S.K., 1986a, Opt. Acta **33**, 207.
SRINIVASAN, S.K., 1986b, Opt. Acta **33**, 835.
STERN, T.E., 1960, IRE Trans. Inf. Theory **IT-6**, 435.
STOLER, D., 1970, Phys. Rev. D **1**, 3217.
STOLER, D., 1971, Phys. Rev. D **4**, 1925.
STOLER, D., 1974, Phys. Rev. Lett. **33**, 1397.
STOLER, D., and B. YURKE, 1986, Phys. Rev. A **34**, 3143.
STOLER, D., B.E.A. SALEH and M.C. TEICH, 1985, Opt. Acta **32**, 345.
SZE, S., 1969, Physics of Semiconductor Devices, 1st Ed. (Wiley, New York) p. 421, Eq. (95).
TAKAHASI, H., 1965, Information theory of quantum-mechanical channels, in: Advances in Communication Systems, ed. A.V. Balakrishnan (Academic Press, New York) p. 227.

M. C. Teich and B. E. A. Saleh, "Photon Bunching and Ant bunching," in Progress in Optics, vol. 26, edited by E. Wolf (North-Holland, Amsterdam, 1988), ch. 1, pp. 1-104.

TAPSTER, P.R., J.G. RARITY and J.S. SATCHELL, 1987, Europhys. Lett. **4**, 293.
TAPSTER, P.R., J.G. RARITY and J.S. SATCHELL, 1988, Phys. Rev. A, to be published.
TEICH, M.C., 1981, Appl. Opt. **20**, 2457.
TEICH, M.C., and B.I. CANTOR, 1978, IEEE J. Quantum Electron. **QE-14**, 993.
TEICH, M.C., and B.E.A. SALEH, 1981a, Phys. Rev. A **24**, 1651.
TEICH, M.C., and B.E.A. SALEH, 1981b, J. Opt. Soc. Am. **71**, 771.
TEICH, M.C., and B.E.A. SALEH, 1982, Opt. Lett. **7**, 365.
TEICH, M.C., and B.E.A. SALEH, 1983, J. Opt. Soc. Am. **73**, 1876.
TEICH, M.C., and B.E.A. SALEH, 1985, J. Opt. Soc. Am. B **2**, 275.
TEICH, M.C., and B.E.A. SALEH, 1987, J. Mod. Opt. (Opt. Acta) **34**, 1169.
TEICH, M.C., and B.E.A. SALEH, 1988, Squeezed states of light, in: Tutorials in Optics **1**, 1987 OSA Annual Meeting, ed. D.T. Moore (Optical Society of America, Washington, DC).
TEICH, M.C., and G. VANNUCCI, 1978, J. Opt. Soc. Am. **68**, 1338.
TEICH, M.C., P.R. PRUCNAL, G. VANNUCCI, M.E. BRETON and W.J. MCGILL, 1982, Biol. Cybern. **44**, 157.
TEICH, M.C., B.E.A. SALEH and D. STOLER, 1983, Opt. Commun. **46**, 244.
TEICH, M.C., B.E.A. SALEH and J. PEŘINA, 1984, J. Opt. Soc. Am. B **1**, 366.
TEICH, M.C., B.E.A. SALEH and T. LARCHUK, 1984, Observation of sub-Poisson Franck–Hertz light at 253.7 nm, in: Digest XIII Int. Quantum Electron. Conf., 1984, Anaheim, CA (Optical Society of America, Washington, DC) paper PD-A6, p. PD-A6-1.
TEICH, M.C., K. MATSUO and B.E.A. SALEH, 1986, IEEE J. Quantum Electron. **22**, 1184.
TEICH, M.C., F. CAPASSO and B.E.A. SALEH, 1987, J. Opt. Soc. Am. B **4**, 1663.
THOMPSON, B.J., D.O. NORTH and W.A. HARRIS, 1940, RCA Rev. **4**, 269, 441; **5**, 106, 244.
THOMPSON, B.J., D.O. NORTH and W.A. HARRIS, 1941, RCA Rev. **5**, 371, 505; **6**, 114.
TITULAER, U.M., and R.J. GLAUBER, 1965, Phys. Rev. **140**, B676.
TORNAU, N., and A. BACH, 1974, Opt. Commun. **11**, 46.
TROUP, G.J., 1965, Phys. Lett. **17**, 264.
TWISS, R.Q., and A.G. LITTLE, 1959, Aust. J. Phys. **12**, 77.
WALKER, J.G., 1986, Opt. Acta **33**, 213.
WALKER, J.G., 1987, J. Mod. Opt. (Opt. Acta) **34**, 813.
WALKER, J.G., and E. JAKEMAN, 1985a, Proc. Soc. Photo-Opt. Instrum. Eng. **492**, 274.
WALKER, J.G., and E. JAKEMAN, 1985b, Opt. Acta **32**, 1303.
WALLS, D.F., 1979, Nature **280**, 451.
WALLS, D.F., 1983, Nature **306**, 141.
WHINNERY, J.R., 1959, Scientia Electrica **5**, 219.
WOLF, E., 1979, Opt. News **5**, 24.
WU, L.-A., H.J. KIMBLE, J.L. HALL and H. WU, 1986, Phys. Rev. Lett. **57**, 2520.
YAMAMOTO, Y., and H.A. HAUS, 1986, Rev. Mod. Phys. **58**, 1001.
YAMAMOTO, Y., and S. MACHIDA, 1987, Phys. Rev. A **35**, 5114.
YAMAMOTO, Y., S. MACHIDA and O. NILSSON, 1986, Phys. Rev. A **34**, 4025.
YAMAMOTO, Y., N. IMOTO and S. MACHIDA, 1986a, Phys. Rev. A **33**, 3243.
YAMAMOTO, Y., N. IMOTO and S. MACHIDA, 1986b, Quantum nondemolition measurement of photon number and number–phase minimum uncertainty state, in: 2nd Int. Symp. on Foundations of Quantum Mechanics, Tokyo, Japan, 1986, p. 265.
YAMAMOTO, Y., S. MACHIDA, N. IMOTO, M. KITAGAWA and G. BJÖRK, 1987, J. Opt. Soc. Am. B **4**, 1645.
YUEN, H.P., 1976, Phys. Rev. A **13**, 2226.
YUEN, H.P., 1986, Phys. Rev. Lett. **56**, 2176.
YUEN, H.P., and J.H. SHAPIRO, 1978, IEEE Trans. Inf. Theory **IT-24**, 657.
YUEN, H.P., and J.H. SHAPIRO, 1980, IEEE Trans. Inf. Theory **IT-26**, 78.

M. C. Teich and B. E. A. Saleh, "Photon Bunching and Ant bunching," in Progress in Optics, vol. 26, edited by E. Wolf (North-Holland, Amsterdam, 1988), ch. 1, pp. 1-104.